PL-TR-95-2169   SSS-DTR-95-15259

Investigations of the Seismic Characteristics of Rockbursts

Theron J. Bennett
Keith L. McLaughlin
Margaret E. Marshall
Brian W. Barker
John R. Murphy

Maxwell Laboratories, Incorporated
S-CUBED Division
P. O. Box 1620
La Jolla, CA   92038-1620

December, 1995

Scientific Report No. 1   **19960227 006**

Approved for public release; distribution unlimited

DTIC QUALITY INSPECTED 1

"This technical report has been reviewed and is approved for publication."

DELAINE REITER
Contract Manager

JAMES F. LEWKOWICZ
Director
Earth Sciences Division

This report has been reviewed by the ESD Public Affairs Office (PA) and is releasable to the National Technical Information Service (NTIS).

Qualified requestors may obtain additional copies from the Defense Technical Information Center. All others should apply to the National Technical Information Service.

If your address has changed, or if you wish to be removed from the mailing list, or if the addressee is no longer employed by your organization, please notify PL/IM, 29 Randolph Road, Hanscom AFB, MA 01731-3010. This will assist us in maintaining a current mailing list.

Do not return copies of this report unless contractual obligations or notices on a specific document requires that it be returned.

REPORT DOCUMENTATION PAGE

Form Approved
OMB No. 0704-0188

1. AGENCY USE ONLY *(Leave blank)*	2. REPORT DATE December, 1995	3. REPORT TYPE AND DATES COVERED Scientific No. 1

4. TITLE AND SUBTITLE

INVESTIGATIONS OF THE SEISMIC CHARACTERISTICS OF ROCKBURSTS

6. AUTHOR(S)

Theron J. Bennett, K. L. McLaughlin, M. E. Marshall, B. W. Barker, and J. R. Murphy

5. FUNDING NUMBERS

Contract:
F19628-94-C-0083

PE 61102F
PR 2309
TA G2
WU BR

7. PERFORMING ORGANIZATION NAME(S) AND ADDRESS(ES)

Maxwell Laboratories, Inc.
S-CUBED Division
P.O. Box 1620
La Jolla, CA 92038-1620

8. PERFORMING ORGANIZATION REPORT NUMBER

SSS-DTR-95-15259

9. SPONSORING/MONITORING AGENCY NAME(S) AND ADDRESS(ES)

Phillips Laboratory
29 Randolph Road
Hanscom AFB, MA 01731-3010

Contract Manager: Delaine Reiter/GPE

10. SPONSORING/MONITORING AGENCY REPORT NUMBER

PL-TR-95-2169

11. SUPPLEMENTARY NOTES

12a. DISTRIBUTION/AVAILABILITY STATEMENT

Approved for public release; distribution unlimited

12b. DISTRIBUTION CODE

13. ABSTRACT *(Maximum 200 words)*

This research is directed at improving understanding of rockbursts and related mine tremors as seismic sources and at distinguishing them from other source types based on characteristics of their signals. In addition, this effort seeks to gain insight into controllability of rockbursts and its relevance to possible clandestine testing of small nuclear explosions. An observational element of this research has focused on identifying the characteristics of the seismic signals from rockbursts in areas around the world and, in particular, on the behavior of several prominent rockbursts in specific areas which have occurred within the past few years. A number of features have been identified which may be distinctive for rockbursts relative to other source types. A theoretical aspect of the research effort has been directed at refining the description of the rockburst source and relating the seismic source description to physical properties of the mine environment. For the latter, observed rockburst phenomenology is being used to define source models, for several of the more prominent recent events, which satisfactorily predict many of the salient features of the observed seismic signals.

14. SUBJECT TERMS

Seismic	Rockbursts	North America	South Africa
Discrimination	Mechanisms	Europe	Evasion

15. NUMBER OF PAGES 90

16. PRICE CODE

17. SECURITY CLASSIFICATION OF REPORT	18. SECURITY CLASSIFICATION OF THIS PAGE	19. SECURITY CLASSIFICATION OF ABSTRACT	20. LIMITATION OF ABSTRACT
UNCLASSIFIED	UNCLASSIFIED	UNCLASSIFIED	UNLIMITED

Table of Contents

iv

List of Illustrations

List of Tables

1. Introduction

1.1 Objective

The prospects of a Comprehensive Test Ban Treaty (CTBT) have increased attention on seismic monitoring of small events including a variety of different source types. In addition to the discrimination of underground nuclear explosion tests from earthquakes, under a CTBT chemical blasts and rockbursts, or related mining-induced tremors, could represent a significant problem for seismic identification schemes. In particular, these latter events may be quite frequent at the lower magnitude thresholds of interest in CTBT monitoring, the source mechanisms may be different from those for earthquakes which form the bases for many traditional seismic discriminants, and ability to control the occurrence of the events could provide an opportunity to conceal a concurrent clandestine nuclear explosion test in the region adjacent to the source. The research effort described here is directed at improving understanding of rockbursts and related mining-induced tremors as seismic sources and at distinguishing them from other source types based on the characteristics of their signals. In the course of this research, we are also seeking to gain insight into the controllability of rockbursts and the relevance of such control to the issue of covert testing of small nuclear explosions.

1.2 Overview

Rockbursts and related events occur in mines throughout the world (cf. Figure 1) due to the perturbation, caused by the excavation, to the ambient stress field in the vicinity of the mine. In some cases the man-made perturbation alone can be enough to generate the stress field and release associated with the rockburst or tremor. However, in other cases the perturbation may act as a trigger to the regional tectonic stress which is released in the rockburst. Mining-induced events are often small (less than magnitude 3), but they have also occasionally been large (greater than magnitude 5) in some areas. The events are frequent in some mines and rare in others depending on factors like rate of excavation, rock properties, tectonic conditions, and details of the mining practice.

In a previous report (cf. Bennett et al., 1994) we reviewed several source mechanisms associated with mining-induced seismicity and suggested some implications that the different mechanisms might have for discrimination. It

1
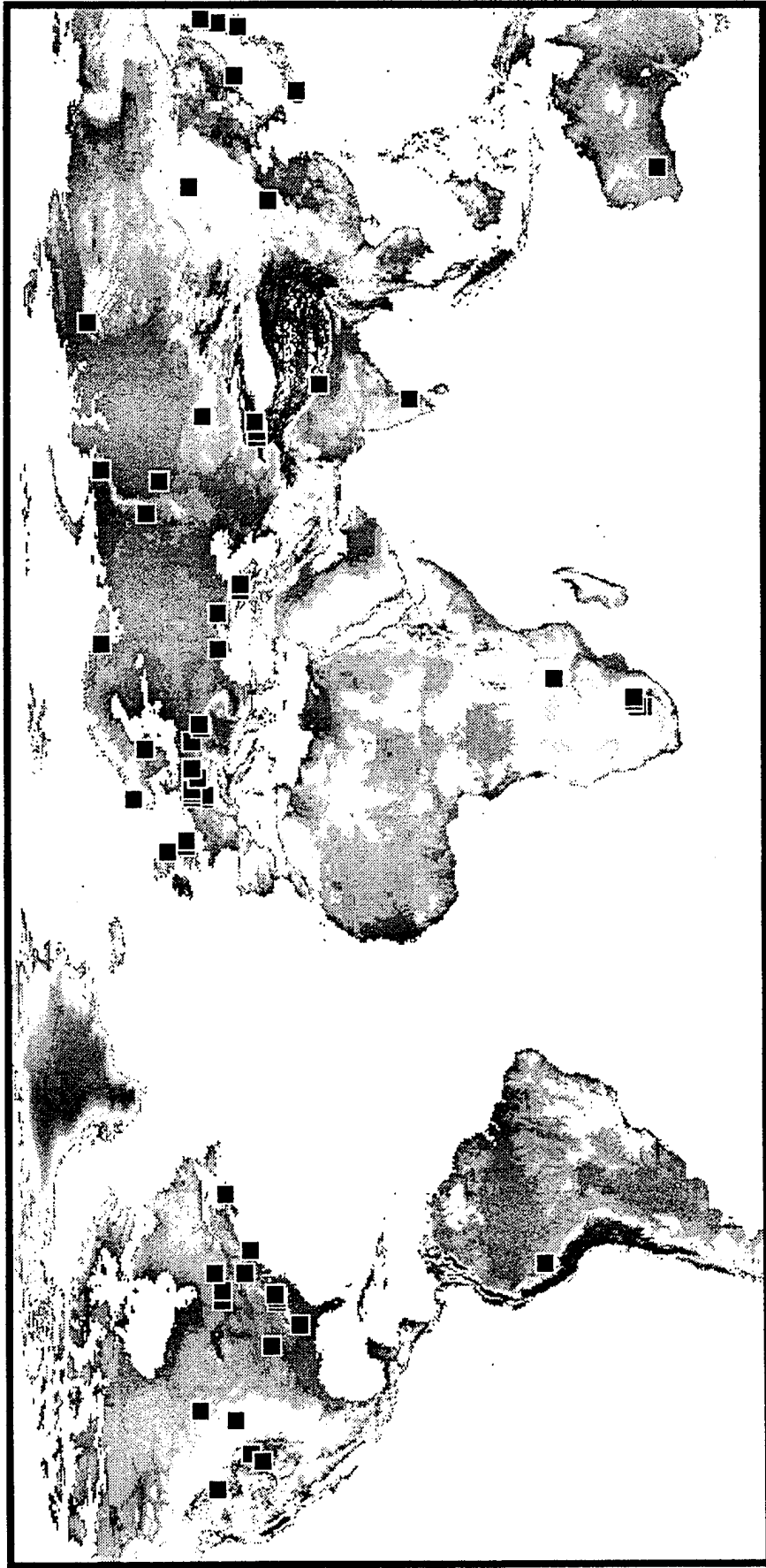
Figure 1. Locations of mining areas with reported rockbursts or tremors.

should be noted that, for the purpose of this and our prior studies, we consider a rather wide range of mining-induced seismic events under the term "rockburst"; whereas in a strict sense rockbursts are events in which rock or sections of rock are suddenly displaced or projected into the mine opening. Throughout this report we have used "rockburst" to refer to any mining-induced event which releases strain energy in the surrounding rock.

Interest in rockbursts and related events has been stimulated in recent years. However, this increased awareness is only partly related to the knowledge that such events affect seismic discrimination. A far greater influence has been the occurrence of several large, catastrophic rockbursts at mines in different parts of the world. These events have drawn public attention because of the extensive damage and, in some cases, fatalities which they have caused.

Some of the more prominent of these rockbursts (cf. Figure 2), responsible for this increased attention, have been the April 13, 1989 Völkershausen, Germany mine collapse, the February 3, 1995 southwestern Wyoming mine collapse, and the October 30, 1994 mine tremor in the Orange Free State, South Africa. These events were three of the largest rockbursts to have ever occurred anywhere. In addition, a few recent events have come to attention because they were fairly large and occurred in regions where seismic events of that size are unusual. These include the January 5, 1995 seismic event in the Ural mountains of Russia and the March 11, 1995 coal mine bump in eastern Kentucky. In the course of our investigations, we have had the opportunity to take a closer look at each of these events.

We reported on the 1989 Völkershausen, Germany mine collapse in our prior report (cf. Bennett et al., 1994) and described a discrimination analysis of the 1995 Urals event in another report (cf. Bennett et al., 1995). In this report we focus on the Wyoming mine collapse and the Orange Free State, South Africa mine tremor. In addition, we describe some on-going work on coal mine bumps in eastern North America and preliminary investigations of the database of central European rockbursts which we are developing. Finally, we have begun a modeling effort to investigate how rockburst mechanisms, focal depths, and nearby stress conditions and rock properties affect the observed seismic signals. As part of this modeling effort, we are also seeking to identify to what extent mining practice might be used to control the rockburst source with respect to timing, size, and other source properties.

3

Figure 2. Locations of recent significant rockbursts which are being analyzed.

4

1.3 Report Organization

This report is divided into six sections including these introductory remarks. In Section 2 we describe our investigations of the seismic signals from the February 3, 1995 Wyoming mine collapse and compare the observations to other event types and similar sources in other source regions. Section 3 deals with the October 30, 1994 South African mine tremor and our analyses of the seismic signals from that and other tremors from the nearby mines. In Section 4 we briefly review our on-going work with rockbursts in other source regions including Polish rockbursts in central Europe, coal mine bumps in the eastern U.S., and the January 5, 1995 Urals event. Section 5 reviews our approach to modeling the seismic signals from rockbursts and how source properties and mechanisms are expected to influence observations. Finally, in Section 6 we summarize our observations thus far and outline our directions for future investigations.

2. Wyoming Mine Collapse of February 3, 1995

2.1 Background

On February 3, 1995 a large seismic event, which has been identified as a rockburst or mine collapse, occurred in southwestern Wyoming. The event had a magnitude of 5.2 m_b, reported by NEIS, and occurred at 41.5° N 109.8° W in a relatively aseismic region; over the past 30 years only seven events (all with magnitudes less than 3) have been located within 50 km of this event (cf. Pechmann et al., 1995). In locating the event the focal depth was constrained at 4 km, but the depth cannot be precisely determined from the seismic data alone, so there is associated uncertainty in the location. The event location places it in proximity (less than 5 km separation) to the Solvay mine. This mine extracts trona, an evaporite mineral used as a source of sodium-based chemicals, at depths near 0.5 km. The mine experienced considerable damage at the time of the seismic event, several miners were temporarily trapped and injured, and one miner died.

2.2 Events and Data Sources

Our investigation of the Wyoming mine collapse has focused on analyses of data from several regional/far-regional seismic stations. We have sought to compare observations from the mine collapse with similar recordings from other source types at similar distances in the western U.S. Figure 3 shows the locations of the February 3, 1995 mine collapse in southwestern Wyoming near the Utah border along with recording stations and events used in our comparisons. The events and recording station information are summarized in Table 1. Records for the mine collapse were clipped at the nearby Pinedale station, but regional phase signals were well recorded at several other stations throughout the western and central U.S.

In our initial analyses of this event, we have relied heavily on the records from the Texas array station at Lajitas; some of these were obtained from the ARPA Center for Monitoring Research database while others were obtained directly from Southern Methodist University Department of Geological Sciences (Herrin, 1995). The most direct comparison that we have is for the northwestern Colorado earthquake of March 20, 1995, although for this event the magnitude is somewhat smaller (viz. 4.1 m_b) and the epicentral distance is a little less (1300 km versus 1470 km for the Wyoming mine collapse). Nevertheless, the
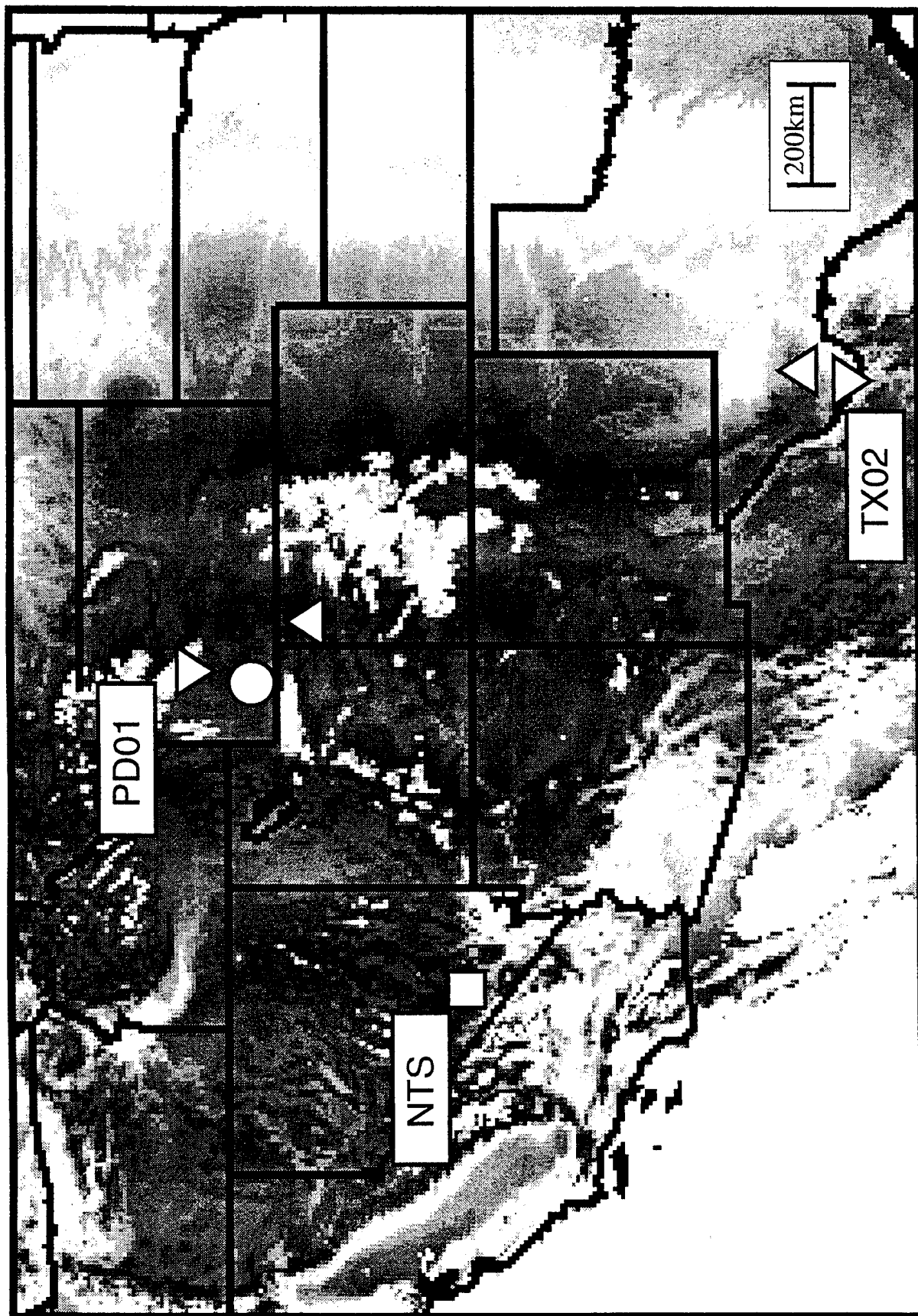
Figure 3. Locations of southwestern Wyoming rockburst of February 3, 1995 (◯), earthquakes (△) and nuclear explosions (☐) used in comparisons and regional seismic stations (▽).

Table 1

Selected Western U.S. Sources

Events	Latitude	Longitude	mb	MS	Distance
Wyoming Mine Collapse 2/03/95 15:26:11	41.53 N	109.81 W	5.2	4.6	1460 km (to Lajitas)
Colorado Earthquake 3/20/95 12:46:19	40.33 N	108.55 W	4.1	-	1300 km (to Lajitas)
Texas Earthquake 4/14/95 00:32:55	30.26 N	103.33 W	5.7	5.6	1470 km (to Pinedale)
NTS Explosion JUNCTION 3/26/92 16:30:00	37.27 N	116.36 W	5.5	4.2	1500 km (to Lajitas)

Selected Western U.S. Seismic Stations

Station	Latitude	Longitude
Texas Array (Lajitas)	29.33 N	103.66 W
Pinedale Array	42.78 N	109.58 W

paths are quite similar. We also compared the Wyoming collapse signals recorded at the Texas array with regional signals recorded at the Pinedale, Wyoming array from the earthquake (5.7 mb) of April 14, 1995 in southwestern Texas. The latter represents a nearly reciprocal path as can be seen in Figure 3, with an epicentral distance somewhat greater (1500 km) for the Texas earthquake record. Possibly the most relevant comparison from the standpoint of discrimination is between the mine collapse and NTS nuclear explosions recorded at the Texas array station. Although the propagation path is clearly somewhat different, the epicentral distance is almost exactly the same (1470 km for both); so we would not expect propagation effects to be greatly different. In our comparison we have used the observations from the NTS explosion JUNCTION on March 26, 1992 which had a magnitude (5.5 mb) close to that of the mine collapse.

2.3 Earthquake Comparison

Our principal analysis tool in these studies has been band-pass filter processing. A series of narrow band-pass filters with progressively higher corner frequencies was applied to each vertical-component record, with the same set of filters used for each of the events. Figure 4 shows the results of this band-pass filter analysis applied to the Wyoming mine collapse recorded at the Texas array. It should be noted that the sequence of eight filters covers overlapping passbands of 0.05 - 0.1 Hz, 0.1 - 1.0 Hz, 0.5 - 2.0 Hz, 1.0 - 3.0 Hz, 2.0 - 4.0 Hz, 3.0 - 6.0 Hz, 4.0 - 8.0 Hz, 6.0 - 12.0 Hz; and the traces corresponding to each filter output have been individually normalized.

The most prominent features of the signals are the emergent, long-duration regional P phases and relatively large L_g in bands from just below 1 Hz to 3 Hz. Over this frequency band the L_g/P ratio is about two or more. Above 3 Hz the regional phase signals are less coherent, except for an apparent P_g phase which dominates the 2 - 4 Hz passband; the source of the late-arriving, high-frequency signals in the bands above 4 Hz is unknown but does not seem to be associated with the mine collapse event. In the very low-frequency band (0.05 - 0.1 Hz) we see a clear indication of a fundamental mode Rayleigh wave, which rises above the background at a time just after the L_g signal time.

Figure 5 shows the results of applying the same set of band-pass filters to the record for the March 20, 1995 Colorado earthquake. On the broadband
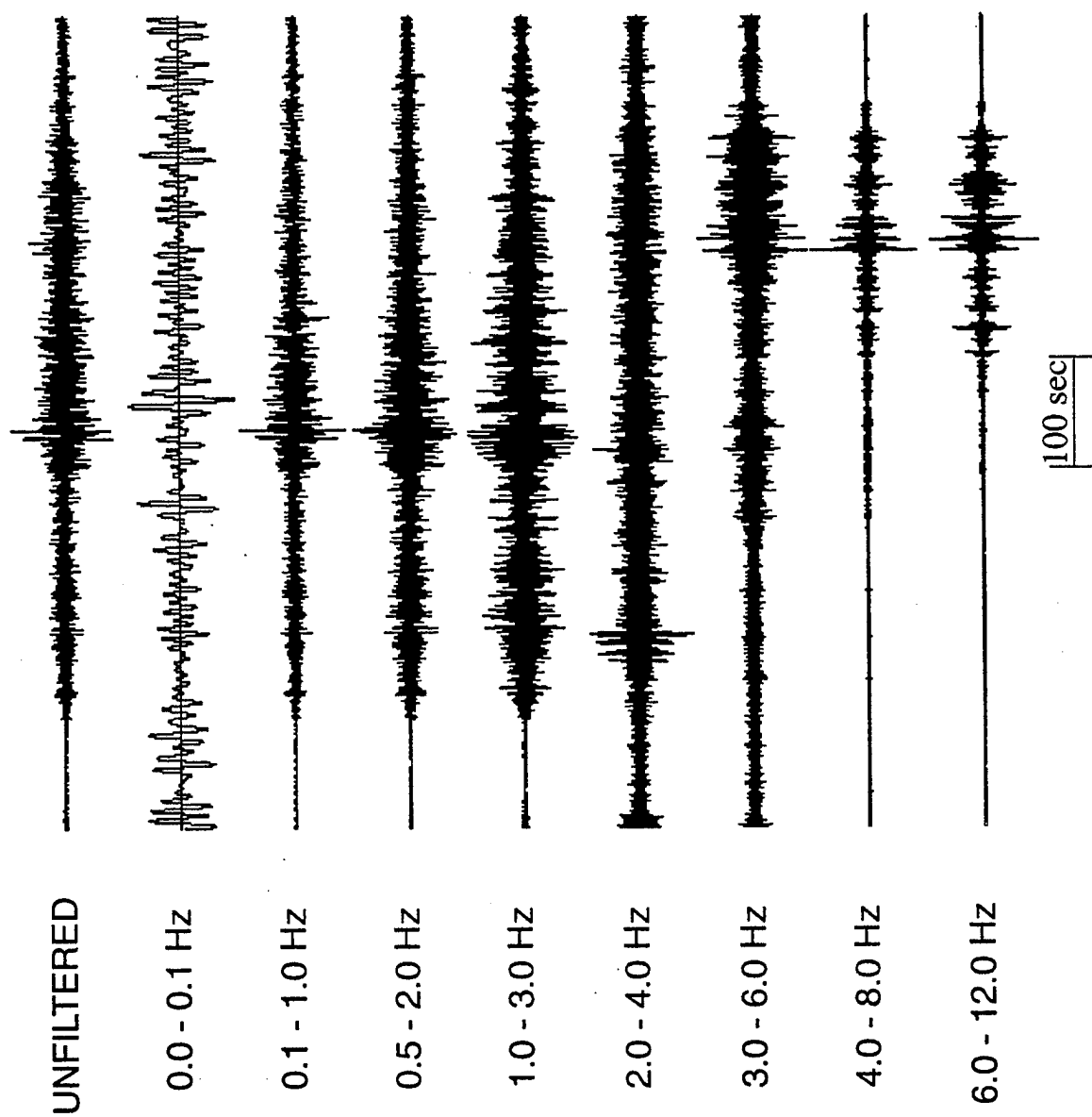
Figure 4. Bandpass filter analysis of southwestern Wyoming rockburst of February 3, 1995 recorded at Texas array (R = 1470 km).

UNFILTERED

0.0 - 0.1 Hz

0.1 - 1.0 Hz

0.5 - 2.0 Hz

1.0 - 3.0 Hz

2.0 - 4.0 Hz

3.0 - 6.0 Hz

4.0 - 8.0 Hz

6.0 - 12.0 Hz

100 sec
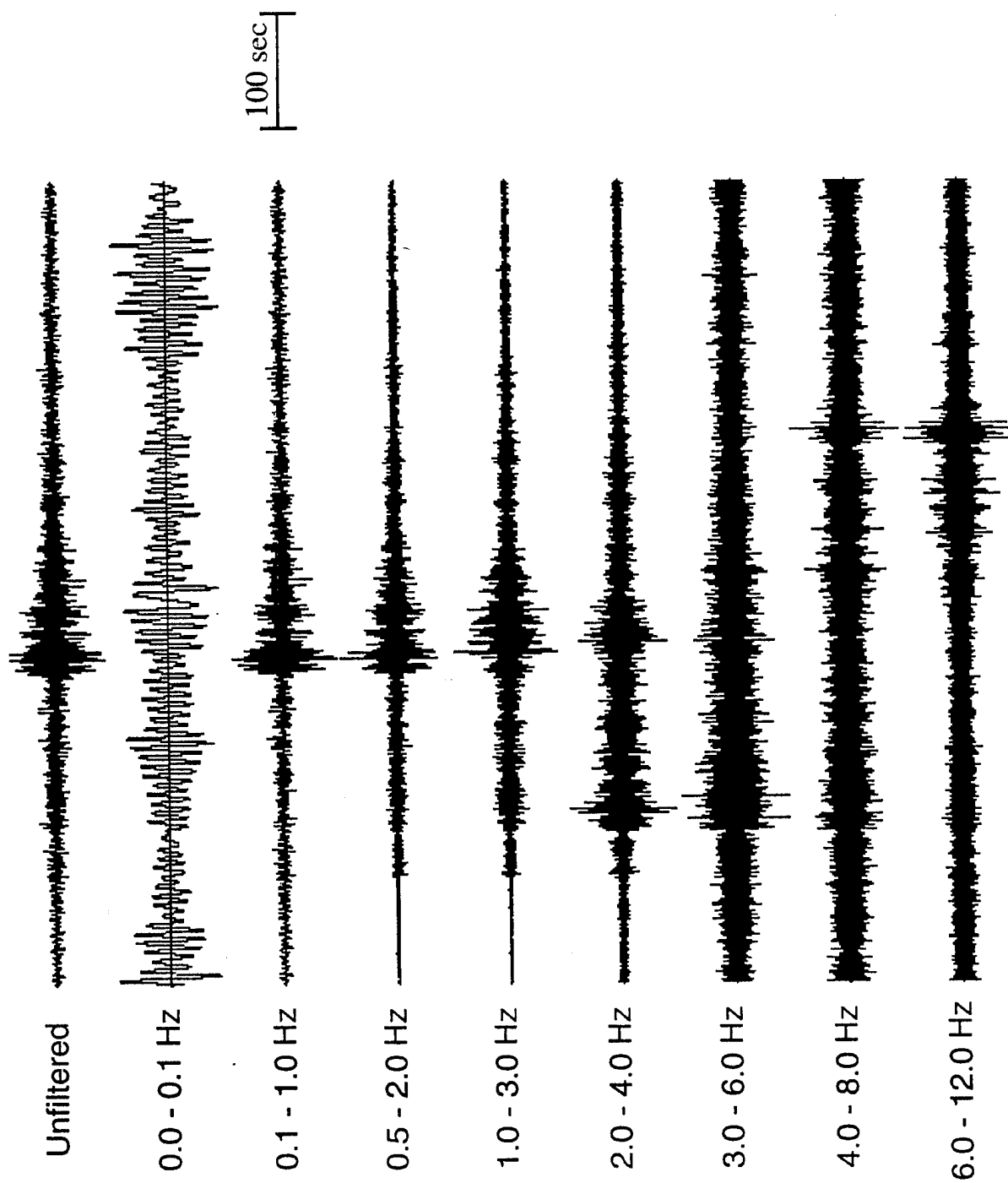
Figure 5. Bandpass filter analysis of northern Colorado earthquake of March 20, 1995 recorded at Texas array (R = 1300 km).

(unfiltered) traces the signals appear to be quite similar except that the signal-to-noise level is lower for the smaller-magnitude event (i.e. the earthquake). The regional P phases look alike in the frequency bands between about 1 Hz and 3 Hz for the earthquake and the mine collapse. One interesting feature of the earthquake record is an apparent enhancement of higher frequencies in the regional signals, which is seen in the 2 - 4 Hz passband. In fact, absolute amplitude levels in this band are smaller for the earthquake than for the mine collapse; so that the observation can probably be explained as a reduction in background noise and shift to slightly higher corner frequency for the smaller magnitude event (i.e. the earthquake).

The long-period Rayleigh-wave signal is not clear in the low-frequency passband for the earthquake record; however, the perturbation of the long-period microseisms shortly after the L_g time might correspond to the signal. If so, the signal level is down around the microseism noise level, which means that the long-period Rayleigh wave signal level for the earthquake would be about a factor of two or so lower than the long-period Rayleigh wave for the mine collapse at this single station. Assuming that radiation pattern effects are similar for the two events and also assuming that this single-station observation is representative of the long-period Rayleigh-wave excitation for the events, the observations suggest that the M_S for the earthquake would be approximately 0.3 - 0.4 magnitude units smaller than the mine collapse M_S. It could be inferred from this that the earthquake M_S is about 4.2 - 4.3, which is approximately equal to its body-wave magnitude.

2.4 Reciprocal Event Comparison

We next compare the Wyoming mine collapse signals processed using the band-pass filters with results obtained from similar processing of the southwestern Texas earthquake recorded at Pinedale, Wyoming. As we pointed-out above in Figure 3, the event-station pairs form a nearly reciprocal relationship with approximately equivalent propagation path elements. The difference in epicentral distance between the two is only about 30 km. Thus, any differences in the regional signal behavior are more likely to be related to source differences.

Figure 6 shows the results of the band-pass filter processing of the Texas earthquake. The dominant features of the regional signals from the earthquake appear quite similar to those seen in Figure 4 above for the mine collapse;

12
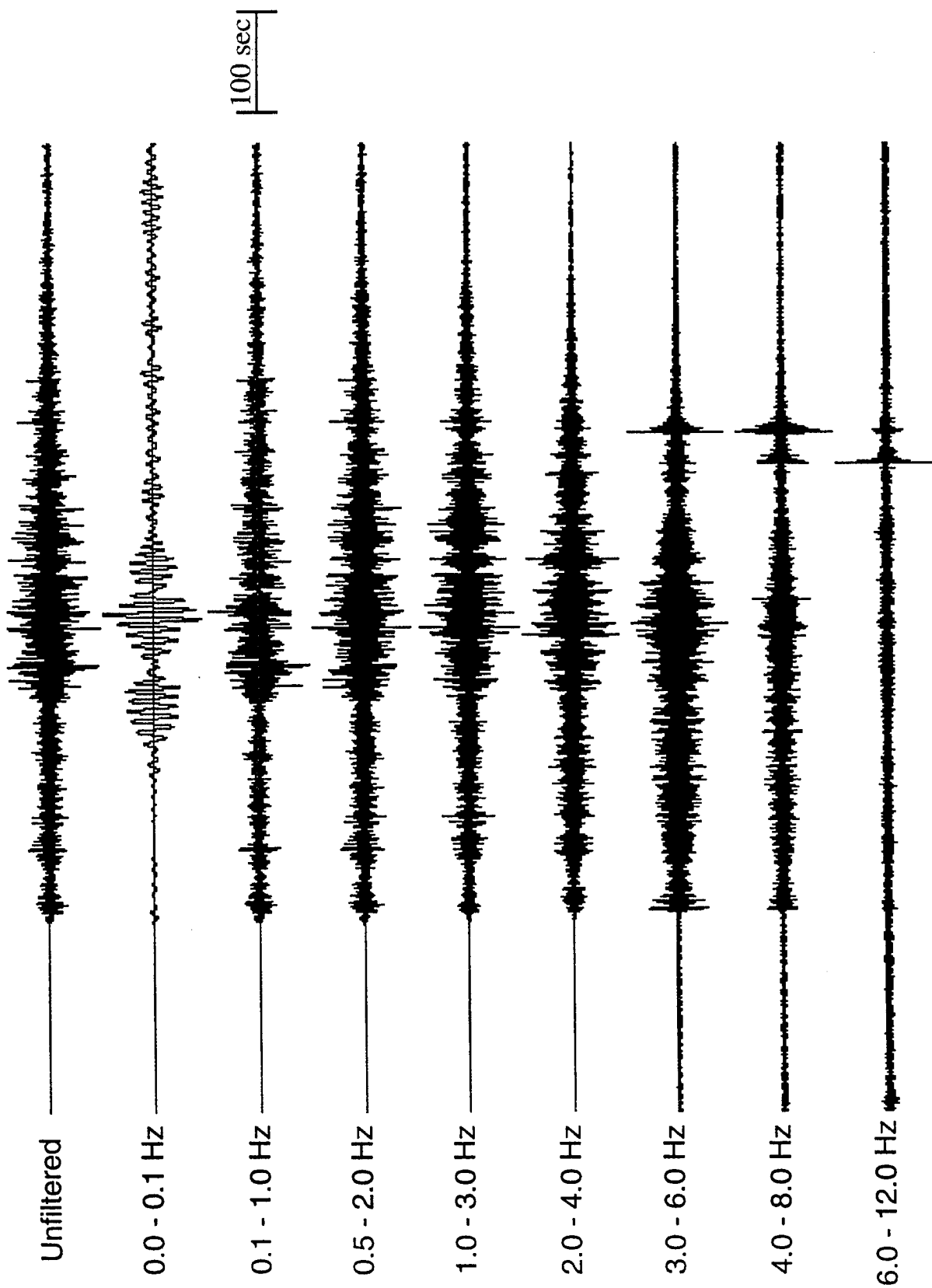
Figure 6. Bandpass filter analysis of south Texas earthquake of April 14, 1995 recorded at Pinedale array (R = 1500 km).

Unfiltered

0.0 - 0.1 Hz

0.1 - 1.0 Hz

0.5 - 2.0 Hz

1.0 - 3.0 Hz

2.0 - 4.0 Hz

3.0 - 6.0 Hz

4.0 - 8.0 Hz

6.0 - 12.0 Hz

100 sec

however, there are some differences in detail. For the frequency bands in the range 0.1 to 3 Hz, we again see emergent, long-duration P and Lg phases; the Lg/P ratio is greater than two. Within these bands P phases appear to be somewhat more coherent for the earthquake than for the mine collapse. At higher frequencies the earthquake signals appear to be much more distinct and energetic than was seen for the mine collapse. Ignoring the late-time pulses in the bands from 3 to 12 Hz, which again appear to be local noise, unrelated to the earthquake, regional P and Lg phases are seen to be well above the background noise. The apparent differences do not seem to be attributable to different background noise conditions but might be associated with recording system response differences between the Pinedale and Texas array stations.

The surface-wave signals in the 0.05 - 0.1 Hz passband appear to be strong but rather complex for the southwestern Texas earthquake. In particular, the record shows several distinct energy packets. The long-period surface-wave signal levels for the Texas earthquake are well above the microseism background noise. The observation of a strong fundamental-mode Rayleigh wave from the April 14, 1995 southwest Texas earthquake would appear to be consistent with the large MS of 5.6 reported for the event, which is approximately equal to the mb of 5.7 reported by NEIS. We have not resolved the instrument response differences between the Pinedale and Texas array stations; but we anticipate that, after accounting for the response differences, more direct comparisons can be made between the signals for the mine collapse and earthquake in Figures 4 and 6 respectively.

2.5 Nuclear Explosion Comparison

The Nevada Test Site (NTS) is located 1470 km west-northwest of the Texas array site at Lajitas, which is the same distance as the Texas array from the Wyoming collapse. In testing regional seismic discrimination methods, we would like to be able to compare observations from different source types in the same source area. However, observations which meet these requirements are rare; and we are often required to relax our restrictions. In comparing the Wyoming mine collapse with the NTS nuclear explosion JUNCTION both recorded at the Texas array, we at least eliminate most differences attributable to recording station site response. As can be seen in Figure 3 above, there are some clear propagation differences for the two events; the path to NTS follows along the southern edge of the Colorado plateau, while the path for the

14

Wyoming event cuts through the highest parts of the plateau, the Rocky Mountains. Nevertheless, propagation conditions are at least somewhat similar; and the choice of events with common epicentral distances should help to reduce the effects of any propagation differences.

Figure 7 shows the results of the band-pass filter analysis applied to the JUNCTION nuclear test. Regional P and L_g phases are clearly discernible. In this case the P phase has a very sharp onset, unlike the emergent signals seen for the mine collapse and earthquakes. The L_g signal is also apparent in the frequency bands for the range from 0.1 to 3 Hz, but the signal level is reduced in duration and in amplitude relative to P. In addition, much of the L_g energy appears to be concentrated in the frequency band near 1 Hz. In comparison to the rockburst and earthquake signals, the L_g/P ratios are much lower for the nuclear explosion. Furthermore, these L_g/P differences tend to be enhanced at high frequencies where the L_g signal vanishes into the noise for the explosion, at frequencies above about 3 Hz. It should be noted again that late-time high-frequency bursts present on the bottom two traces of Figure 7 are thought to be noise and have been disregarded in our analysis. The difference in L_g/P ratios between nuclear explosions and other source types appears to be quite distinctive and has been identified in past studies as a prospective discriminant for explosions, earthquakes, as well as rockbursts (cf. Blandford, 1981; Pomeroy et al., 1982; Bennett et al., 1992, 1994). These observations appear to support the previous findings.

In the low-frequency pass-band 0.05 - 0.1 Hz, the record for the JUNCTION nuclear test shows a surprisingly strong fundamental-mode Rayleigh wave signal. The signal has some similarities to the Rayleigh wave observed in the same passband for the Wyoming mine collapse (cf. Figure 4 above). The periods of the signals are similar, and the amplitude level is nearly the same or slightly smaller for the mine collapse. Although both events were recorded at essentially the same site, there could be some differences in instrument response over time which might affect these types of amplitude comparisons. We are attempting to resolve instrument response issues, so that more precise comparisons can be made between the observed absolute signal levels for the different source types.

UNFILTERED

0.0 - 0.1 Hz

0.1 - 1.0 Hz

0.5 - 2.0 Hz

1.0 - 3.0 Hz

2.0 - 4.0 Hz

3.0 - 6.0 Hz

4.0 - 8.0 Hz

6.0 - 12.0 Hz

100 sec
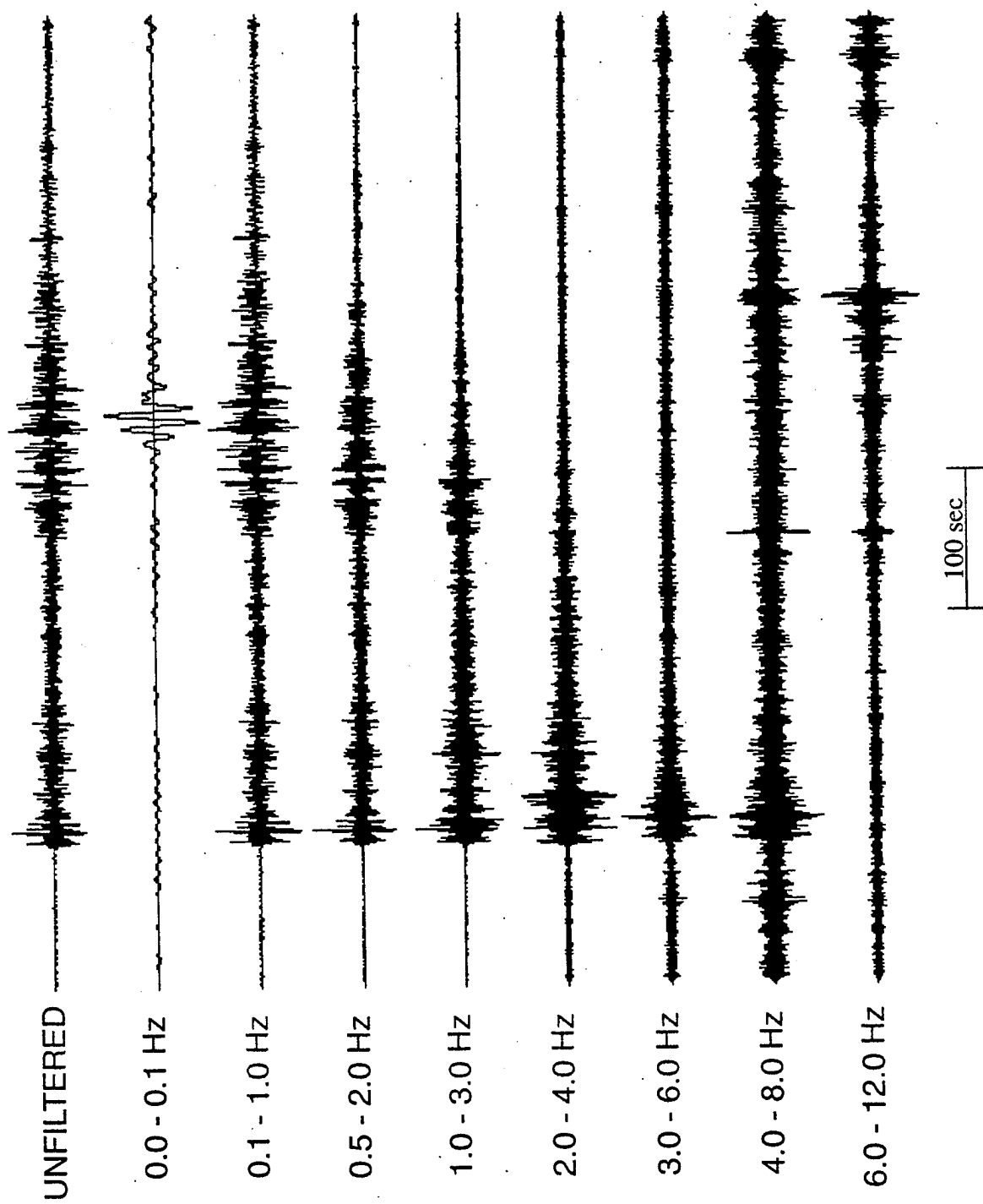
Figure 7. Bandpass filter analysis of the JUNCTION nuclear test recorded at the Texas array (R = 1470 km).

2.6 Comparison to Other Mine Collapses

As can be seen in Table 2, the Wyoming mine collapse has several similarities to the 1989 Völkershausen, Germany mine collapse, which we analyzed in a previous report (cf. Bennett et al., 1994). The body-wave magnitudes are both quite large for this type of event. Rockbursts with magnitudes as great as 5 m_b are rare, with the possible exception of South Africa where the historical record appears to include several large-magnitude mine tremors. The surface-wave magnitudes, M_S, reported by NEIS are more than 0.5 magnitude units lower than mb, which also seems to be consistent with our past experience for this source type (cf. Bennett et al., 1994). Both events appear to be associated with relatively sudden collapse over large horizontal areas projecting upward from the mine workings (cf. Ahorner, 1989; Minkley, 1993; Pechmann et al., 1995). Pechmann et al. (1995) report nearly all dilatational first motions for the Wyoming mine collapse and suggest that the first motion pattern could be represented either by an implosional mechanism or by a normal dip-slip fault mechanism. This is like the situation observed from the Völkershausen event (cf. Ahorner, 1989; Knoll, 1990; Bennett et al., 1994) where nearly all stations (except a few distant stations with low signal-to-noise conditions) reported dilatational first motions, and the mechanism was determined to have a strong implosional component which could be interpreted as a simple collapse. However, there does seem to be some difference in the gravitational potential energy loss estimates for the simple collapse models of the two events. The energy in the Völkershausen mine collapse is about a factor of eight larger, which is too large considering the magnitude difference is small. One explanation for this observation could be a difference in seismic efficiency between the two sources. Even though the two events seem to be reasonably represented by simple down-dropped blocks above the mine workings, it seems quite likely that there could be significant differences in details which may not be accounted for in our original simple model. In future work we plan to evaluate how factors like collapse timing and duration and variations in the displacement across the block might affect the seismic signals.

17

Table 2

Comparison of the 1995 Wyoming and 1989 German Mine Collapses

	Solvay Mine	Ernst Thaelmann Mine
Date	2/03/95	3/13/89
Location	41.5 N 109.8 W Little America, WY	50.7 N 9.9 E Völkershausen, Germany
Depth	0.5 km	0.9 km
mb	5.2	5.4
MS	4.6	4.7
Collapse Area	2 km x 1 km	3 km x 3 km
Average Collapse Displacement	60 cm	70 cm
Mineral	Trona	Potash
Gravitational Energy	1.4×10^{20} ergs	1.1×10^{21} ergs

3. South African Mine Tremor of October 30, 1994

3.1 Background

Another significant mining-induced event occurred on October 30, 1994 in the Orange Free State mining district of South Africa. The gold-mining region around Johannesburg has historically been the site of frequent and large mine tremors. The induced seismicity there follows a somewhat arcuate, northeast-southwest trend about 250 km in length corresponding to the location of the deep mines, with the Orange Free State mines lying at the far southwestern end of the trend. Many of the mine tremors from the South African region have had magnitudes greater than 5; the October 30, 1994 event had a magnitude of 5.6 mb.

This event is unusual because it is one of the largest to have occurred in this area, some authors (cf. Fan and Wallace, 1995) have attributed the event to a deep tectonic source, and the event produced excellent on-scale records at a broad-band, near-regional station (viz. BOSA), which has recorded numerous smaller mine tremors from the same general area. Our analyses have focused on a comparison of the October 30, 1994 event with several other mine tremors from this area, and in particular comparisons of the regional seismic signals at BOSA from these events.

3.2 Comparisons to Other Events from the Mining Region

The October 30, 1994 Orange Free State event was large and, as would be expected, was well-recorded at stations all over the world. We will briefly consider some of the teleseismic observations below, but we concentrate here on the regional signals. Figure 8 shows the location of the October 30 event relative to station BOSA and several gold-mining areas where historically mine tremors have frequently been associated with on-going mining activity. In each of these mining areas, mine tremors have been reported with magnitudes in excess of 5.0 mb; and events with M_L near 3 occur on a routine basis. The epicentral distance from BOSA to the October 30, 1994 event and the Orange Free State mining area is approximately 160 km, while the distances from BOSA to the other mining areas are 240 km to Klerksdorp, 310 km to Far West Rand, 375 km to Central Rand, and 390 km to East Rand.

Figures 9 and 10 show the sz and bz recordings at BOSA from ten recent presumed mine tremors in four of the five mining districts identified above. The
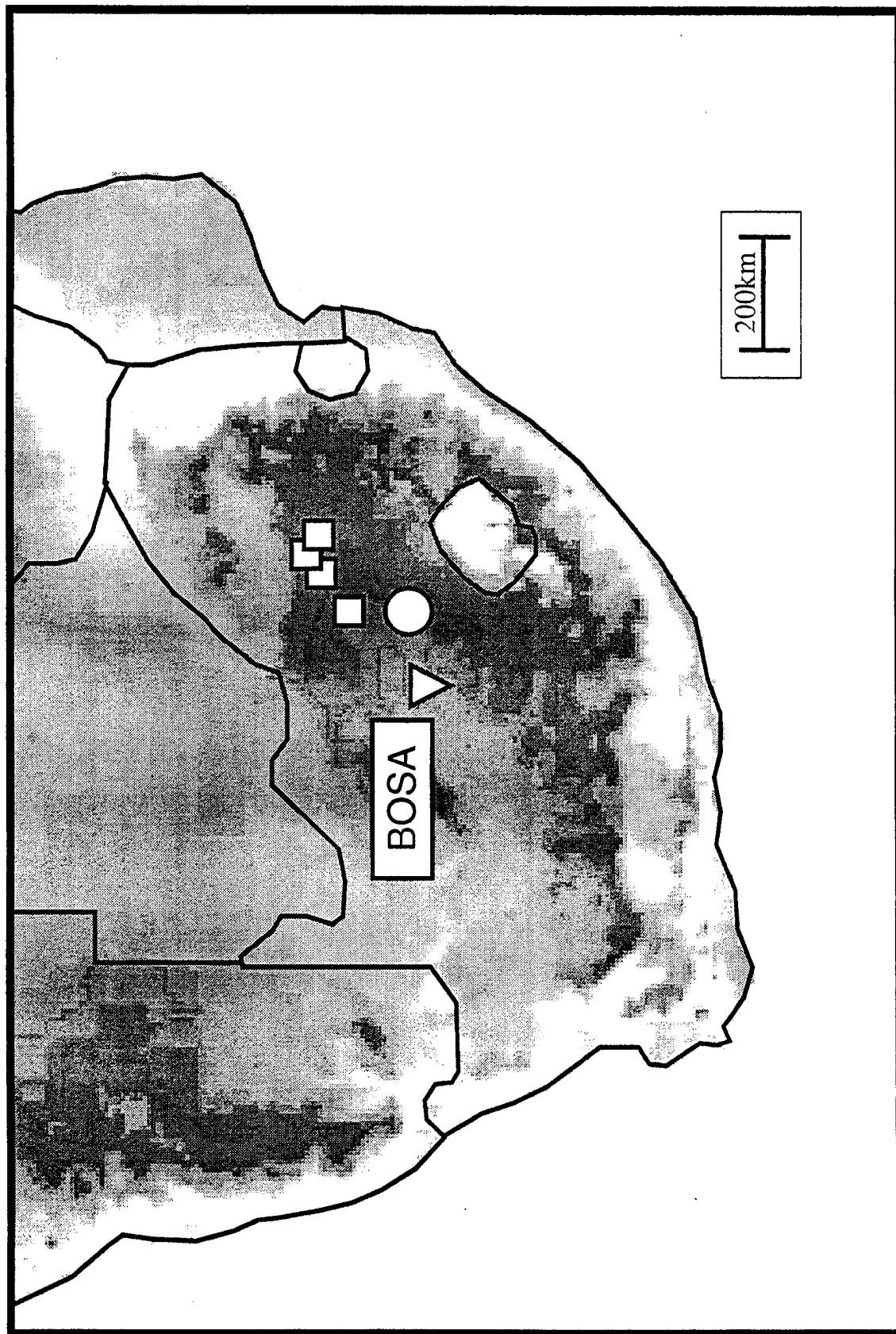
Figure 8. Locations of Orange Free State mine tremor of October, 1994 (◯) and adjacent tremor-producing mine areas (☐) relative to the near-regional seismic station at Boshof, South Africa (▽).
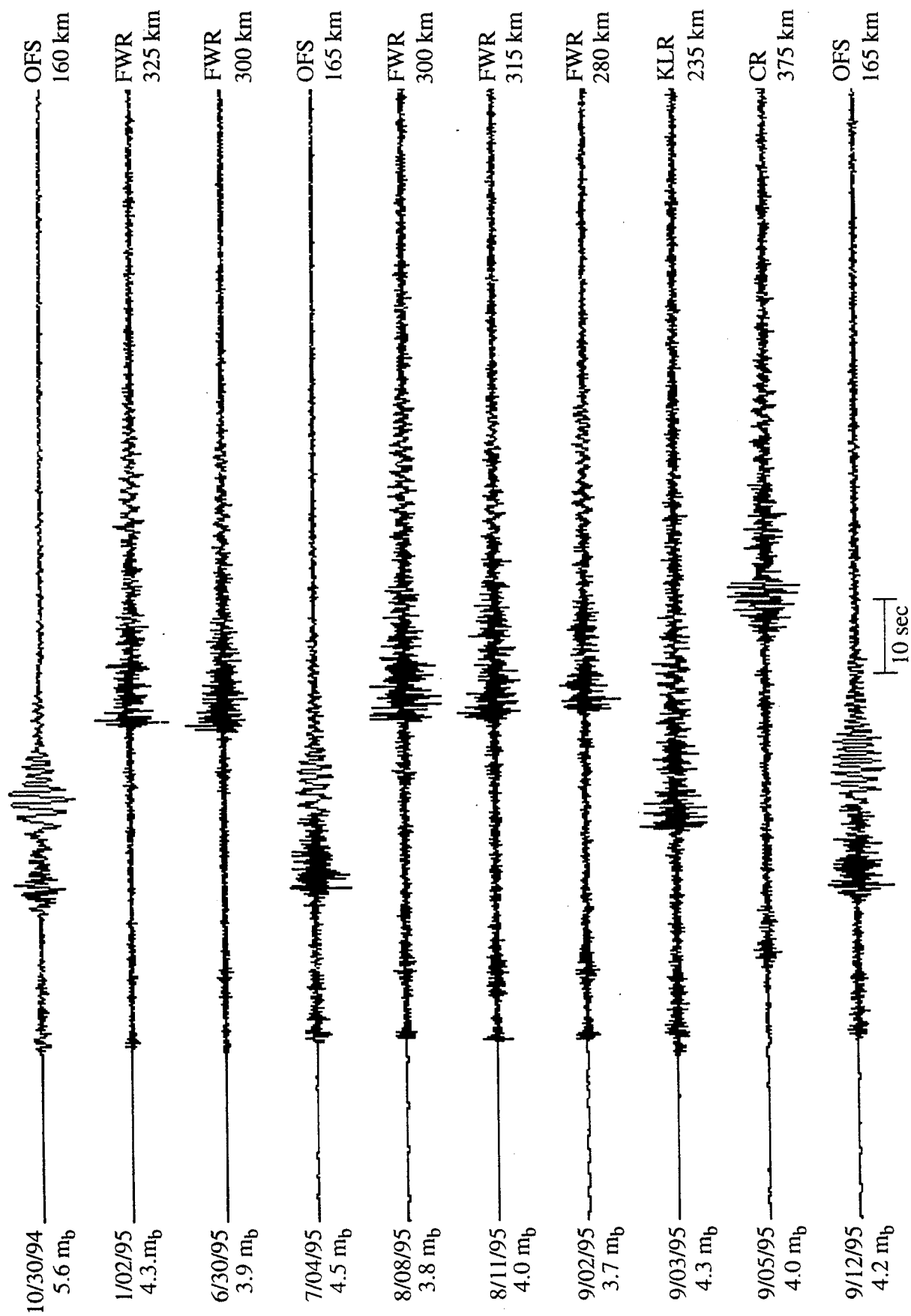
Figure 9. Short-period vertical-component (sz) records at BOSA for 10 South African mine tremors from Orange Free State (OFS), Klerksdorp (KLR), Far West Rand (FWR), and Central Rand (CR) mining districts.
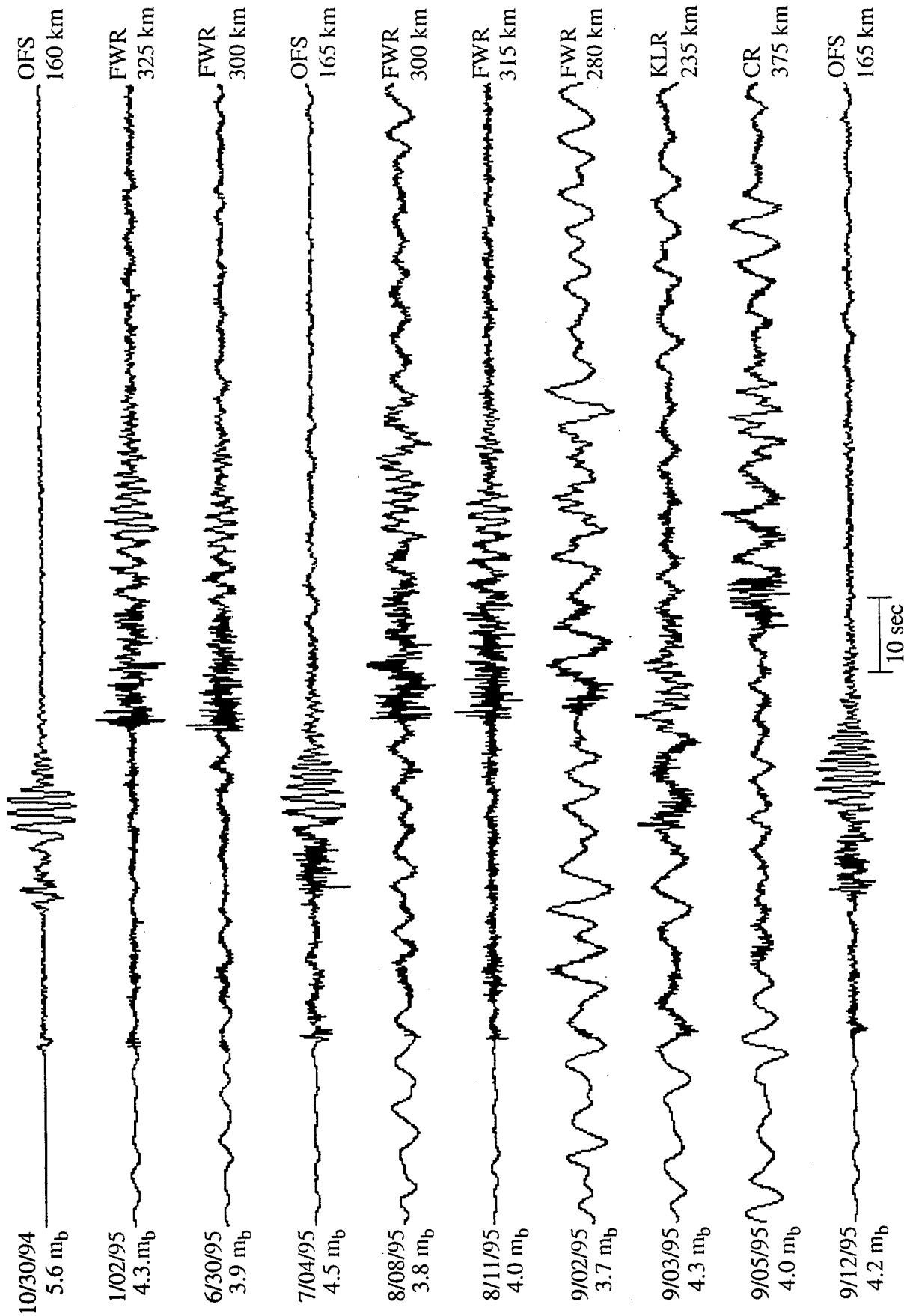
Figure 10. Broad-band vertical-component (bz) records at BOSA for 10 South African mine tremors from Orange Free State (OFS), Klerksdorp (KLR), Far West Rand (FWR), and Central Rand (CR) mining districts.

22

events range in magnitude from 3.65 mb to 5.6 mb and are located at ranges between 160 km and 375 km from BOSA. It should be noted though that, for the smaller and more recent events, the magnitudes and locations have been obtained from the IDC database at CMR, and not the usual NEIC or South African bulletin sources. In general, the signals appear to be quite similar between the sz and bz traces; the higher frequencies are more prominent on the sz and the signals are more easily distinguished against the low-frequency microseisms. Longer periods, including short-period Rg, are more prominent of the bz channel records. On the regional records there is a Pg phase, which is separated from a preceding Pn phase at distances beyond 200 km, followed by a strong Lg, and Rg from nearly all the events.

The record traces for the October 30, 1994 Orange Free State event are seen at the top of the record suite in Figures 9 and 10. The regional phases for this event appear to have low frequencies enhanced relative to high frequencies, possibly indicating a lower corner frequency for this larger magnitude event. An Rg phase with a dominant period of 1.0 - 1.5 seconds is the most prominent phase on the record for the October 30, 1994 event. This phase is usually attributed to excitation of short-period fundamental-mode Rayleigh waves in the shallow crustal waveguide and is, therefore, associated with shallow focus events (cf. Kafka, 1990). Deeper sources normally do not excite Rg or produce only weak Rg. This evidence would seem to be contrary to the 9 - 12 km focal depth attributed to this event by Fan and Wallace (1995). The region surrounding the gold-mining area of South Africa includes a sedimentary layer with an average thickness estimated at about 3 km (cf. Gane et al., 1956; Shapira, 1988; Fan and Wallace, 1995). Considering the mechanism for excitation of Rg, it seems unlikely that the October 30, 1994 Orange Free State event could have a depth much deeper than this 3 km; but we will take a closer look at this issue in our future work on this project with future theoretical modeling studies of regional phase signals from specific rockburst mechanisms. The finding by Shapira (1985) that South African mine tremors typically do excite strong Rg signals appears to corroborate the conclusion that the October 30, 1994 event is more likely to be mining induced than tectonic in origin. This is not to say that the event mechanism may not have a fault origin or that the event cannot be influenced by the ambient regional tectonic stress conditions. We will return to this topic below in discussing South African mine tremor mechanisms.

The records in Figures 9 and 10 which provide the most direct comparisons to the October 30, 1994 event with respect to source location and propagation path are from two other events in the Orange Free State mining area: the July 4, 1995 event (4.5 m_b, IDC) and the September 12, 1995 event (4.2 m_b, IDC). For both of these events the high frequencies appear to be more strongly excited relative to low frequencies in the regional P, P coda, and L_g windows; and the R_g phase appears somewhat less prominent. Nevertheless, the records from these two events appear to be remarkably similar to those from the October 30, 1994 event; and this consistency suggests that the events have similar mechanisms and source attributions. The strong R_g phase is again thought to be indicative of a shallow source, probably within the upper few kilometers of the crust. The events from the Klerksdorp and Far West Rand mining areas (viz. September 3, 1995, January 2, 1995, June 30, 1995, August 8, 1995, August 11, 1995, and September 2, 1995) all show a strong Lg phase with a sharp onset. P_n is fairly strong and simple, preceding a longer duration P_g phase by 3 to 6 seconds. The R_g phase is also well-developed as a dispersed signal, again indicating the shallow focus of these events and continuity of the shallow crustal waveguide out to these ranges. Finally, the September 5, 1995 event from the Central Rand district seems to show a somewhat more emergent L_g signal and has a relatively weak P_n arriving well in front of a rather strong P_g, as is appropriate for the greater epicentral distance. This event also has indications of a weaker R_g.

The L_g/P ratios for all the events in Figures 9 and 10 are large. The ratios are at least 2:1 and as great as 5:1 on both the sz and bz records. These large L_g/P ratios are typical of what we have seen in the past from rockbursts and earthquakes (cf. Bennett et al., 1994). For comparison purposes Figure 11 shows L_g versus P for presumed earthquakes and presumed mine tremors in South Africa, which we measured in a previous study (cf. Bennett et al., 1993). We concluded there that the L_g/P ratios at the near-regional DWWSSN station SLR tended to be well above one and intermingled for the earthquakes and mine tremors. Our current observations appear to fall into this same range for the L_g/P ratios.

3.3 Band-Pass Filter Analysis

To provide additional insight into the character of the near-regional signals from the South African mine tremors, we performed narrow band-pass

Figure 11. Comparison of the maximum P versus maximum Lg amplitudes measured from
time-domain records at DWWSSN station SLR from 31 mine tremors and 10 southern Africa
earthquakes (after Bennett et al., 1993).
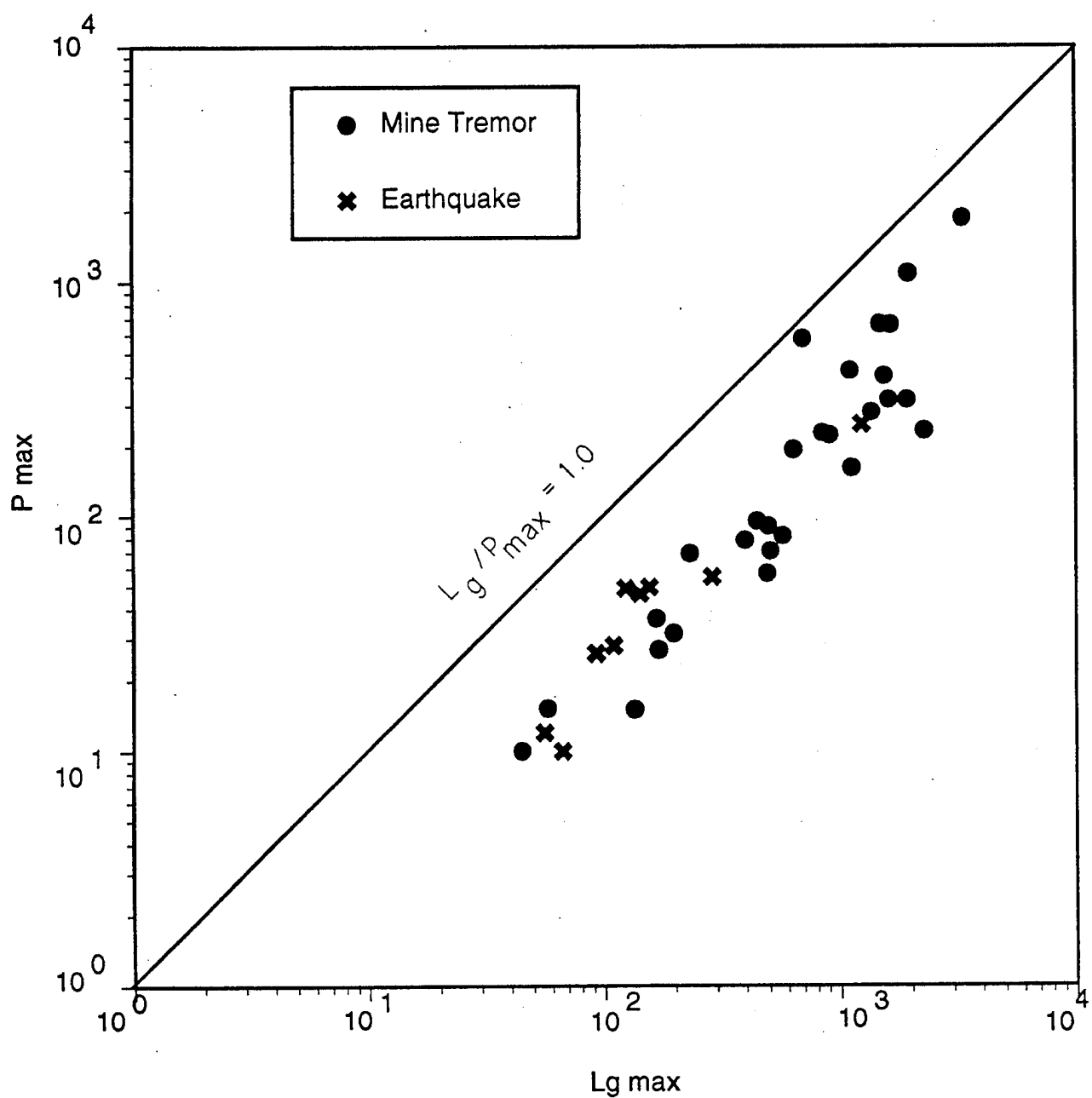
filter analysis of the broadband, vertical-component records at station BOSA for several events. The band-pass filter analysis used here was exactly the same as that applied to the western U.S. events, as described above in Section 2.3. Figure 12 shows the results of the band-pass filter analysis applied to the October 30, 1994 event. Although the original, unfiltered records shows little evidence of the high frequencies in the signals, the filtered traces show the presence of the high frequencies in the regional P and Lg signals in filter passbands between about 1 Hz and 10 Hz. In each of these bands, the Lg/P ratio is seen to be well above one with ratios ranging from about 2:1 to near 5:1. In the lower frequency passbands between about 0.5 and 3 Hz, the Rg signal is strong and shows a normal dispersion pattern. One interesting feature seen in the lowest frequency passband (viz. 0.05 - 0.1 Hz) is the long-period surface wave signal. This signal appears to have a dominant period in the 12 - 15 second range and seems to correspond to a fundamental-mode Rayleigh wave. Considering that rockbursts frequently produce surface-wave magnitudes, M_S, which are low relative to m_b, the relative amplitude of this signal might prove to be useful in identifying the source. We discuss this observation more fully in the following section of this report.

The same band-pass filter analysis has been applied to the broadband records for two other South African events from Figure 10. Figure 13 shows the results from analysis of the July 4, 1995 Orange Free State event. Although we see some differences in individual passbands, the overall behavior is very much the same as that seen in Figure 12 for the October 30, 1994 event. In particular, over the high-frequency bands (viz. between 1 Hz and 10 Hz) we see the strong Lg and regional P signals, with Lg/P ratios from about 2:1 to 3:1. Rg is prominent in the band from about 0.5 Hz to 3 Hz and shows roughly the same dispersion as seen in Figure 12. The fundamental -mode Rayleigh wave is not apparent in the low-frequency passband (viz. 0.05 - 0.1 Hz) and is apparently at or below the noise level caused by the long-period microseisms.

To provide some insight into sensitivity to source area, we performed the same band-pass filter analysis on the January 2, 1995 event from the Far West Rand mining area. The result is shown in Figure 14. The epicentral distance here is nearly twice as great, so that the regional signals appear more separated and of longer duration. In the high-frequency passbands, we see the same behavior in the Lg/P ratios as observed for the nearer events; the Lg/P ratios are between about 2:1 and 10:1, with the maximum ratio observed in the
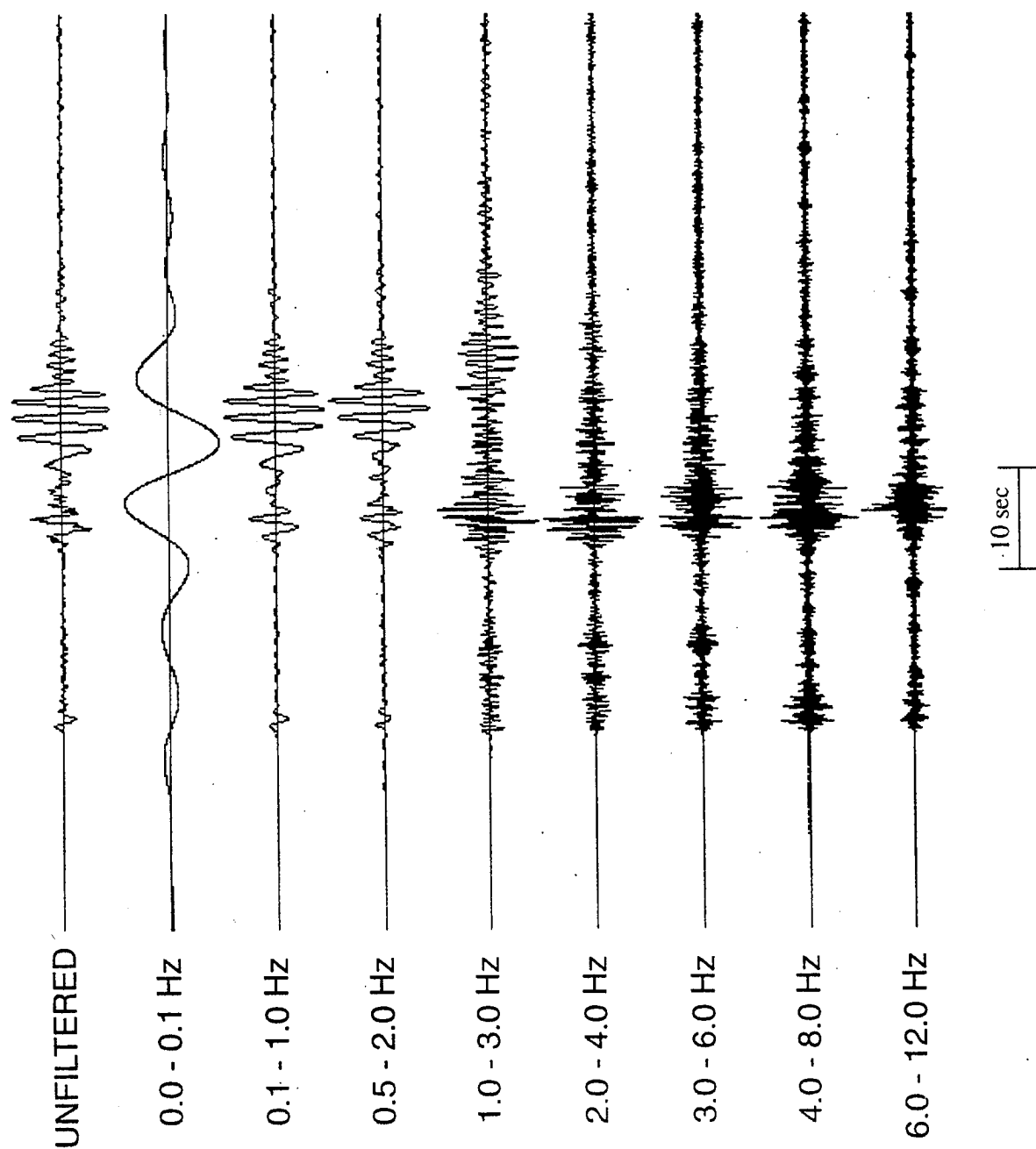
Figure 12. Bandpass filter analysis of large South African rockburst of October 30, 1994 recorded at station BOSA (R = 155 km).

UNFILTERED

0.0 - 0.1 Hz

0.1 - 1.0 Hz

0.5 - 2.0 Hz

1.0 - 3.0 Hz

2.0 - 4.0 Hz

3.0 - 6.0 Hz

4.0 - 8.0 Hz

6.0 - 12.0 Hz

10 sec

UNFILTERED

0.0 - 0.1 Hz

0.1 - 1.0 Hz

0.5 - 2.0 Hz

1.0 - 3.0 Hz

2.0 - 4.0 Hz

3.0 - 6.0 Hz

4.0 - 8.0 Hz

6.0 - 12.0 Hz

10 sec
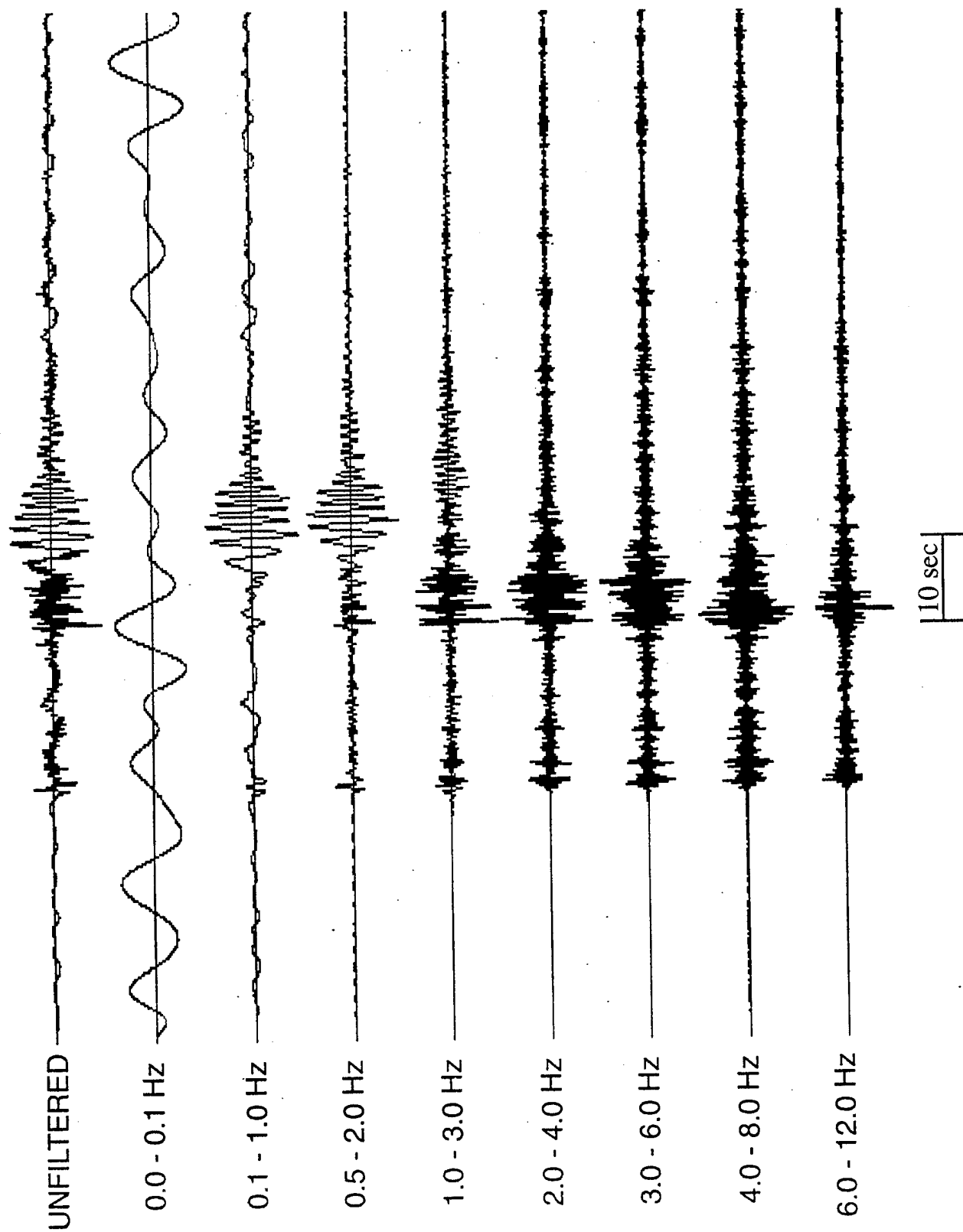
Figure 13. Bandpass filter analysis of South African rockburst of July 4, 1995 (4.5 mb) recorded at station BOSA (R = 165 km).

UNFILTERED

0.0 - 0.1 Hz

0.1 - 1.0 Hz

0.5 - 2.0 Hz

1.0 - 3.0 Hz

2.0 - 4.0 Hz

3.0 - 6.0 Hz

4.0 - 8.0 Hz

6.0 - 12.0 Hz

10 sec
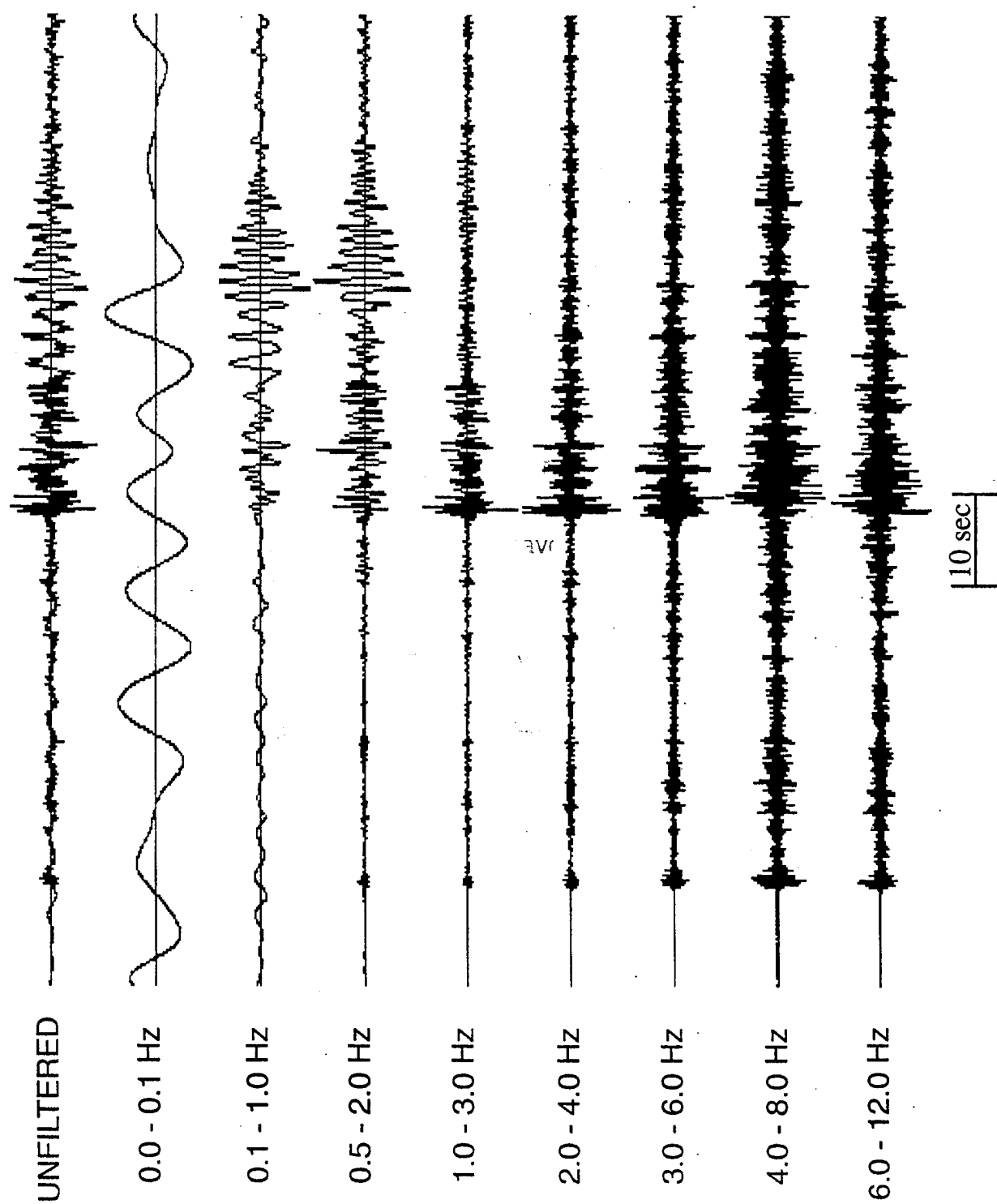
Figure 14. Bandpass filter analysis of South African rockburst of January 2, 1995 (4.3 mb) recorded at station BOSA (R = 325 km).

1 - 3 Hz band. The R$_g$ phase is well dispersed in bands from 0.5 to 3 Hz. In the lowest frequency passband, we see possible evidence of a long-period Rayleigh wave with a dominant period of 12 - 15 seconds, but the signal level appears to be only slightly greater than the long-period microseisms. In general, then, we seem to see very similar behavior in the most prominent regional signals from presumed mine tremors in the different South African source areas, which suggests that the observations could be characteristic of the source.

3.4 Surface Waves from South African Mine Tremors

Evidence from several rockbursts and related mining-induced events around the world, which we have described in some of our previous reports (cf. Bennett et al., 1993; 1994), seems to suggest that the surface-wave magnitudes, M$_S$, tend to be low relative to mb for this event type. Unfortunately, the amount of data supporting this observation is very limited. The principal limitation is that the majority of these mining-induced events are small and, therefore, are not well recorded at teleseismic stations which traditionally provide estimates of M$_S$ magnitudes. The recording problem is, of course, exacerbated because this event type seems to be a poor generator of the long-period surface waves, used to determine M$_S$; so that even rockburst events with relatively large mb may not produce the Rayleigh waves needed to determine M$_S$ at a network of teleseismic stations. Therefore, a rare event like the large October 30, 1994 Orange Free State mine tremor, which produced a teleseismic M$_S$ measurement, provides a valuable data point for the relationship between M$_S$ and m$_b$ for these and similar events. The M$_S$ for the October 30, 1995 mine tremor was reported by NEIS as 4.7, which is almost one magnitude unit lower than the reported body-wave magnitude, 5.6 m$_b$. In Figure 15 we compare the M$_S$-versus-m$_b$ measurements for a sample of mining-induced events obtained from a careful search of the worldwide database. For comparison we show observations from two South African earthquakes away from the gold-mining region and a large European earthquake. The plot also includes several of the large recent rockburst events referred to elsewhere in this report (viz. the February 3, 1995 Wyoming mine collapse, the March 13, 1989 German mine collapse, and the January 5, 1995 Urals event).
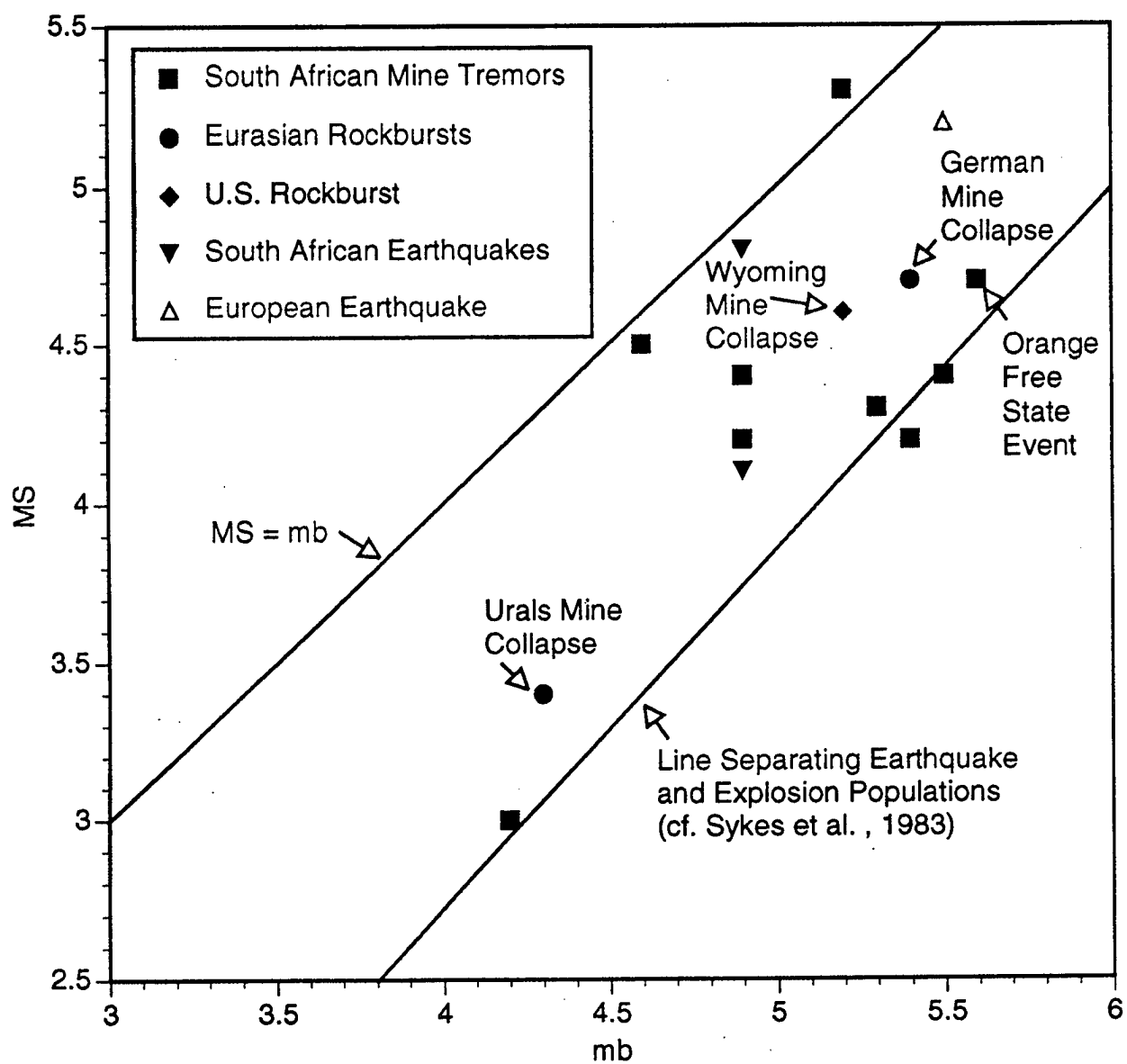
Figure 15. Comparison of MS versus mb for large rockbursts in four source regions with similar observations for earthquakes in the same regions.

In originally defining the earthquake magnitude scales, the scale parameters were set so that m_b would be on average equal to M_S for large worldwide earthquakes (cf. Gutenberg and Richter, 1956; Richter, 1957; Båth, 1979). However, it was later found (cf. Richter, 1957) that, below magnitude 7, M_S tended to be lower than m_b; while, above magnitude 7, M_S tended to be larger than m_b. Investigations of the teleseismic M_S-versus-m_b discriminant (cf. Marshall and Basham, 1972; Sykes et al., 1983) indicate that, in the magnitude range 4 to 6 m_b, earthquake M_S values tend to be about a half magnitude unit low relative to m_b. However, there is considerable scatter about the mean line, and M_S - m_b differences range from -1 to +1 for earthquakes with many of the low-M_S events at lower magnitudes. We have also superimposed on the plot in Figure 15 a line identified from the work of Sykes et al. (1983) as separating the earthquake and explosion populations with respect to M_S versus m_b (cf. Office of Technology Assessment, 1988). Several of the mining-induced events shown have M_S values which are from 0.5 to 1 magnitude unit lower than mb and would be in the lower part of the earthquake range, or even into the explosion population. This is somewhat unusual considering that the events are shallow and suggests that the rockburst mechanism may not be an efficient generator of long-period Rayleigh waves.

In two previous reports on the surface waves from South African mine tremors (cf. Bennett et al., 1993, 1994), we reached a similar conclusion from the long-period Rayleigh-wave signals recorded at the African station, BCAO, at a distance of about 32° from 18 events with mb magnitudes in the range 4.2 to 5.2. There we used the Prague formula (cf. Båth, 1979) to compute M_S from the output of a band-pass filter centered at a period near 20 seconds. Nearly 90 percent of those events would fall into the explosion population based on the decision line described above, derived from the results of Sykes et al. (1983).

In Figure 12 above we saw that the narrow band-pass filtering of the October 30, 1994 South African mine tremor recorded at station BOSA showed a clear long-period Rayleigh wave in the lowest frequency band (viz. 0.05 - 0.1 Hz). To estimate the long-period Rayleigh wave excitation, we passed the broad-band vertical-component records at BOSA from all ten of the mine tremors in Figures 9 and 10 through the same low-frequency band-pass filter. However, we found only a few cases where the Rayleigh wave signals were visible above the long-period background microseism noise. In cases where the Rayleigh wave wasn't apparent, we determined the microseismic noise

level in this passband and used that amplitude as an upper-bound limit of the long-period Rayleigh-wave excitation. We tied the Rayleigh-wave amplitudes for the South African mine tremors to M_S using the knowledge that the October 30, 1994 event had a M_S of 4.7. We then took the logarithm of the ratio of the measured amplitude for the selected event to the amplitude measured for the October 30, 1994 mine tremor and applied that as an adjustment to the 4.7 M_S; a second adjustment was made to the M_S estimate for attenuation from the events at the more distant mines.

Figure 16 compares these M_S estimates at station BOSA for the South African mine tremors with the reported m_b's. It should be noted that only two of the events plotted here had m_b's reported by NEIS; for the remainder we used the m_b values determined by the IDC at CMR, which could be subject to revision. With this caveat we can note that the M_S estimates for all ten mine tremors fall well below the corresponding m_b values. In many cases (about 80 percent) the difference is more than one magnitude unit. It should also be noted that in most cases the M_S values are upper-bound estimates, so that actual M_S values for these events are likely to be lower than shown here. It is not entirely unexpected that M_S should be low for these small events. Gutenberg and Richter (cf. Richter, 1957) found that earthquakes with $m_b < 7$ tended to have M_S values below m_b with greater differences for smaller events. As a reference in Figure 15, we have again plotted the line separating the earthquake and explosion populations with respect to M_S versus m_b, as determined from the work of Sykes et al. (1983). It appears from this that these mine tremors are tending to produce relatively low M_S values; the M_S values are often near the bottom of the earthquake population and in some cases fall below the line into the region normally associated with explosions. This situation could lead to false alarms and should be investigated further for a wider range of events in this and other source areas.

3.5 South African Mine Tremor Mechanisms

The mechanisms of South African mine tremors have been investigated for many years. Unlike the collapse models described above, which seem to best represent the mechanism of the February 3, 1995 Wyoming event and the March 13, 1989 eastern Germany event, the mechanisms for South African events have often been associated with faulting in the vicinity of the mine opening. Spottiswoode et al. (1971) and Spottiswoode (1980) found that large
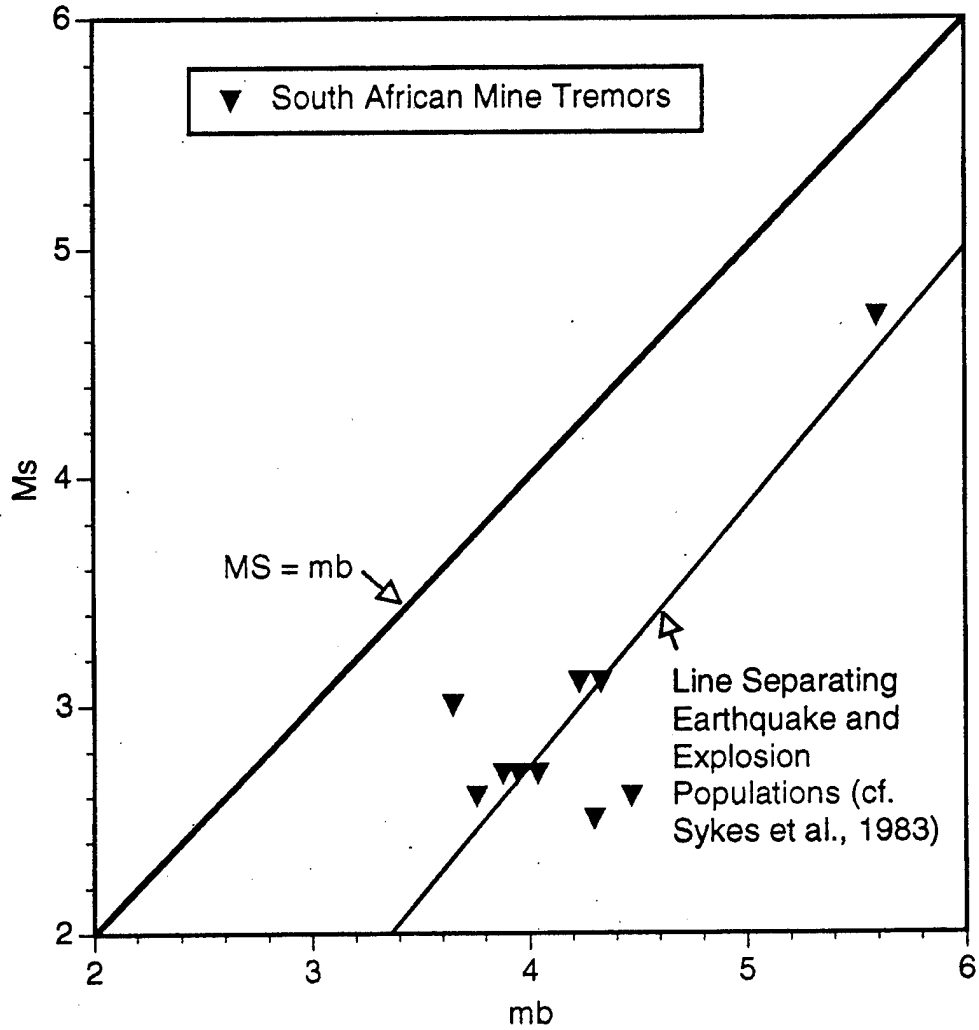
Figure 16. MS versus mb inferred for some recent South African mine tremors based on comparison of long-period amplitude levels observed at station BOSA for the events relative to similar amplitude levels for the October 30, 1994 tremor (4.7 MS). Note that MS values for several smaller events are estimated as upper bounds.

South African mine tremors in the East Rand area typically produced four-lobed radiation patterns for the P-wave first motions, like those in the double-couple mechanisms associated with most earthquakes. Potgieter and Roering (1982) also determined quadrantal distributions of first motion for mine tremors in the Klerksdorp mining district and associated the tremors with shear failure along pre-existing faults or dykes adjacent to the mine. McGarr (1971, 1992) points out that the underground manifestation of South African mine tremors is often a fresh shear zone. However, McGarr (1992) also notes that some mechanisms from this same general source area include strong non-shear, volumetric components. Rorke and Roering (1984) discovered a two-lobe radiation pattern in first motions from some South African mine tremors, which they attribute to sudden failure of rock on one side of a pre-existing discontinuity. Several studies (e.g. Gane, 1952; Joughin, 1966) of South African mine tremors found in some areas a preponderance of dilatational first motions at nearby stations which could be attributed to a strong implosional component, but poor station distribution about the source often made these and similar early observations inconclusive. Nevertheless, it is now generally believed (cf. Joughin and Jager, 1983) that there are at least two types of mine tremor mechanisms active in the gold-mining region of South Africa: one involving volumetric failure of rock in the vicinity of an excavation and the second corresponding to slipping along pre-existing faults or zones of weakness.

Most historical studies associate nearly all the seismicity in the deep-gold-mining area of South Africa with the mining (cf. Fernandez, and Guzman, 1979). There was practically no record of seismicity in the area prior to mining and activity dramatically increased in frequency and event size as mining progressed to greater depths. Even large seismic events, which appear to produce a release of energy greater than the amount of strain energy stored in the surrounding rock as a result of mining, appear to be connected to mining (cf. Gay et al., 1984) as a trigger or through other indirect mechanisms. However, a recent study by Fan and Wallace (1995) suggests that the large seismic event of October 30, 1994 in the Orange Free State region is tectonic in origin and unrelated to mining. Their best-fit focal mechanism obtained from a moment tensor inversion applied to the very broadband signals at two regional stations corresponds to normal faulting with a very steeply dipping pressure axis and a more nearly horizontal tension axis. This mechanism is consistent with that seen in many mine tremors from this same general area and also agrees with

35

in-situ stress results found by Gay (1975). The in-situ stress measurements obtained from the deep mines also indicated nearly vertical pressure and nearly horizontal tension axes in most cases, although in one or two areas stresses appeared to be reoriented by local structure causing both pressure and tension axes to take on horizontal orientations. As noted above, one mine tremor model (cf. Gay et al., 1984) calls for pre-existing faults on zones of weakness which are favorably oriented in the ambient stress field (which could be related to the larger scale regional tectonics) to be triggered because the mining activity perturbs local equilibrium conditions at points along the fault. So, the mechanism for the October 30, 1994 event, as determined by Fan and Wallace (1995), seems reasonable but does not preclude the event from being a mine tremor. The primary reason for concluding that the event is unrelated to mining would appear to be if it can be shown conclusively that the source depth is much below the mining activity. Fan and Wallace estimate the depth at between 9 and 12 km from their inversion, but this does not seem to agree with the strong Rg phase observed from the event. We plan to conduct additional investigations and modeling of the regional signals, including the strong Rg phase, to help resolve this issue.

4. Rockbursts in Other Regions

4.1 Investigations in Other Source Regions

In addition to the large rockbursts described in Sections 2 and 3, we have also been investigating somewhat smaller rockbursts in several other source regions. These include the recurring rockburst activity in Poland, a rare event in the Ural mountains of Russia associated with mining, and a rockburst in the eastern U.S. in Kentucky which has been the source of prior similar events. Because of the nature of rockburst activity in these different areas and specific investigative goals for some events, the research on these events has followed somewhat different paths and some analyses are still in progress.

4.2 European Rockbursts

In several of our previous reports on rockbursts (cf. Bennett et al., 1993, 1994), we have looked at the regional signals from specific events (e.g. the 1989 Völkershausen, Germany mine collapse) or from groups of events in specific source regions (e.g. Polish rockbursts) within central Europe. The rockbursts from Polish coal and copper mines have been under investigation for many years and have been the subject of several excellent prior reports (e.g. Gibowicz, 1984; Gibowicz and Sileny, 1994). The events are concentrated in two main source areas; one in the vicinity of copper mines near Lubin at about 51.5° N 16.1° E and the second associated with coal mining below ground in Upper Silesia near 50.3° N 18.9° E extending northeastward to a surface coal mine at Belchatow near 51.3° N 19.4° E. In each of these areas the rockburst activity has been frequent and occasionally large. Historic rockburst events in the Lubin area have been assigned magnitudes as high as 5.3 m_b by NEIS, and events in the Upper Silesia/Belchatow area have had magnitudes as large as 4.6 m_b. Furthermore, these areas are two of the most active zones of recent seismicity in central Europe; it is not unusual for several events per week to be reported from these areas. The GESETT-1 and GESETT-2 experiments found many events in these areas which were detected and located by the GERESS regional array in Germany, and similar events continue to be reported from these same areas in the ongoing GESETT-3 experiment.

For the past few years, we have been attempting to put together a database of regional recordings from rockbursts in these Polish mining areas. In most cases we do not have "ground truth" but presume that the events are

rockbursts based on their location in proximity to these mines. For the older events we relied primarily on records from the Grafenburg array station, GRFO, which we occasionally supplemented with more-distant regional records for some of the larger events. The distance to GRFO from these source areas is about 400 km for Lubin, 555 km for Upper Silesia, and 610 km for Belchatow. However, it should be noted that the distances for specific events may vary about those specified here because mine locations are spread out and epicenter locations have some uncertainty. For many of the more recent events, we have drawn data primarily from stations in the GERESS regional array. The corresponding distances are 340 km from Lubin, 400 km from Upper Silesia, and 490 km from Belchatow. Our database currently includes 76 rockbursts from the Polish mining areas and selected additional events from other central European sources, including some non-rockburst sources for use in comparison to the regional rockburst signals. The Polish rockbursts in the current database fall in the magnitude range from about 2.8 m_b to 5.3 m_b. We are continuing to add to this database. Figure 17 shows a map of the locations of the events for which we currently have regional data.

Up to this point we have not conducted a systematic analysis of all these Polish rockburst data but have instead performed analyses and comparisons of the regional signals for selected events. In particular, Figure 18 shows a bandpass filter analysis applied to the GRFO record for a Polish rockburst (4.0 m_b) from the Lubin area (R $\approx$ 390 km). The record is dominated by the short-period regional phases, including an initial P_n phase, followed by a somewhat larger P_g, and a strong L_g signal. This record presents approximately the same behavior as we have seen for other rockburst here and in other parts of the world. The S/P or L_g/P ratio is 1.0 or greater in all frequency bands. One interesting feature of the record is the apparent tendency in the L_g window for high frequencies to be clustered near the front of the window, while low-frequencies tend to be more spread out or clustered toward the back of the L_g window. Thus, the L_g signals have an apparent inverse dispersion on these records. The regional records from the Polish rockbursts do not show the prominent R_g phase that we saw in some of the other source areas (e.g. South Africa), but this might be related to propagation path influences (e.g. a disruption in the crustal waveguide).

For the waveform data collected most recently, Figures 19 and 20 show some examples of the vertical-component records at the GERESS regional
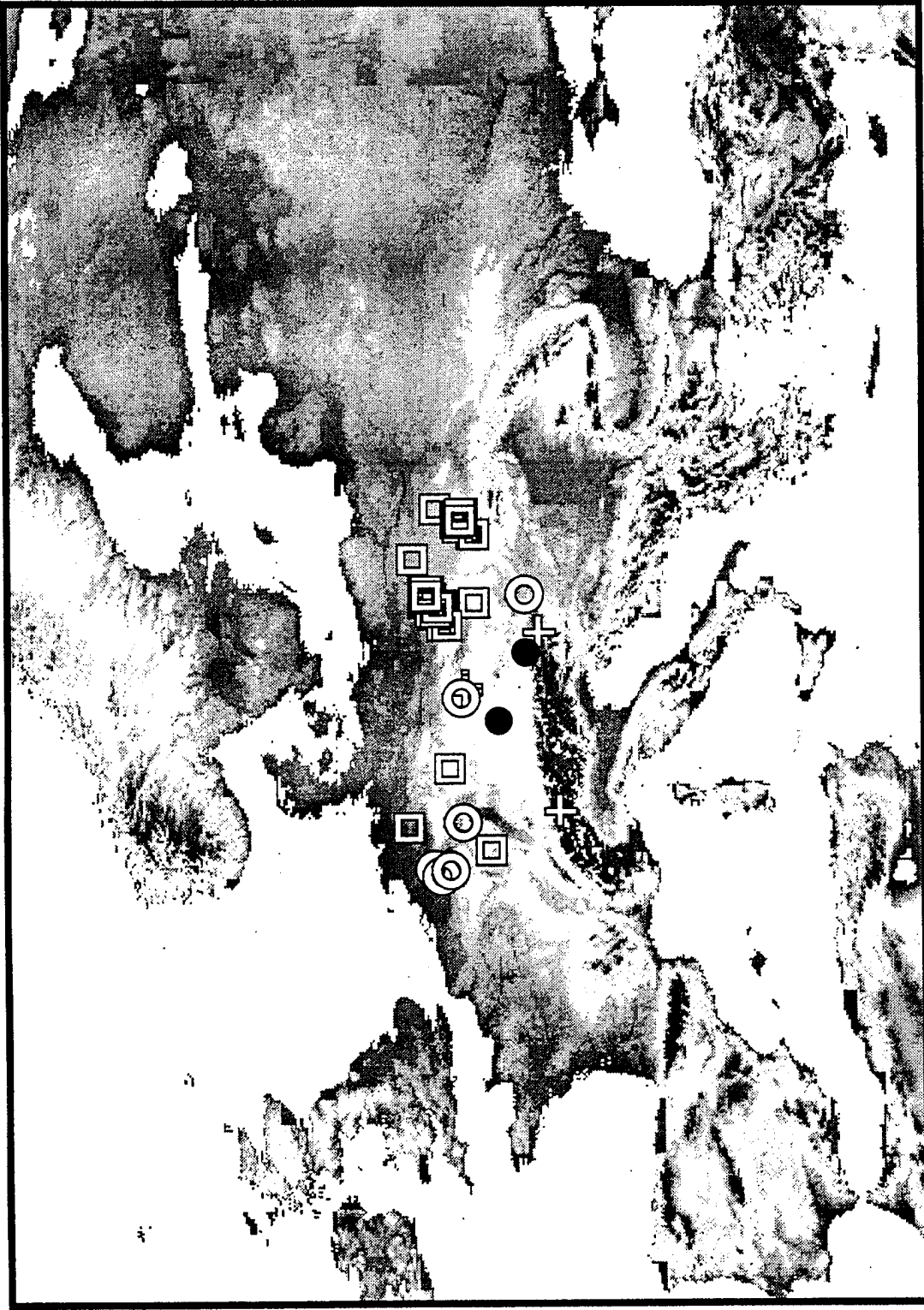
Figure 17. Locations of rockbursts (▣) in central Europe and selected other source types (earthquakes- ⊙, blasts- ✛) used in comparisons and seismic stations (●) GRFO (farther west) and GERESS (farther east).
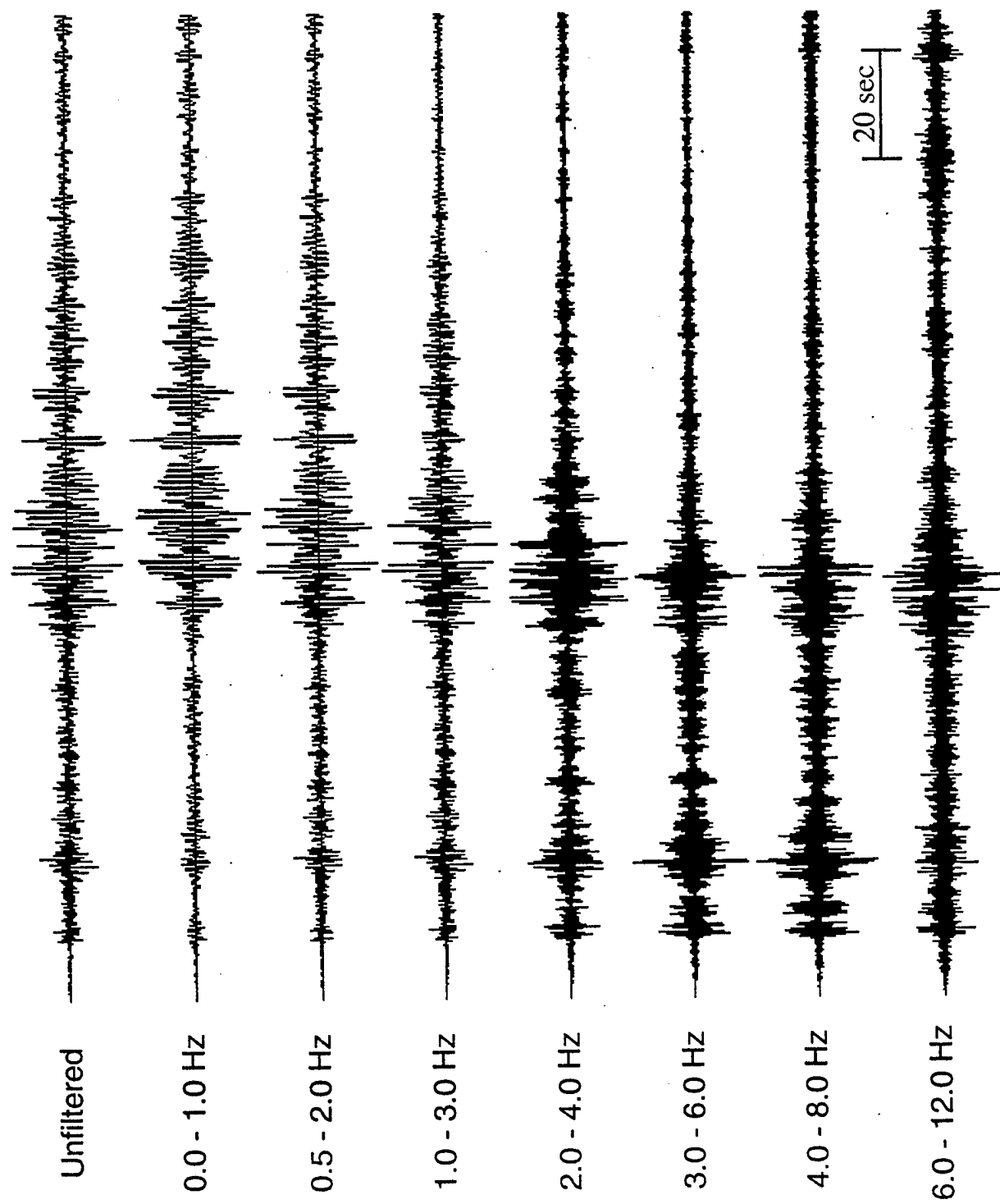
Figure 18. Bandpass filter analysis of the Polish rockburst of August 15, 1981 recorded at station GRFO (R =390 km).

Unfiltered

0.0 - 1.0 Hz

0.5 - 2.0 Hz

1.0 - 3.0 Hz

2.0 - 4.0 Hz

3.0 - 6.0 Hz

4.0 - 8.0 Hz

6.0 - 12.0 Hz

20 sec

40
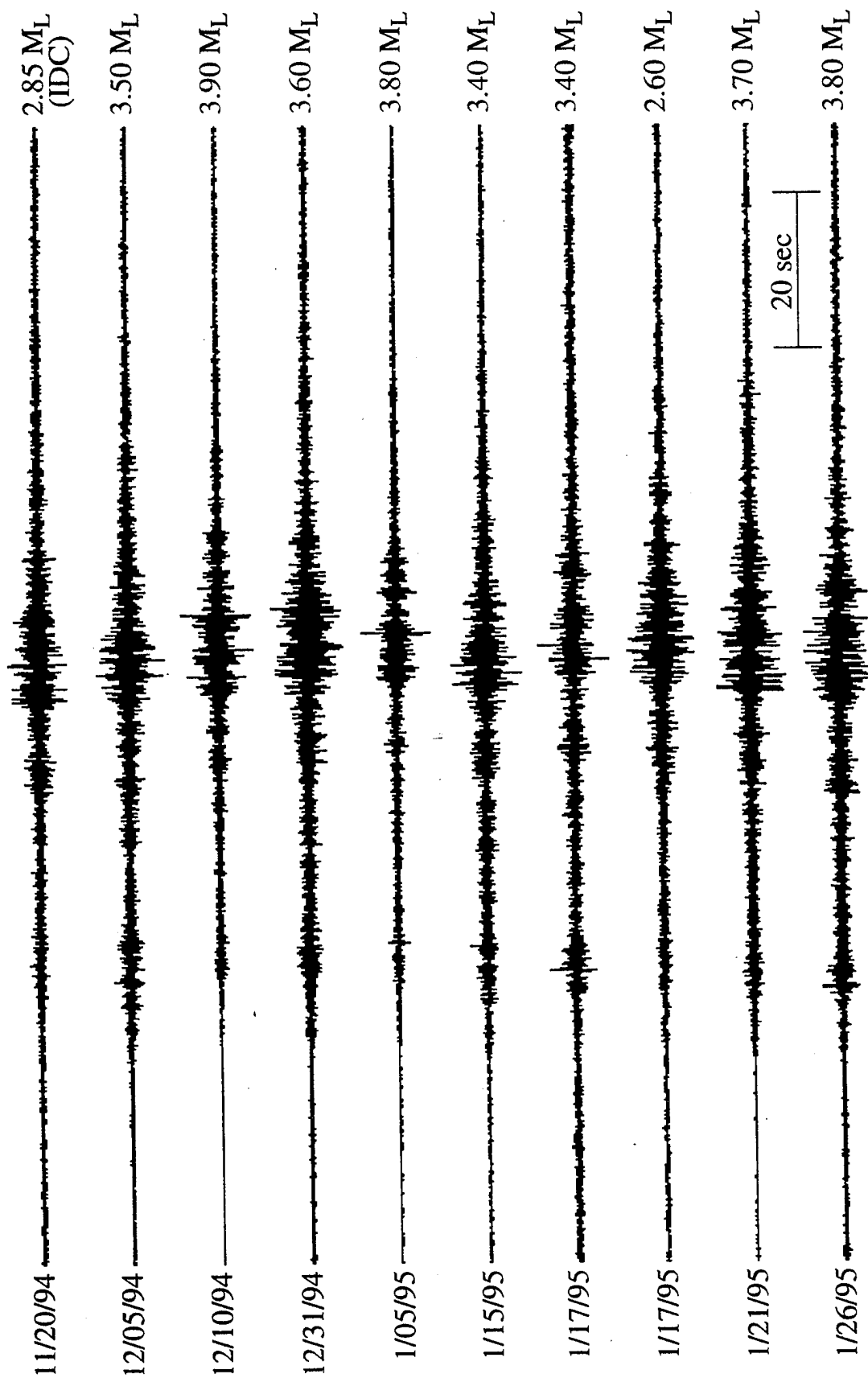
Figure 19. Short-period vertical-component (sz) records at GERESS for 10 Polish rockbursts from the vicinity of the Lubin mining area (290km $\leq$ R $\leq$ 365km).

41
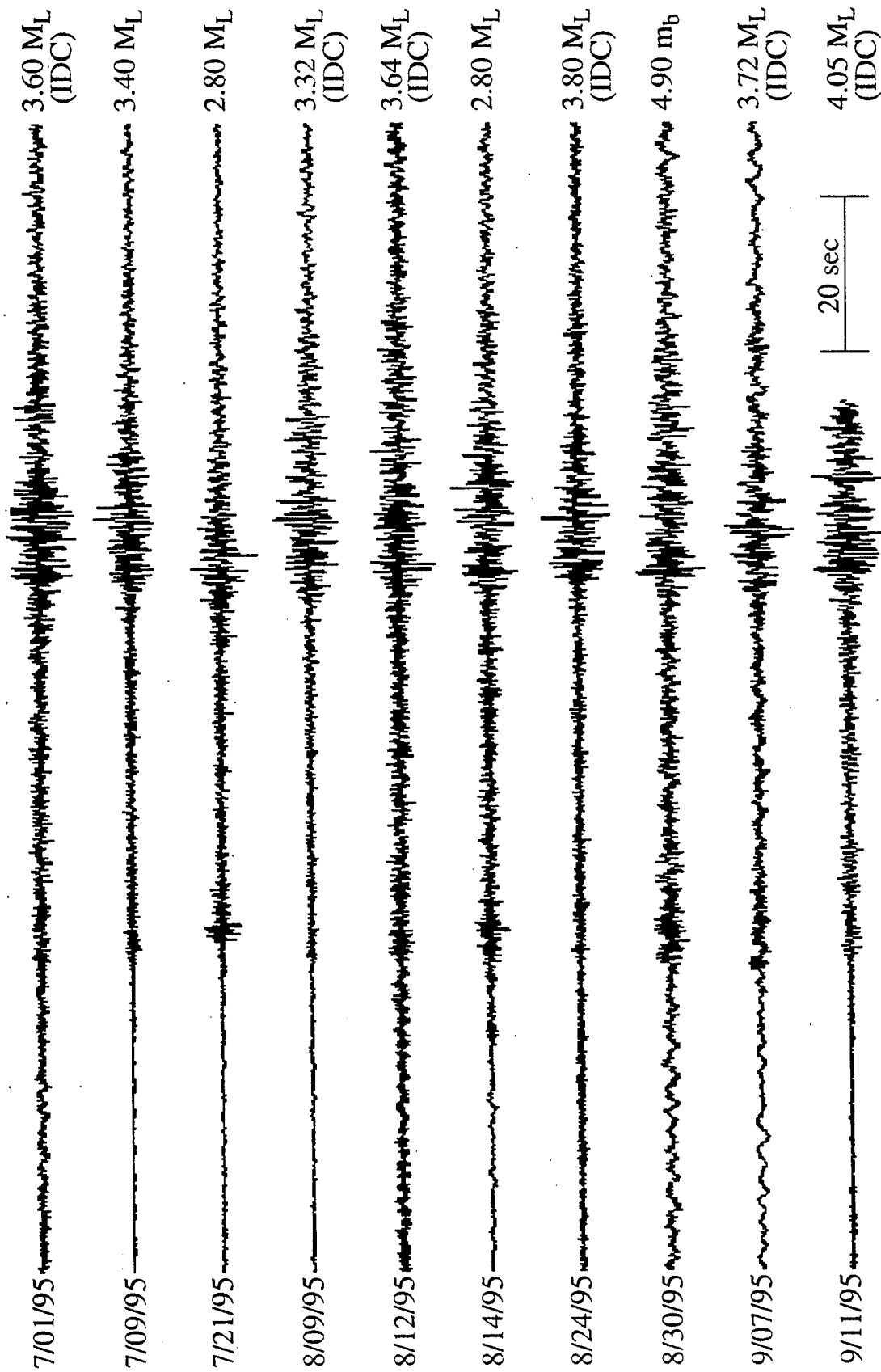
Figure 20. Short-period vertical-component (sz) records at GERESS for 10 Polish rockbursts from the vicinity of the Upper Silesia/Belchatow mining area (360km $\leq$ R $\leq$ 435km).

array station for 10 rockbursts from the Lubin source zone (R ≈ 340 km) and 10 rockbursts from the Upper Silesia/Belchatow source zone (R ≈ 400 km) respectively. It should be noted that the epicentral distances associated with specific events are not always accurate due to location uncertainty; similarity in relative times and characteristics of regional phases, as seen by comparison with other records, may often be indicative of proximity between event sources. For the Lubin source zone (cf. Figure 19), the rockbursts shown have magnitudes between about 2.6 and 3.9 M_L, as reported by NEIS. These records all appear to be generally similar to what we saw above in Figure 18, prior to filtering. In almost all cases there is evidence of a P_n phase, followed by a stronger P_g, and a stronger still L_g. On these sz components the L_g/P ratios are generally in the range from 3:1 to 4:1. On several records there is also evidence of an S-wave train preceding the strong L_g phase. For the Upper Silesia/Belchatow source zone (cf. Figure 20), the rockbursts shown have local magnitudes between about 2.8 and 3.4 M_L (NEIS); it should be noted that for many of the more recent events we have only the M_L magnitudes reported by IDC. The records for these events are more spread out in time and have generally lower signal-to-noise ratios because of the greater distance and somewhat smaller magnitudes. The P_n phases are barely visible above the background noise, but the subsequent P_g phases usually stand out. The later L_g phases are the most prominent signals on the records, and the resulting L_g/P ratios are generally in the range 2:1 to 4:1. There is no apparent regional S phase prior to L_g, as it is lost in the noise and P coda. The large L_g/P ratios, which we see here for Polish rockbursts, appear to be consistent with rockburst behavior that we have seen for other source areas. As our work continues, we will systematically analyze the signals from all these events to identify and quantitatively assess consistent behavior.

With regard to source mechanisms, Polish rockbursts most often appear to have double-couple, shear mechanisms, similar to those described above for South African mine tremors. Gibowicz (1984) shows a fault-plane solution, based on P-wave first motions, for a rockburst in the Lubin area as having a nearly vertical pressure axis and a nearly horizontal tension axis, which would correspond most closely to a normal fault. In the same study he finds for coal mines in Upper Silesia one rockburst mechanism which is normal, dip-slip and another which is strike-slip with a reverse component; so there appears to be some variability within a given source zone, possibly dependent on the

43

geologic conditions or mining practice. In the Belchatow source area to the north, Gibowicz (1984) reports ambiguous fault-plane solutions which could be strike-slip or reverse. The latter would appear to correspond quite nicely with the interpretation of the rockburst as post-excavation rebound at the surface mine. To the south of Upper Silesia in the coal-mining region of the former Czechoslovakia, Sileny (1989) finds in one area rockburst mechanisms are dominated by shear (although there is often a smaller implosional component) with normal faulting, which may be related to triggered fault movement in response to larger scale tectonic stresses. However, in another nearby mining area, Sileny finds stronger implosional components to the events and less evidence of a tie to the regional tectonics. At mines elsewhere in Europe, Gibowicz (1990) suggests a connection between tectonics and rockbursts in the Ruhr mining district of Germany, where horizontal stresses are significantly larger than lithostatic stress at mining depths. In such cases rockbursts apparently result from the interaction between the tectonic stresses, lithostatic stress, and local stresses introduced by the mining operation. Similar to behavior reported in some Polish mines by Orsepowski and Bachowski (1992), Gibowicz et al. (1990) report rather strong variations in stress drop between mining-induced events in the Ruhr; and they suggest that this could have implications with regard to the relative amplitude and frequency content of the P-wave and S-wave signals which are generated by such events. This clearly has some relevance with regard to the L_g/P regional discriminant which we have been discussing. We are attempting to investigate the significance of these kinds of mechanism effects with our model studies of regional phases from rockburst sources.

4.3 North American Rockbursts

Aside from our analysis of the 1995 Wyoming mine collapse and identification of specific mining areas in the U.S. and Canada which have experienced rockbursts, our investigation of mining-induced seismicity in North America has been very limited. Rockbursts do occur in mining regions throughout much of North America. In the eastern U.S. many of the rockbursts occur in association with coal mining in the form of "mine bumps." The history of such bumps dates back to the 1920's; over that period some of the heaviest concentrations of coal mine bumps, as documented by the U.S. Bureau of Mines (cf. Iannacchione and Zelanko, 1995), has been in the states of West

Virginia, Virginia, and Kentucky with 53, 40, and 19 events respectively. It should be noted that this event count may not be complete because it was developed mainly from accident reports by the various mines, and reporting procedures may have been uneven particularly for smaller, non-injurious or older events. Even today there are no systematic requirements for seismic monitoring in such mines or for reporting results from proprietary monitoring efforts. Iannacchione and Zelanko (1995) report local seismic magnitudes for selected mine bumps for the 30-year period between 1965 and 1994. The largest reported magnitudes for the three eastern states noted above were 3.4 M_L for West Virginia, 4.5 M_L for Virginia, and 3.8 M_L for Kentucky. Some larger coal bumps may have occurred prior to this time period, but it nevertheless appears that large-magnitude events of this type are relatively rare in eastern North America.

One such coal bump occurred in eastern Kentucky on March 11, 1995 and had a body-wave magnitude of 3.6 m_b. The event apparently occurred as one in a series of bumps in the Lynch mine, which has been the site of similar activity in the past. The same mine experienced bumps on August 3, 1994 and October 5, 1994, both with magnitudes greater than 3; and other mine bumps have occurred there and at other nearby coal mines in the past. The March 11 mine bump was well-recorded at regional stations primarily in the southeastern U.S. at ranges from 230 km to 640 km. Figure 21 shows the location of the mine bump and regional seismic stations which provided records with good signal-to-noise levels.

Figure 22 shows a bandpass filter analysis applied to the vertical-component record at the Blacksburg, Virginia station, BLA (R ≈ 230 km). At this distance range P_n and P_g phases would be expected to arrive nearly simultaneously and do not appear to be distinct phases on the records. The regional P phase appears fairly complex and increases in relative prominence and duration in the higher-frequency passbands. In most bands the L_g/P ratio is large, ranging from near 5:1 at frequencies between 1 Hz and 3 Hz to just greater than 1:1 for the high-frequency bands. The long-period surface wave is difficult to discern in the lowest-frequency passband, but there is the slight hint of an R_g signal in the 0.1 to 1 Hz band. We will be analyzing regional records from this and other eastern U.S. mine bumps in greater detail to identify any peculiarities associated with this type of rockburst mechanism.

45
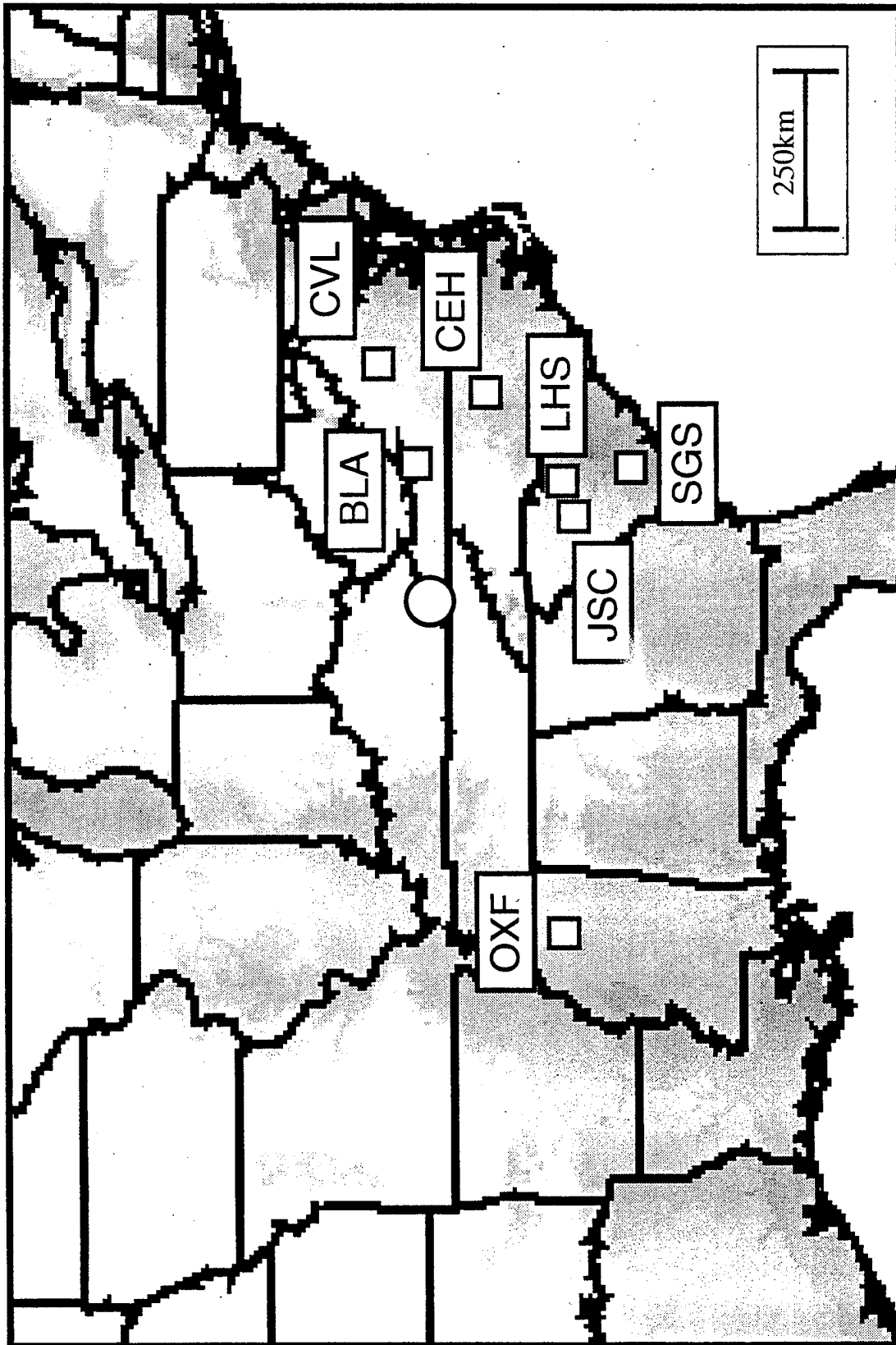
Figure 21. Selected regional seismic stations which recorded the eastern Kentucky mine bump of March 11, 1995.
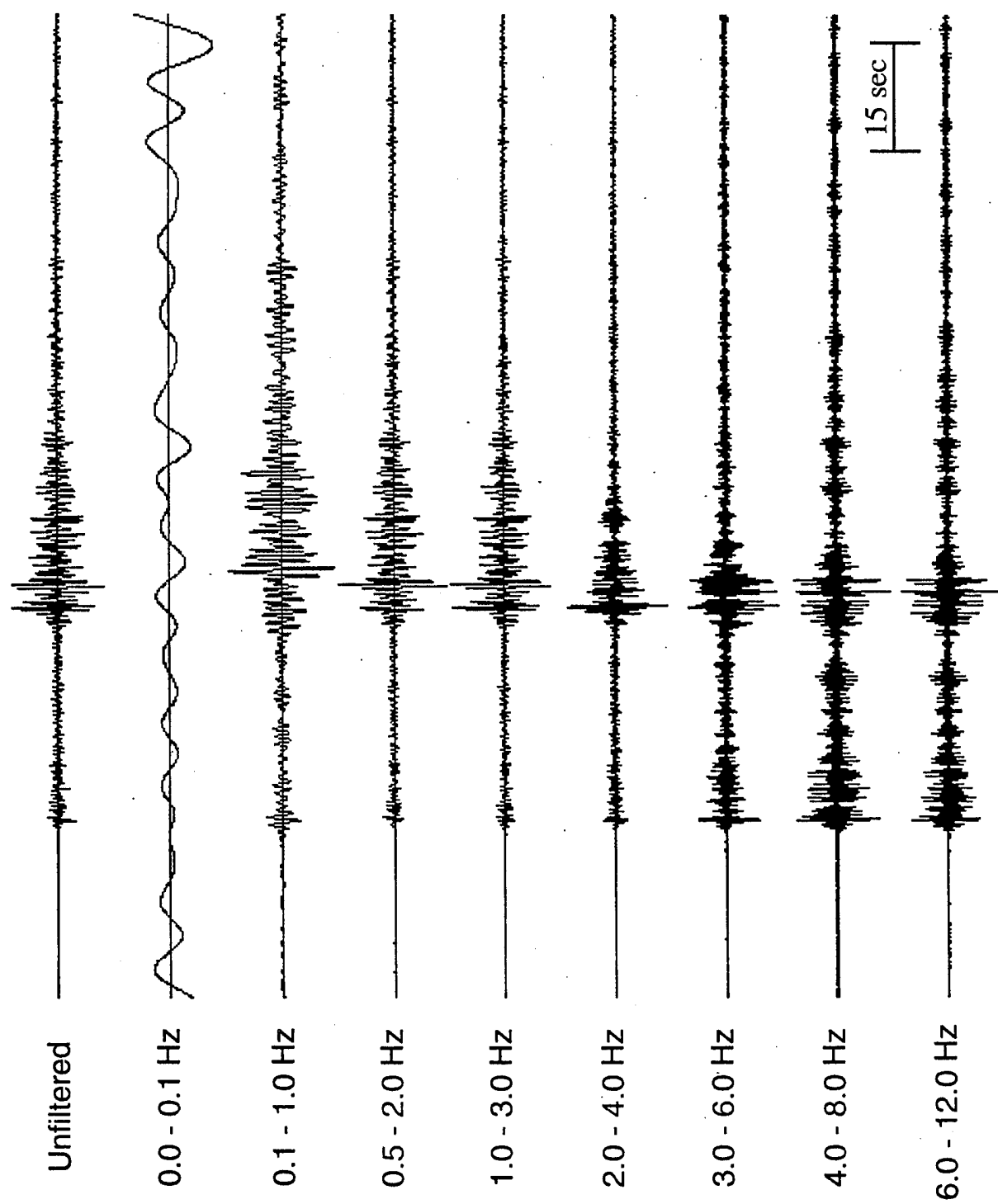
Figure 22. Bandpass filter analysis of the eastern Kentucky rockburst of March 11, 1995 recorded at station BLA (R = 230 km).

Unfiltered

0.0 - 0.1 Hz

0.1 - 1.0 Hz

0.5 - 2.0 Hz

1.0 - 3.0 Hz

2.0 - 4.0 Hz

3.0 - 6.0 Hz

4.0 - 8.0 Hz

6.0 - 12.0 Hz

15 sec

4.4 Urals Rockburst

The Ural mountains of Russia, where an apparent rockburst occurred on January 5, 1995, are in a relatively aseismic region. Figure 23 is a map of the general region showing the location of this rockburst and the seismicity for the past ten years reported by NEIS. Very little natural earthquake activity has occurred in this region; however, a number of Russian PNE's have been located in the Ural mountains (including seven within about three degrees of this event). This area is known to be a mining region. We also show on the map the locations for two regional IRIS stations whose records were used in the analysis of this event. In a previous study (cf. Bennett et al., 1995) we described the details of a discrimination analysis performed on this event; we will review here a few of the main observations leading to the conclusion that this event was most likely a rockburst or mine collapse.

The January 5, 1995 event in the Urals was originally reported by the IDC at the Center for Monitoring Research to have had a magnitude of 4.35 mb, but the magnitude subsequently reported by NEIS for the event was 4.7 mb. In our investigation of the event, we focused on the records from the digital stations at ARU (R = 360 km) and OBN (R = 1280 km), two of the best-quality regional stations in that area. Figure 24 shows the results of a bandpass filter analysis performed on the vertical-component record at ARU. The record is rather complex and shows several distinct regional phase arrivals, which has led some investigators to postulate a multiple source (cf. REFS). This hypothesis needs further study, but it is clear from Figure 24 that many of the distinct arrivals can be explained by the normal regional phases seen from a single source at the appropriate epicentral distance. In the lowest frequency passbands the records show a strong, well-dispersed R_g phase, which we take to be indicative of a shallow focus. We found similar R_g phases from rockbursts in several other source regions, as described elsewhere in this report. The lower frequency bands (up to about 3 Hz) are dominated by the R_g and L_g phases. In these bands L_g/P ratios are between 3:1 and 4:1. Above 3 Hz the regional P and S phases are most prominent. S/P ratios remain at about 1:1 except in the band from 3 Hz to 6 Hz where they fall to about 1:2. In these high-frequency bands the P phases are rather simple and impulsive.

To provide a basis for comparison in our prior analysis, we looked at similar bandpass filter analyses for a rockburst, explosion, and earthquake recorded at station GRFO, for which the epicentral distance was almost the

48
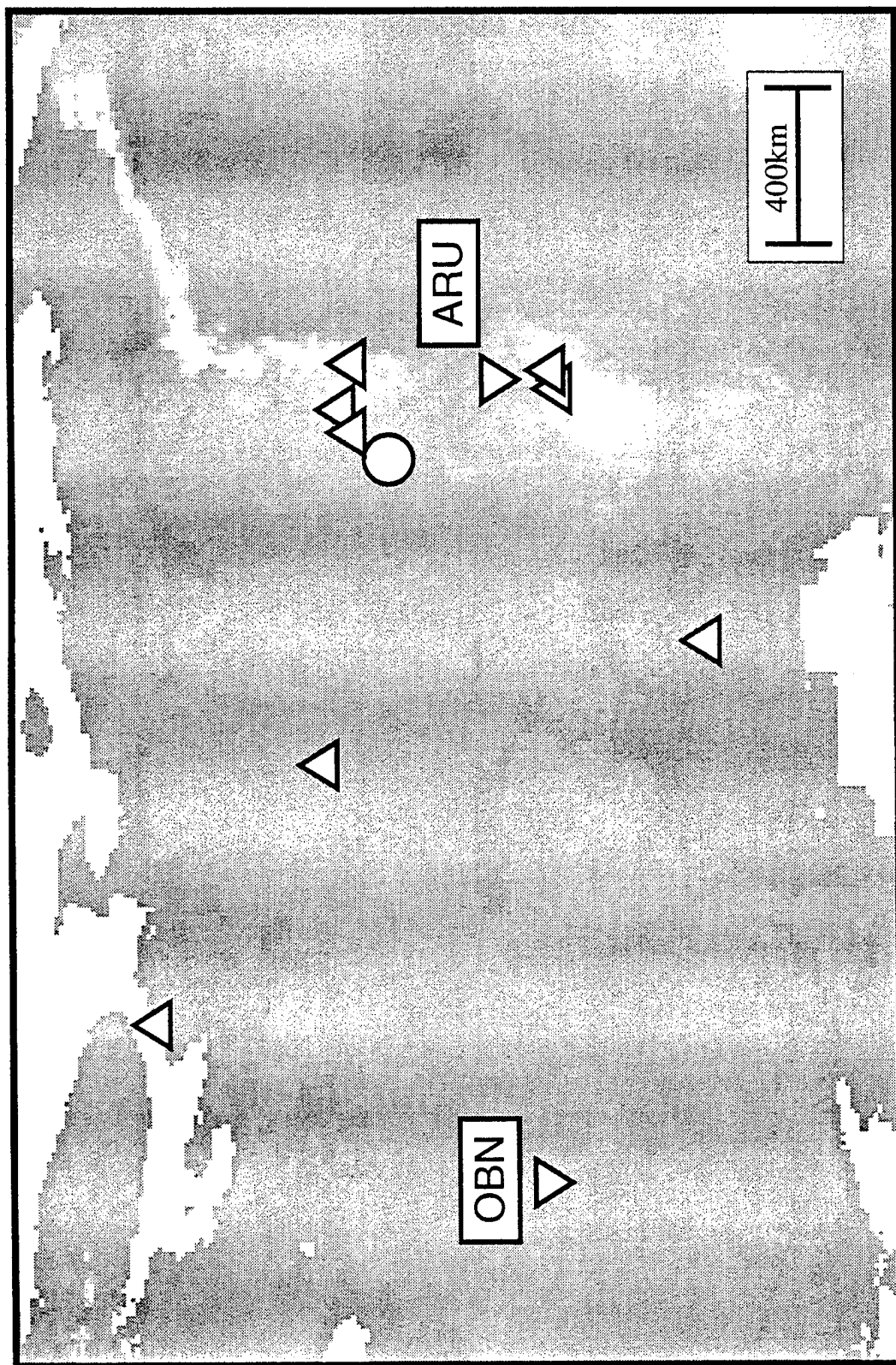
Figure 23. Locations of the central Urals rockburst (○), seismicity of the past decade reported by NEIS (△) , and regional seismic stations (▽) used in analysis.
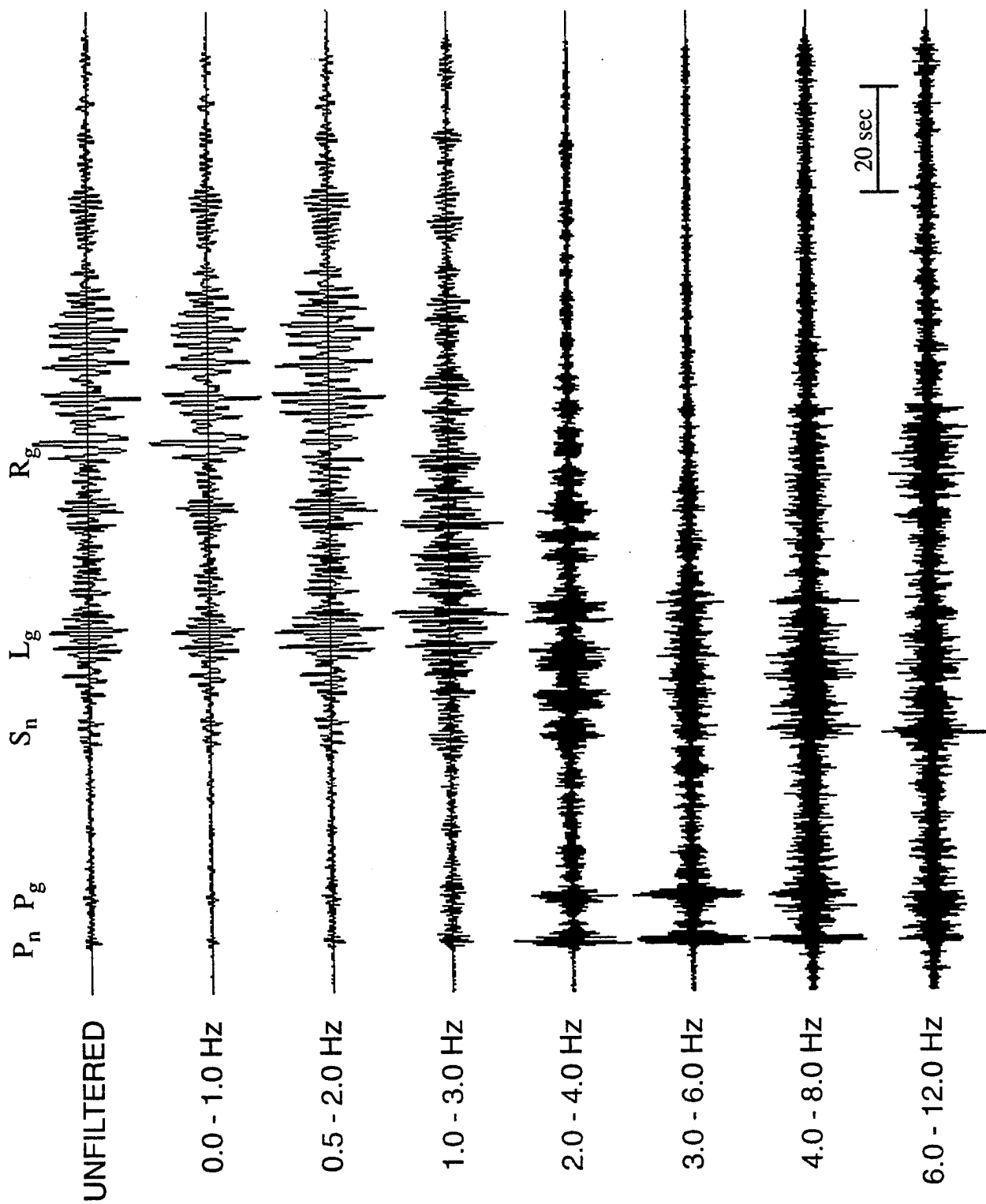
Figure 24. Bandpass filter analysis of the ARU record for the Urals event of January 5, 1995. Note an instrument correction has been applied to make the response equivalent to GRFO for comparison to other events.

same as that for the Urals event at ARU. As seen above in Figure 18, the filter results (after adjusting for instrument differences) appear quite similar for the Urals event at ARU and the Polish rockburst at GRFO. Comparisons for the other source types were less similar (cf. Bennett et al., 1995).

Independent of the analysis shown in Figure 24, Stevens (1995) investigated the long-period surface waves from the January 5 Urals event recorded at station OBN. Based on these records he determined a single-station M_S of 3.38 for the event. Thus, this single-station M_S would appear to be low by at least one magnitude unit compared to the IDC m_b of 4.35 and to the NEIS m_b of 4.7. This result is shown in Figure 15 above and is consistent with the behavior which we have reported elsewhere in this report for rockbursts in other source regions. More complete analyses of the surface-wave signals at these and other stations could provide a more reliable M_S estimate for this event.

In our prior report, we concluded that the January 5, 1995 Urals event was clearly shallow based on the strong R_g phase observed at ARU. We also noted that the relatively weak M_S and simple P phases were more typical of explosions or rockbursts. However, what we considered to be most diagnostic was the large L_g/P and S/P ratios which were observed over fairly broad ranges in frequency. This latter behavior is not consistent with explosion observations but does agree with what we have seen for rockbursts in many different source regions. The conclusion that this event was most likely a rockburst or mine collapse appears to be supported by the fact that the event occurred in an area of known below-ground mining and by damage reports from a Russian mine near the epicenter. We hope to obtain additional details from the mine which can help define the mechanism for this event and to use the results to model the observed regional signals.

5. Rockburst Mechanisms

5.1 Implications for MS-versus-mb and Regional Phases

There are several examples of events variously described in the literature as rockbursts, collapses, or mine bumps that exhibit explosion-like (viz. small) 20-second surface-wave MS magnitudes with respect to short-period magnitudes such as mb, ML, or mb(Lg). Some of these events include the 1981 Gentry mine collapse (Taylor, 1994) in Utah, the 1989 Völkershausen mine collapse in Germany (Ahorner, 1993; Bowers, 1995), the 1995 Urals event (Bennett et al., 1995), the 1995 Solvay mine rockburst in Wyoming (Pechmann et al., 1995), and the 1995 Lynch mine bump in Kentucky. In each case the long-period fundamental-mode surface waves were smaller than what would be expected from a shallow crustal earthquake when compared to the short-period magnitudes of the events. Therefore, these events appeared "explosion-like" from the MS-versus-mb point of view. Clearly, none of these events were explosions; but they were rather mine-related collapses with varying amounts of tectonic release. There have been several papers written on the mechanisms of some of these events, and the seismic mechanisms are somewhat controversial. In several cases, local networks observed P-wave first-motion dilatations from large fractions of the focal sphere of the event. Such observations have sometimes led workers to assume an implosion or thrust mechanism (Bowers, 1995). First-motion studies are limited for most of the events; local networks were not available, more distant P-wave first motions were emergent and masked by noise, or the event was complex and preceded by a smaller foreshock. In some cases, the search for possible seismic moment tensors was constrained to double-couple mechanisms and the modeling results led to a thrust mechanism (Bowers, 1995). In at least two cases, authors have allowed the possibility of a general seismic moment tensor "collapse" mechanism that was not purely implosional. In these cases they have found that the best solution was not a double-couple or a pure implosion but a mechanism closer to a closing tension crack (Pechmann et al., 1995, Taylor, 1994).

It is the purpose of this short section to discuss moment tensor representations of a mine collapse in the context of mb-versus-MS and short-period Lg/P discriminants. First, we review some moment tensor decompositions for the tension crack (TC) and compensated linear-vector

dipole (CLVD). Then, we use a non-linear discrete element code to show that the stress field introduced by a large room collapse is probably best represented by a closing tension crack. Finally, we compute some Green's functions from several moment tensor representations and show that very small M_S values may be best explained by the shallow tension crack model. This is a direct result of the inefficient excitation of the fundamental-mode Rayleigh wave by a shallow tension crack. Furthermore, it is highly likely that the P-wave first motions from a closing tension crack will be consistent with a thrust mechanism.

Clearly, we should expect that no single moment-tensor model will fit all mine-related tremors; but it is clear that there should be a class of events that are dominated in the long period by the collapse of a large volume with a large aspect ratio (long and wide with respect to height). This class of events should in the long-period seismic band be best represented by the moment tensor representation of a closing tension crack plus some component of tectonic release (pure deviatoric). We would expect there to be a spectrum of events ranging from little or no tectonic component to those dominated by the tectonic component. Events with little or no tectonic component are the most interesting since these events should have "explosion-like" m_b-versus-M_S. On average, a couple of these events occur each year with short-period magnitudes greater than 4 (equivalent to tamped explosions greater than a kiloton). The extent to which these events look "explosion-like" will depend upon the ratio of tectonic-release moment to the tension-crack moment and the time functions for the two mechanisms.

5.2 Moment Tensor Representations

We can represent the equivalent far-field seismic source for an event as a moment tensor with six independent time series. For most events we can assume that all components of the source have the same time dependence and at periods longer than the characteristic time of all near-field motion, we can assume also that all components of the moment tensor are indeed the same. However, in the case of a rockburst plus mine collapse, we may at short-periods have two or more related time series involved (movement on a fault and gravity collapse). For the purpose of our discussion we will use a few simple decompositions of the moment tensor (Aki and Richards, 1980). It should be noted that we could use as a basis any linear combination of the basic moment tensors we use here; the explosion/implosion, the horizontal tension crack, the

horizontal CLVD, the thrust fault, the dip-slip, the strike-slip, and the horizontal slip.

Explosion: $M = M_{EX} \begin{bmatrix} 1 & 0 & 0 \\ 0 & 1 & 0 \\ 0 & 0 & 1 \end{bmatrix}$

Opening / Closing Horizontal Tension Crack: $M = \dfrac{M_{TC}}{\lambda + 2\mu} \begin{bmatrix} \dfrac{\lambda}{\lambda + 2\mu} & 0 & 0 \\ 0 & \dfrac{\lambda}{\lambda + 2\mu} & 0 \\ 0 & 0 & 1 \end{bmatrix}$

$$= \frac{M_{TC}}{\lambda + 2\mu} \left((\lambda + \frac{2}{3}\mu) \begin{bmatrix} 1 & 0 & 0 \\ 0 & 1 & 0 \\ 0 & 0 & 1 \end{bmatrix} - \frac{4\mu}{3} \begin{bmatrix} 1/2 & 0 & 0 \\ 0 & 1/2 & 0 \\ 0 & 0 & -1 \end{bmatrix} \right)$$

Vertical CLVD: $M = M_{CLVD} \begin{bmatrix} 1/2 & 0 & 0 \\ 0 & 1/2 & 0 \\ 0 & 0 & -1 \end{bmatrix} = \dfrac{M_{CLVD}}{2} \left(\begin{bmatrix} 1 & 0 & 0 \\ 0 & 0 & 0 \\ 0 & 0 & -1 \end{bmatrix} + \begin{bmatrix} 0 & 0 & 0 \\ 0 & 1 & 0 \\ 0 & 0 & -1 \end{bmatrix} \right)$

45 Degree Dipping Pure Thrust with Strike 0 Degrees: $M = M_{TH1} \begin{bmatrix} 0 & 0 & 0 \\ 0 & 1 & 0 \\ 0 & 0 & -1 \end{bmatrix}$

45 Degree Dipping Pure Thrust with Strike 90 Degrees: $M = M_{TH2} \begin{bmatrix} 1 & 0 & 0 \\ 0 & 0 & 0 \\ 0 & 0 & -1 \end{bmatrix}$

Pure Dip - Slip with Strike 45 Degrees: $M = M_{DS} \begin{bmatrix} 0 & 0 & 1 \\ 0 & 0 & -1 \\ 1 & -1 & 0 \end{bmatrix}$

Pure Strike - Slip with Strike 45 Degrees: $M = M_{SS} \begin{bmatrix} -1 & 0 & 0 \\ 0 & 1 & 0 \\ 0 & 0 & 0 \end{bmatrix}$

Pure Horizontal Slip with Strike 45 Degrees: $M = M_{H} \begin{bmatrix} 0 & 0 & \frac{-1}{\sqrt{2}} \\ 0 & 1 & \frac{-1}{\sqrt{2}} \\ \frac{-1}{\sqrt{2}} & \frac{-1}{\sqrt{2}} & 0 \end{bmatrix}$

It is useful to remember that the scale moment for a tension crack is M_{TC} = $(\lambda + 2\mu)Ad$, where A is the fault/crack surface and d is the crack opening/closing displacement, in contrast to the more familiar scalar moment for a double-couple, $M = \mu Ad$.

Note that the explosion/implosion, the opening/closing horizontal tension crack, and the vertical CLVD have no off-diagonal elements; and hence these fundamental sources have no azimuthal radiation patterns, and they excite no Love waves. Also, note that the opening/closing horizontal tension crack can be decomposed into an explosion/implosion plus a vertical CLVD, and that the vertical CLVD may be decomposed into two 45-degree dipping thrust faults that strike at 90 degrees to each other. These two identities are very useful for constructing synthetic seismograms.

Another useful relation for the tension crack source is that the shallow horizontal tension crack source may be replaced by an equivalent vertical point force on the surface (Day et al., 1983; and Day and McLaughlin, 1991). For wavelengths longer than the depth to the tension crack, we can replace the tension crack moment-tensor source, $M_{TC}(t) = (\lambda + 2\mu)Ad(t)$, with an equivalent point force, $F_z(t) = -hpA\dot{d}(t)$, where h is the depth of the tension crack, p is the material density, A is the area of the crack, $d(t)$ is the displacement time history, and $\dot{d}(t)$ is the first derivative of the displacement time history. Since $m = hpA$ is the mass of the material above the tension crack, we can see that the equivalent force can be interpreted as the momentum of the material above the closing crack. This long-period approximation is useful since it demonstrates that the long-period excitation will be proportional to the mass of material above the collapse; excitation from the tension crack goes to zero as the tension crack depth goes to zero.

It is clear from examination of the CLVD thrust fault identity, that if the modeling of seismic waves cannot determine the azimuth of a thrust mechanism, then the modeling cannot exclude a vertical CLVD from the solution space. In earthquake modeling, it is often assumed that the trace of the moment tensor is zero (no explosion/implosion component) and furthermore that the motion is purely double-couple (no CLVD components). Bowers (1995) modeled fundamental-mode surface waves and broadband P-waves from the Völkershausen mine collapse constrained to use only double-couple sources and found that a thrust mechanism with any azimuth could explain the observed radiation patterns. Therefore, he could not rule-out a vertical CLVD source

which is the average of the sources in his solution space. Figure 25 shows the P-wave radiation patterns from the thrust (strike 0 and -90), the CLVD, and the tension crack. Clearly, based on P-wave radiation patterns alone, unless nodes can be identified on the focal sphere, the CLVD, thrust, and tension crack will be indistinguishable.

5.3 Simulations Using A Discrete Element Code

We have used a discrete element code, UDEC (Universal Distinct Element Code), to model the collapse of a large cavity (cf. Itasca, 1991). The calculations are 2-D plane-strain and simulate the stress-field changes produced by the excavation of a cavity, and the subsequent "failure" of a pillar and the collapse of the roof of the cavity. These calculations proceed in a stepwise manner.

1. The first step is to define the characteristics of the country rock (bulk modulus, shear modulus, density, tensile strength, etc.), the boundary conditions (such as a free surface on the top of the model), and any faults that cut through the model (slip surfaces with a specified friction law). A computational grid is established to perform the subsequent calculations.

2. The computational mesh is defined and the initial stress and displacement conditions are allowed to reach a static solution. At this stage, the rock mass will be in lithostatic equilibrium with the boundary conditions, gravitational forces, and slip surfaces (faults).

3. Volumes of rock are cut-out and removed to create a mined out cavity. The stresses and displacements are again allowed to reach a static solution. This step may be repeated several times.

4. Finally, in order to simulate a collapse, we cut-out and remove the last pillars or activate a fault surface, and allow the program to integrate the equations of motion and reach a final static state.

Figure 26 illustrates a computational mesh for our simulation after completion of steps 1-3. Only a limited portion of the model is shown. A 3-m high by 40-m wide cavity at a depth of 50 m with two support pillars (2-m wide) is shown. There is a fault passing through the model from the upper right-hand corner with a dip of 45 degrees. The fault passes through the right-hand pillar. No initial tectonic stress field is imposed besides the lithostatic field imposed by gravity. A minuscule amount of sagging in the roof of the cavity and uplift in the floor of the cavity has occurred following the removal of the cavity material.
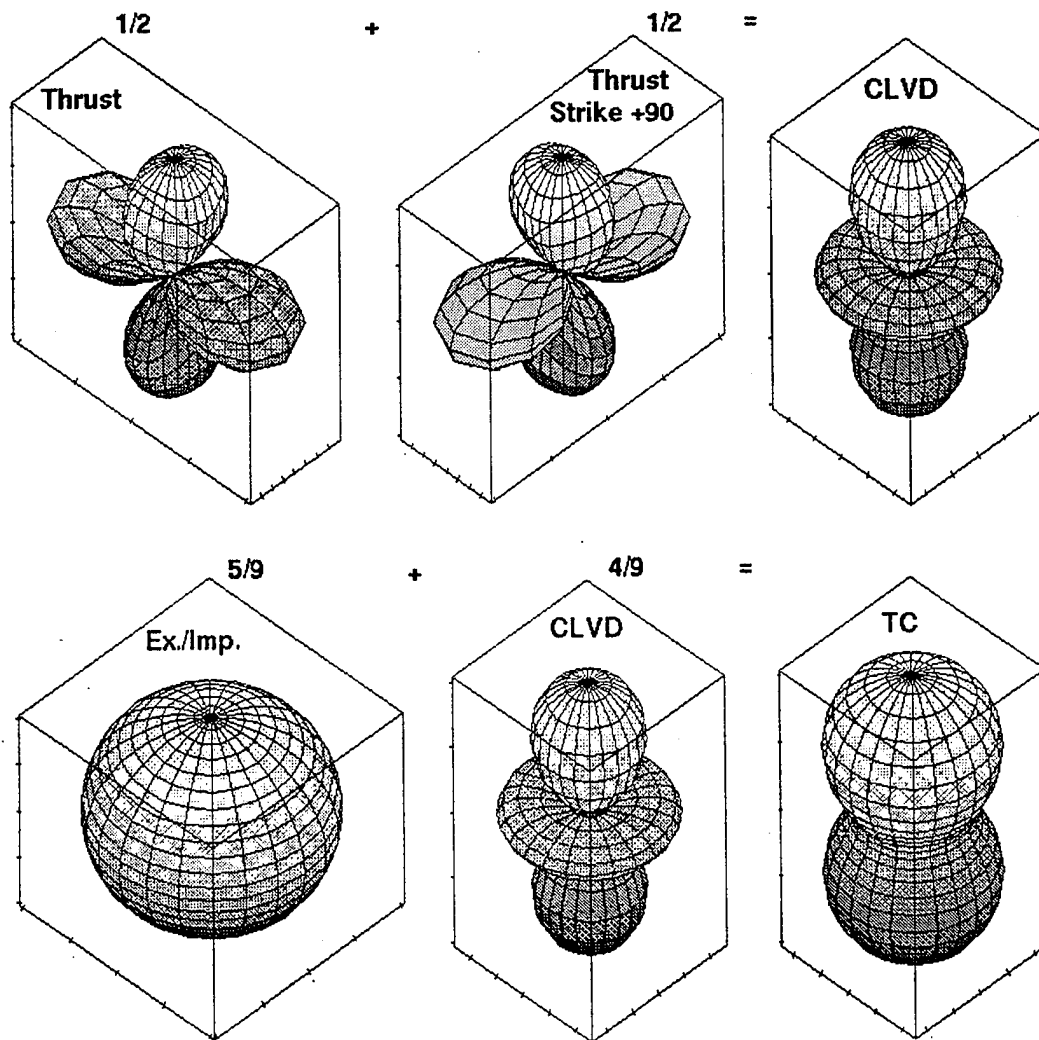
Figure 25. P-wave radiation patterns for 45-degree dipping pure thrust (strike 0 and -90 degrees) double-couple, vertical CLVD, vertical opening/closing horizontal tension crack (Poisson's ratio of 1/4), and explosion/implosion. Note that the CLVD is the average of thrust faults with strikes from 0 to 360, and that the tension crack is the (4/9)'s CLVD plus (5/9)'s explosion/implosion.
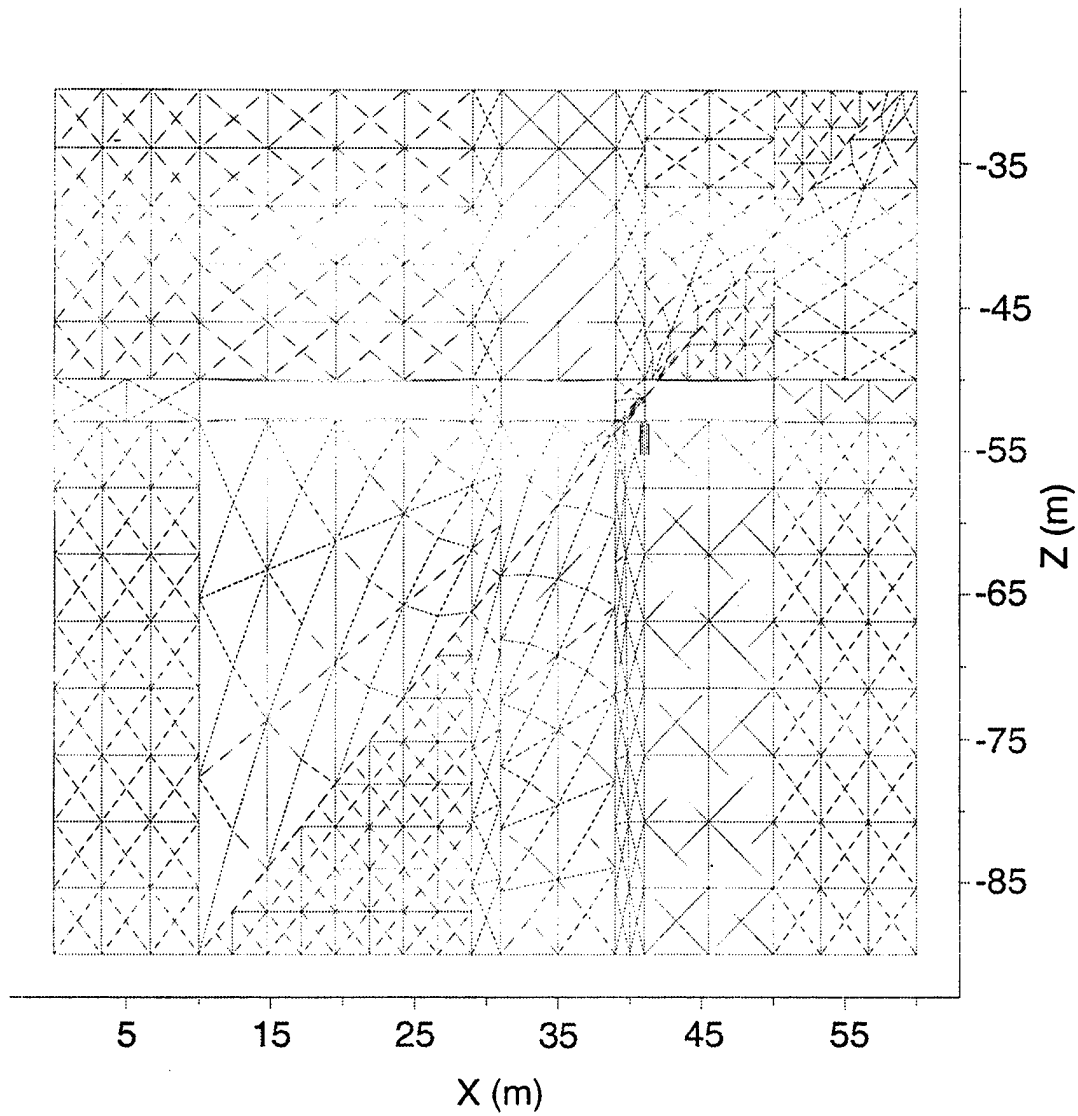
Figure 26. Computational triangular grid for the UDEC plane-strain simulation. A 3m high, 40m wide cavity is shown with two 2m wide pillars. A fault (frictional slip surface) passes through the right-hand pillar. Only a portion of the model is shown.

A small displacement (0.022 m maximum) has occurred along the fault in response to the creation of the cavity and the stress-field adjustments. Figure 27 shows the principal directions of stress at this stage. The stress field is largely lithostatic except in close proximity to the fault surface, in the pillars, and near the ends of the cavity. Figure 28 shows the exaggerated final displacement field (0.33 m maximum) that results from the simultaneous removal of both pillars. The motion is largely that of a collapse into the cavity despite the presence of the fault (0.19 m maximum slip). Figure 29 illustrates the stress field resulting from the collapse. Note that the stress field is dominated by the cavity collapse despite the fact that motion has occurred along the fault. Tensile failure has occurred in limited rock volumes in the cavity roof and in a small region of the cavity floor. The stress field that results looks very much like that of a closing tension crack or perhaps a CLVD. It is this stress-field change that excites the long-period seismic radiation.

5.4 Green's Functions

In order to illustrate the relative efficiency of various basic moment tensor sources we have computed wavenumber integration Green's functions for a 1.5 * 10^{16} Nt-m step-function source at a depth of 900 m and a vertical receiver at a range of 340 km. The layered earth model is described in Table 3 and was modified from models proposed for the region of the KTB-Oberpfalz deep drill hole near the Bavaria-Bohemia border (Jan Wuester, 1995). The many randomized layers in the crust contribute to more realistic P_g and L_g waveforms.

Displacement seismograms are shown in Figure 30 for a thrust fault, strike-slip fault, an explosion, a vertical CLVD, and a horizontal tension crack. The seismograms are presented in two passbands, an LP and an SP passband. First note that the LP fundamental-mode Rayleigh wave from the tension crack source is reduced with respect to the other sources by a factor of 10. The SP fundamental-mode (labeled R_g) from the tension crack source is not reduced with respect to the other sources. The excitation of the fundamental-mode Rayleigh wave from a shallow tension crack source is extremely inefficient for wavelengths that are longer than the depth of the source. While this observation has been made previously by Day et al. (1983) and by Day and McLaughlin (1991) in the context of spall sources from explosions, it may not be fully appreciated in the context of shallow collapses. If
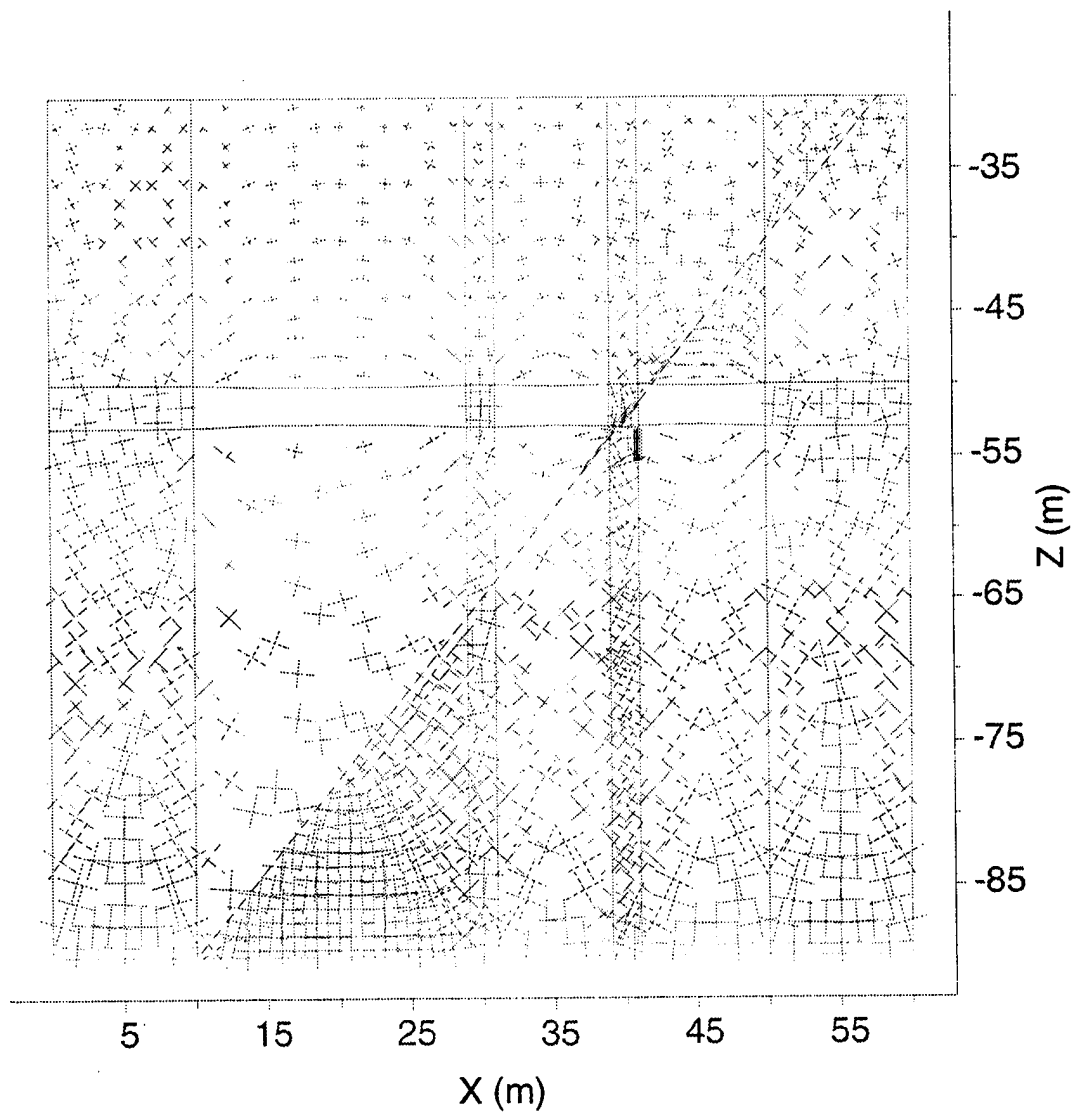
Figure 27. The lithostatic stress field is shown following the re-adjustment of stresses due to the excavation of the cavity.
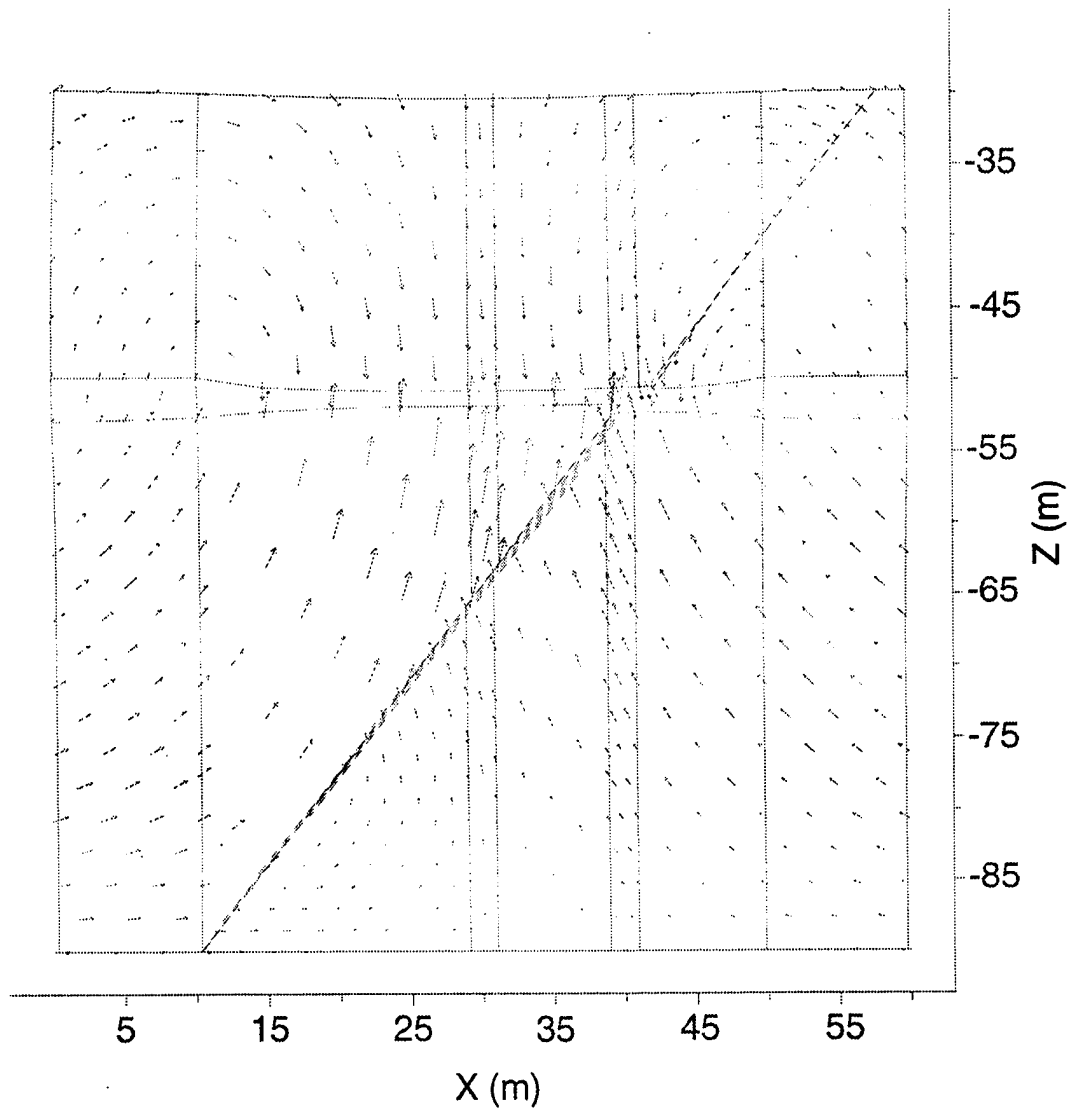
Figure 28. The static displacement field following pillar removal. Maximum displacement is 0.33m. Maximum slip on the fault is 0.19m.
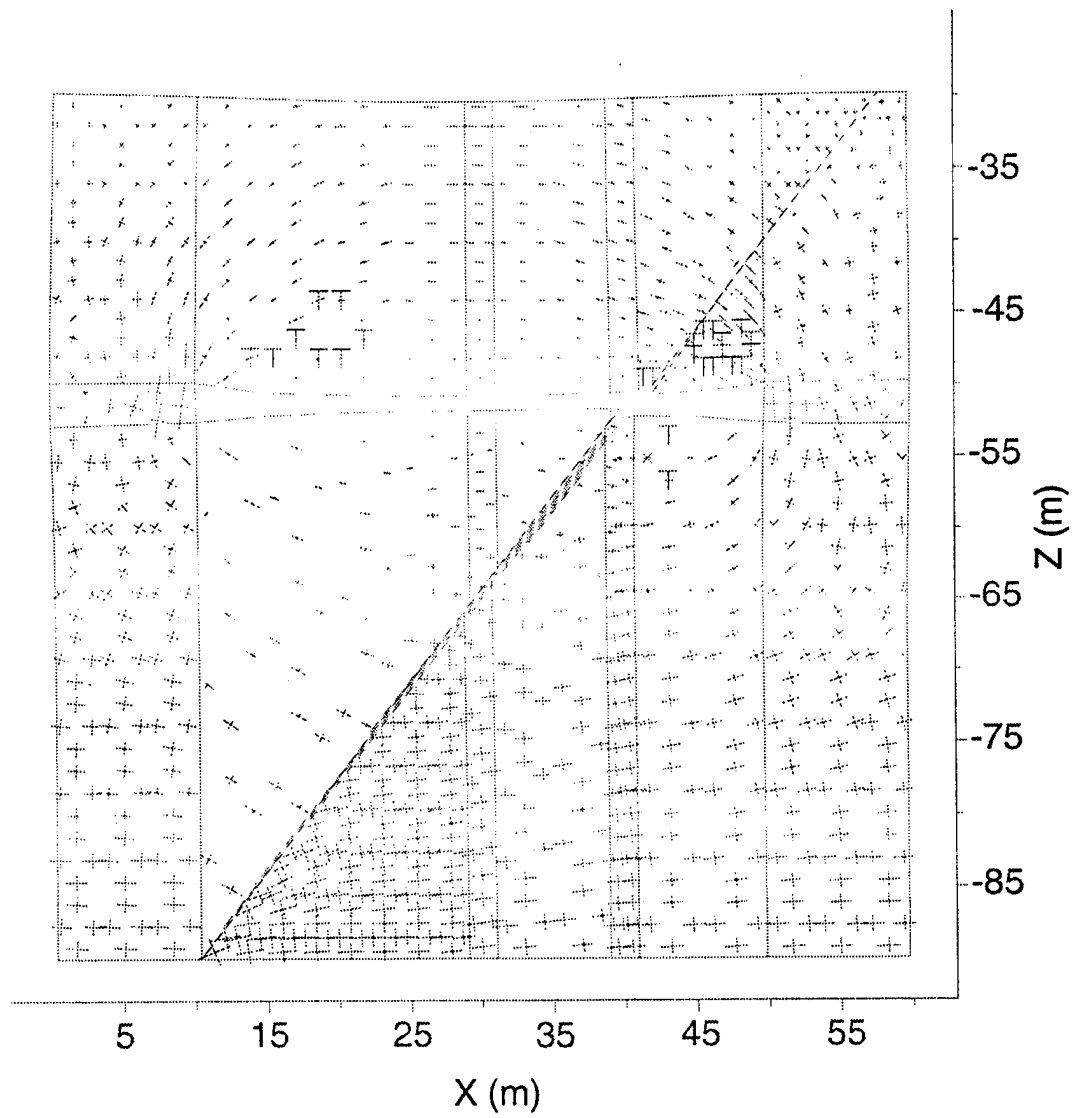
Figure 29. The lithostatic stress field is shown following the pillar removal.

Table 3. Layered Earth Model Used For Synthetics Calculation

H (m)	α (m/s)	β (m/s)	ρ (Kg/m³)	Qμ
500.1	4660.4	2775.8	2537.3	50.0
535.1	5664.2	3188.9	2680.4	100.0
572.4	5650.0	3328.8	2681.4	100.0
613.1	5936.0	3632.0	2764.3	405.6
655.3	5817.5	3347.0	2706.7	393.3
701.7	5898.5	3375.6	2693.2	394.5
750.8	6273.5	3601.7	2773.8	404.2
803.4	5920.7	3440.2	2710.7	397.3
859.7	6068.5	3423.5	2748.6	396.6
920.3	5915.3	3517.7	2739.1	400.6
984.7	5727.0	3310.0	2696.6	391.6
1054.0	6102.3	3404.0	2744.8	395.6
1127.6	6174.8	3548.2	2760.1	401.8
1206.9	5926.8	3451.4	2734.1	397.6
1291.6	6301.0	3600.4	2776.6	404.0
1382.1	6510.4	3498.1	2776.4	399.6
1479.5	6400.1	3483.5	2775.8	398.9
1583.8	5991.5	3550.3	2754.8	401.7
1694.6	6317.9	3568.0	2794.3	402.5
1813.9	6365.6	3555.9	2799.4	401.9
1941.3	6370.1	3659.6	2794.6	406.2
2078.0	6439.1	3736.2	2808.4	409.4
2224.4	6429.0	3778.7	2813.8	411.1
2380.8	6856.4	3961.2	2871.4	418.4
2548.0	7311.0	4068.2	2939.7	422.6
2728.1	8043.4	4522.9	3319.5	440.1
2919.5	8047.0	4762.5	3138.9	448.9
3126.1	8051.0	4643.3	3467.1	444.4
3346.7	8055.2	4670.8	3449.8	445.4
3582.6	8059.7	4764.3	3401.3	448.7
3835.7	8064.6	4653.5	3336.1	444.5
4107.3	8069.8	4795.6	3306.6	449.6
4396.7	8075.4	4706.3	3154.8	446.3
4708.5	8081.3	4618.2	3316.5	442.9
5041.8	8087.7	4652.0	3318.3	444.0
5399.2	8094.6	4661.2	3449.4	444.2
5782.2	8102.0	4913.5	3383.2	453.2
6192.5	8109.8	4895.8	3385.5	452.4
6632.8	8118.3	4887.7	3322.8	451.9
7105.3	8127.3	4751.3	3452.8	446.8
7610.3	8137.0	4775.4	3325.9	447.5
8154.3	8147.5	4566.8	3261.8	439.6
8736.3	8158.7	4650.1	3345.5	442.4
9360.6	8170.6	4683.0	3304.3	443.4
10031.7	8183.5	4768.7	3316.7	446.2
10750.9	8197.3	4736.8	3327.3	444.8
11524.1	8212.2	4774.1	3271.1	445.8
12353.5	8228.1	4782.9	3421.3	445.8
13245.5	8245.2	4868.4	3352.8	448.5

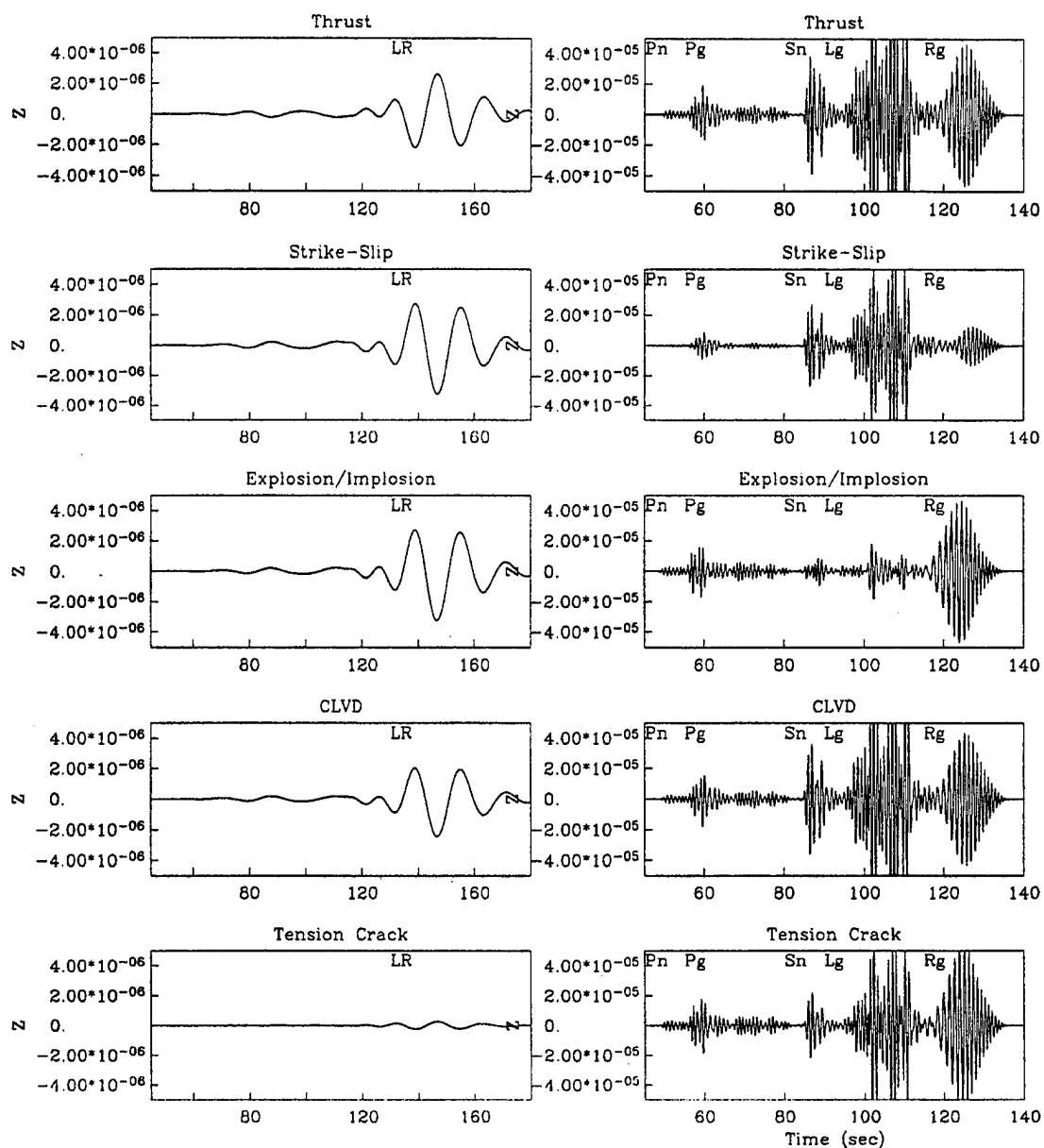Figure 30. Green's functions at a distance of 340km for 900m deep thrust, strike-slip, explosion, CLVD, and tension crack sources (top to bottom) . LP band-passed (0.33-0.66 Hz) seismograms are shown on the left, SP band-passed (0.8-1.2 Hz) seismograms are shown on the right. The same plotting scales are used for all SP and for all LP seismograms.

the moment tensor source from a shallow collapse resembles that of a closing horizontal tension crack, then the fundamental-mode Rayleigh-wave excitation will be very inefficient.

The P_g is about the same amplitude for each source type (somewhat reduced for the strike-slip). As expected, the pure explosion/implosion source has reduced S_n and L_g with respect to all the other sources since SV energy must be generated by conversion from P energy at interfaces in these synthetic seismograms. The P-to-SV energy for the shallow tension crack source resembles the earthquake and CLVD P-to-SV ratios more than the explosion P-to-SV ratio.

Modeling of regional long-period observations from the 1995 Wyoming rockburst by Pechmann et al. (1995) supports the interpretation that the large Solvay mine collapse was predominately a closing tension crack. Figure 31 shows the seismic modeling from Pechmann et al. (1995) for long-period waves at the station ELKO. Three solutions are shown and compared to the observations: (1) collapse of a tension crack, (2) a vertical dip-slip fault (normal), and (3) a strike-slip fault. The two best-fitting double-couple solutions (strike-slip and normal) either over-predict the amount of transverse motion or they predict the transverse motion and are out of phase with the fundamental. The transverse motion is probably caused by the slight off-axis arrival of the Rayleigh wave, and the Love-wave motion at this station is probably in the noise. By far the best fit in this bandwidth is the closing tension crack model.

The estimated moment from the modeling is 4.5 * 10^{16} Nt-m (accounting for a different moment-tensor normalization of Pechmann et al.) and a subsidence region of 1000 m by 2000 m was observed at the surface following the collapse. Using the equation $M_{TC}(t) = (\lambda + 2\mu)Ad$ ($\alpha = 4200$ m/s, $\rho = 2300$ Kg/m^3), we can estimate the average collapse displacement, d = 0.5 m. In the case of the $M_L = 3.5$ Gentry mine collapse of May 14 1981, Patton and Zandt (1991) estimated an isotropic moment of about 4 * 10^{14} Nt-m; and Taylor (1994) reported that a 10,000 m^2 by 4 m high cavity collapsed which implies an average collapse displacement of d = 3 m ($\alpha = 2600$ m/s, $\rho = 2200$ Kg/m^3). Similar calculations can be done for other mine collapses and comparisons made between the observed seismic radiation.
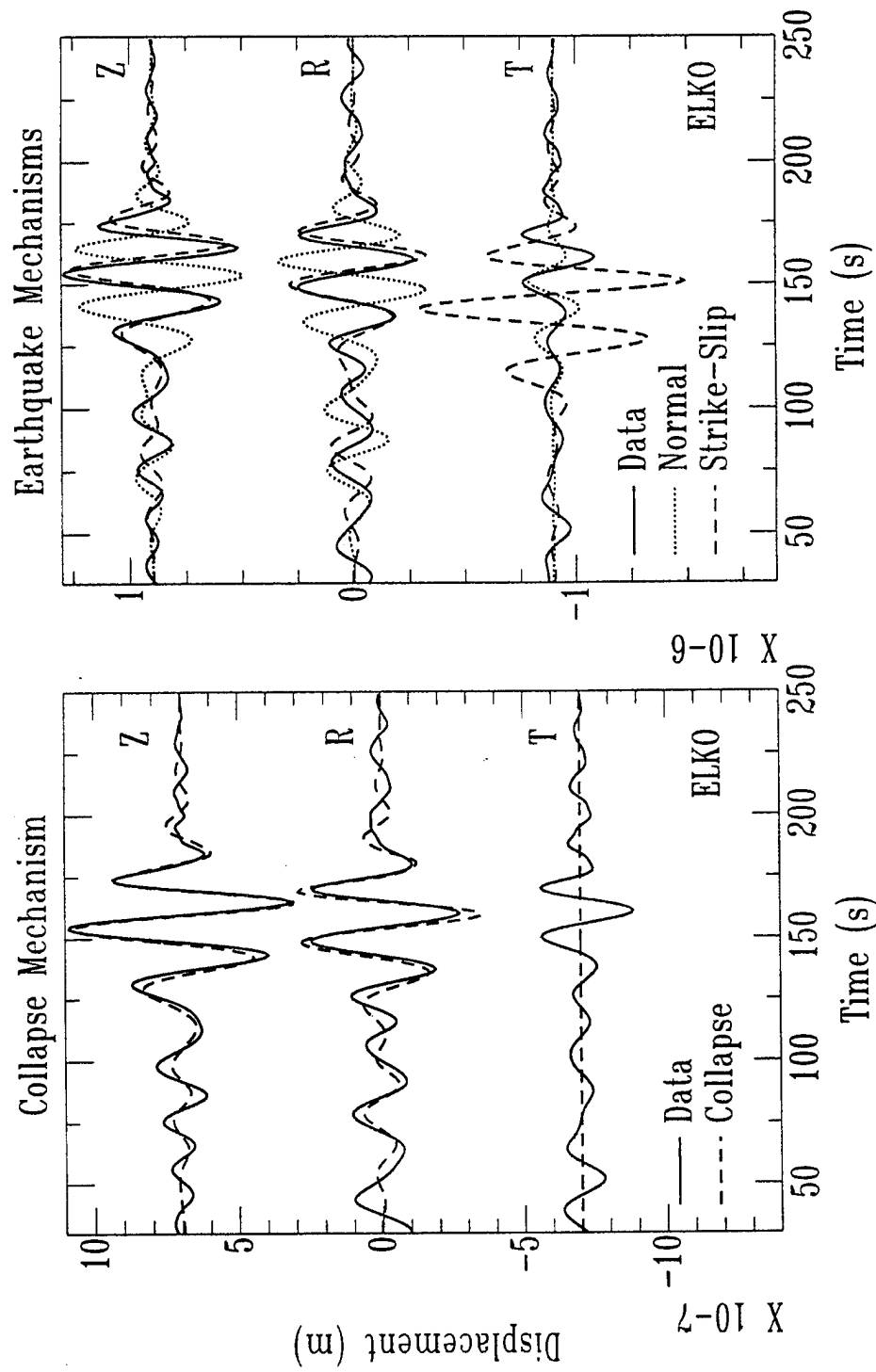
Figure 31. Comparison of the tension crack collapse model and earthquake double-couple synthetics with data from the 1995 Wyoming trona mine collapse (from Pechmann et al. 1995). Note that the two double-couple solutions can not fit both the radial/vertical components and the transverse components at the same time. (Figure courtesy W. R. Walter, LLNL)

66

6. Summary and Conclusions

6.1 Review of Procedures and Main Findings

The primary objective of this research project is to improve understanding of the seismic mechanisms and controllability of rockbursts and related mine tremors. To accomplish this objective we have been seeking to identify the characteristics of seismic signals from rockbursts and the physical properties and phenomenology observed in the vicinity of the mines from such events in a variety of source areas around the world. It is anticipated that this information can be used to investigate and refine mechanisms describing the rockburst source and will help with understanding controllability by adjusting mining practice. During the most recent phase of our research program, we have focused on characterizing the behavior of several recent prominent events including (1) the February 3, 1995 mine collapse in southwestern Wyoming, (2) the October 30, 1994 mine tremor in the Orange Free State and other recent nearby events in South Africa, (3) the January 5, 1995 event in the Ural mountains of Russia, (4) the repetitive rockburst activity associated with copper and coal mines in Poland, and (5) the eastern Kentucky mine bump of March 11, 1995.

For each of these events we have collected seismic waveforms as well as parametric measurements and phenomenological observations. A variety of time-domain and spectral measurements have been performed on the waveform data, which have come primarily from seismic stations at regional to far-regional epicentral distance ranges. Similar measurements from different source types in the same or similar regions have been compared to identify consistent behavior which might be diagnostic of source type. We have also reviewed literature on the physical mechanisms of rockbursts and the properties of the source medium for specific events and specific regions as well as for rockbursts in general. This background information has been used to develop moment-tensor representations of the rockburst sources and to relate such source representations to more physical models, such as descriptions in terms of a discrete-element model which we have implemented in a computer code.

For the southwestern Wyoming mine collapse, we found the event generated relatively low M_S relative to m_b and relatively large L_g/P and S/P ratios over a range of frequencies. In comparison to selected recent western U.S. earthquakes, some regional phases appeared less distinct or coherent for

the mine collapse, particularly at higher frequencies; but Lg/P and S/P ratios were well above 1:1 for both source types. In contrast, P phases for western U.S. nuclear explosions at about the same range and station showed a much stronger onset of regional P and smaller Lg/P ratios (generally less than 1:1) particularly at higher frequencies. This behavior is similar to what we have seen for rockbursts in previous studies; and, in particular, the Wyoming mine collapse has many similarities both in seismic observations and source phenomenology to the 1989 Völkershausen, Germany mine collapse which we have described in prior reports.

For the South African mine tremors, including the October 30, 1994 Orange Free State event, a prominent feature of the near-regional signals was a strong Rg phase, presumably indicative of a shallow focal depth. Lg/P ratios were found to be large (greater than 2:1) on the broadband (unfiltered) records for all of the rockburst records which we have collected from the South African gold-mining region. Results of band-pass filter analyses of several mine tremor records, including that of the October 30, 1994 event, showed remarkable consistency in the behavior of the most prominent regional phases. Teleseismic M_S measurements from large South African mine tremors tended to be low relative to m_b; and upper-bound levels of M_S, which we inferred from long-period signal levels for some of the smaller mine tremors, also seemed to be low. With regard to source mechanisms, many South African mine tremors appear to have mechanisms which are best represented as double couple, like most earthquakes, although some may be more complex and could include implosional components. The October 30, 1994 Orange Free State appears to have had a primarily double-couple mechanism; but its shallow focus (as indicated by Rg), proximity to mines with a history of large mining-induced tremors, and similarity of its near-regional signals with those from other mine tremors suggest that it should be considered a rockburst.

We have also investigated rockbursts in several other areas (viz. central Europe, eastern Kentucky, and the Ural mountains of Russia). Preliminary observations suggest that rockburst events from these areas have shown similar behavior to those in the other areas described above. Specifically, long-period Rayleigh-wave excitation seemed to be low, Lg/P or S/P ratios were consistently large, and regional signals sometimes appeared complex or less distinct.

In our theoretical studies of rockburst mechanisms, we have been seeking to identify ways to represent different types of rockburst sources so as to match the observed seismic signal characteristics. We have found from simulations with a discrete element computer code that, for some large rockbursts (viz. 1989 Völkershausen, Germany, 1995 southwestern Wyoming events, and Gentry Utah rockbursts), which we have been investigating, the seismic source could best be represented as a closing tension crack. Other authors have reached similar conclusions regarding some of these events. An important implication of this model for a shallow source is that it produces poor excitation of long-period fundamental-mode Rayleigh waves, which could explain the consistent reports of low M_S for many rockburst sources. Numerical simulations also have shown that this tension crack source can still produce strong R_g and large and earthquake-like Lg/P or S/P ratios at higher frequencies.

6.2 Future Plans

Our future efforts on this project will continue to include observational and theoretical elements. For the observational element we will seek to enhance our database for specific events and expand observations into any new rockburst areas where data become available. For several of the large events, it would be useful to acquire data from more seismic stations azimuthally distributed about the source. Such data exist for several of the events currently in our database, but effort is needed to retrieve and analyze additional waveforms. For at least two source areas (viz. South Africa and Poland), we have seismic data from numerous events. Systematic review of these waveforms would be useful to identify variability, which may relate to mining practice, in the seismic sources between rockbursts within a common source area.

For the theoretical element of this program, we plan to refine information on collapse area, volume, depth, and rock properties for several specific events. These will be used to model the seismic sources for those rockbursts and to predict characteristics of the seismic signals which can be related to observations. We also plan to conduct some parametric studies of the models which will allow us to assess sensitivities of the seismic signals to some of the source parameters (e.g. depth). In particular, we plan to evaluate the amount of tectonic release (fault movement) required to mask the tension crack source.

69

Acknowledgments

7. References

Ahorner, L. (1989). "Seismologische Untersuchung des Gebirgsschlages am 13. Marz 1989 im Kalisalzbergbau bei Völkershausen, DDR," Gluckauf-Forshungshefte, 50, pp. 224-230.

Aki, K., and P. G. Richards (1980). Quantitative Seismology, W. H. Freeman, San Francisco.

Båth, M. (1979). Introduction to Seismology, Birkhauser Verlag, Basel.

Bennett, T. J., A. K. Campanella, J. F. Scheimer, and J. R. Murphy (1992). "Demonstration of Regional Discrimination of Eurasian Seismic Events Using Observations at Soviet IRIS and CDSN Stations," PL-TR-92-2090, ADA253275.

Bennett, T. J., J. F. Scheimer, A. K. Campanella, and J. R. Murphy (1993). "Seismic Discrimination of Rockbursts for Use in Discrimination," PL-TR-93-2059, ADA266063.

Bennett, T. J., M. E. Marshall, B. W. Barker, and J. R. Murphy (1994). "Characteristics of Rockbursts for Use in Seismic Discrimination," PL-TR-94-2269, ADA290881.

Bennett, T. J., B. W. Barker, M. E. Marshall, and J. R. Murphy (1995). "Detection and Identification of Small Regional Seismic Events," PL-TR-95-2125.

Blandford, R. (1981). "Seismic Discrimination Problems at Regional Distances," in Identification of Seismic Source -Earthquake or Underground Explosion, D. Reidel Publishing Co., pp. 695-740.

Bowers, D. (1995). "An Alternative Interpretation of the Völkershausen Seismic Disturbance," Submitted to BSSA.

Day, S. M., and K. L. McLaughlin (1991). "Seismic Source Representations For Spall," Bull. Seism. Soc. Am., 81, pp. 191-201.

Day, S. M, N. Rimer, J. T. Cherry (1983). "Surface Waves from Underground Explosions with Spall: Analysis of Elastic and Nonlinear Source Models," Bull. Seism. Soc. Am., 73, pp. 247-264.

Fan, G., and T. Wallace (1995). "Focal Mechanism of a Recent Event in South Africa: A Study Using a Sparse Very Broadband Network," Seism. Res. Lett., 66, pp. 13-18.

Fernandez, L. M., and J. A. Guzman (1979). "Seismic History of Southern Africa," Seism. Ser. Geol. Surv. S. Afr., 9.

Gane, P. G., P. Seligman, and J. H. Stephen (1952). "Focal Depths of Witwatersrand Tremors," Bull. Seism. Soc. Am., 42, pp. 239-250.

Gane, P. G., A. R. Atkins, J. P. F. Sellschop, and P. Seligmann (1956). "Crustal Structure in the Transvaal," Bull. Seism. Soc. Am., 46, pp. 293-316.

Gay, N. C. (1975). "In Situ Stress Measurements in Southern Africa," Tectonophysics, 24, pp. 447-459.

Gay, N. C., D. Spencer, J. J. van Wyk, and P. K. van Der Haver (1984). "The Control of Geological and Mining Parameters on Seismicity in the Klerksdorp Gold Mining District," in Proc. 1st Int. Congress on Rockbursts and Seismicity in Mines, SAIMM, Johannesburg, pp. 107-120.

Gibowicz, S. J. (1984). "The Mechanism of Large Mining Tremors in Poland," in Proc. 1st Int. Congress on Rockbursts and Seismicity in Mines, SAIMM, Johannesburg, pp. 17-28.

Gibowicz, S. J. (1990). "The Mechanism of Seismic Events Induced by Mining," in Rockbursts and Seismicity in Mines, C. Fairhurst, editor, A. A. Balkema, Rotterdam, pp. 3-27.

Gibowicz, S. J., and A. Kijko (1994). An Introduction to Mining Seismology, Academic Press, San Diego.

Gibowicz, S. J., H. P. Harjes, and M. Schafer (1990). "Source Parameters of Seismic Events at Heinrich Robert Mine, Ruhr Basin, Federal Republic of Germany: Evidence for Non-Double-Couple Events," Bull. Seism. Soc. Am., 80, pp. 88-109.

Gutenberg, B., an d C. F. Richter (1956). "Magnitude and Energy of Earthquakes," Ann. Geofis, 9, pp. 1-15.

Herrin, Eugene (1995). Personal Communication.

Iannacchione, A. T., and J. C. Zelanko (1995). "Occurrence and Remediation of Coal Mine Bumps: A Historical Review," in Proc. Seminars on Mechanics and Mitigation of Violent Failure in Coal and Hard-Rock Mines, edited by H. Maleki, USBM Special Publication 01-95, pp. 27-67.

Itasca (1992). UDEC - Universal Distinct Element Code Version 1.8, Itasca Consulting Group Inc., Minneapolis.

Joughin, N. C. (1966). "The Measurement and Analysis of Earth Motion Resulting from Underground Rock Failure," Ph.D. Thesis, University of Witwatersrand.

Joughin, N. C., and A. J. Jager (1983). "Fracture of Rock at Stope Faces in South African Gold Mines," in Proc. Symp. Rockbursts: Prediction and Control, IMM, London, pp. 53-66.

Kafka, A. L. (1990). Rg as a Depth Discriminant for Earthquakes and Explosions: A Case Study in New England," Bull. Seism. Soc. Am., 80, pp. 373-394.

Knoll, P. (1990). "The Fluid-Induced Tectonic Rockburst of March 13, 1989, in the "Werra" Potash MIning District of the GDR (First Results)," Gerl. Beitr. Geophysik 99, pp. 239-245.

Marshall, P. D., and P. W. Basham (1972). "Discrimination Between Earthquaeks and Underground Nuclear Explosions Employing an Improved M_S Scale," Geophys. J., 28, pp. 431-458.

McGarr, A. (1971). "Violent Deformation of Rock Near Deep-Level, Tabular Excavations - Seismic Events," Bull. Seism. Soc. Am., 61, pp. 1453-1466.

McGarr, A. (1992). "An Implosive Component in the Seismic Moment Tensor of a MIning-Induced Tremor," Geophys. Res. Lett., 19, pp. 1579-1582.

Minkley, W. (1993). "Zum Herdmechanismus von Großen Seismischen Ereignissen im Kalibergbau," Paper Submitted to Jahr. Deutschen Geophysikalischen Gesellschaft.

Office of Technology Assessment (1988). Seismic Verification of Nuclear Testing Treaties, U. S. Congress OTA Report NO. OTA-ISC-361.

Orsepowski, S., and C. Bachowski (1992). "Source Parameters of Mine-Induced Tremors at Rudna Copper Mine in Poland," Acta Geophysica, 40, pp. 13-24.

Patton, H. J., and G. Zandt (1991). "Seismic Moment Tensors of Western U.S. Earthquakes and Implications for the Tectonic Stress Field," J. Geophys. Res., 96, pp. 245-259.

Pechmann, J. C., W. R. Walter, S. J. Nava, and W. J. Arabasz (1995). "The February 3, 1995, M_L 5.1 Seismic Event in the Trona Mining District of Southwestern Wyoming," Seism. Res. Lett., 66, pp. 25-34.

Pomeroy, P. W., W. J. Best, and T. V. McEvilly (1982). "Test Ban Treaty Verification with Regional Data - A Review," Bull. Seism. Soc. Am., 72, pp. S89-S129.

Potgieter, G. J., and C. Roering (1984). "The Influence of Geology on the Mechanisms of Mining-Associated Seismicity in the Klerksdorp Gold-Field," Proc. 1st Int. Cong. on Rockbursts and Seismicity in Mines, Johannesburg, pp. 45-50.

Richter, C. F. (1957). Elementary Seismology, W. H. Freeman and Co., San Francisco.

Rorke, A. J., and C. Roering (1984). "Source Mechanism Studies of Mine-Induced Seismic Events in a Deep-Level Gold Mine," Proc. 1st Int. Cong. on Rockbursts and Seismicity in Mines, Johannesburg, pp. 51-55.

Shapira, A. (1988). "Rg Waves from Rockbursts in South Africa," Tectonophysics, 156, pp. 267-273.

Sileny, J. (1989). "The Mechanism of Small Mining Tremors from Amplitude Inversion," PAGEOPH, 129, pp. 309-324.

Spottiswoode, S. M. (1980). "Source Mechanism Studies on Witwatersrand Seismic Events," Ph. D. Thesis, University of Witwatersrand.

Spottiswoode, S. M., A. McGarr, and R. W. E. Green (1971). "Focal Mechanisms of Some Large Mine Tremors on the Witwatersrand," Research Report No. 3/71, Chamb. Mines S. Af.

Stevens, J. L. (1995). Personal Communication.

Sykes, L. R., J. F. Evernden, and I. L. Cifuentes (1983). Conference Proceeding 104, American Institute of Physics, pp. 85-133.

Taylor, S. R. (1994). "False Alarms and Mine Seismicity: An Example from the Gentry Mountain Mining Region, Utah," Bull. Seism. Soc. Am., 84, pp. 350-358.

Wuester, J. (1995). Personal Communication.

Prof. Thomas Ahrens
Seismological Lab, 252-21
Division of Geological & Planetary Sciences
California Institute of Technology
Pasadena, CA 91125

Prof. Keiiti Aki
Center for Earth Sciences
University of Southern California
University Park
Los Angeles, CA 90089-0741

Prof. Shelton Alexander
Geosciences Department
403 Deike Building
The Pennsylvania State University
University Park, PA 16802

Prof. Charles B. Archambeau
University of Colorado
JSPC
Campus Box 583
Boulder, CO 80309

Dr. Thomas C. Bache, Jr.
Science Applications Int'l Corp.
10260 Campus Point Drive
San Diego, CA 92121 (2 copies)

Prof. Muawia Barazangi
Cornell University
Institute for the Study of the Continent
3126 SNEE Hall
Ithaca, NY 14853

Dr. Jeff Barker
Department of Geological Sciences
State University of New York
 at Binghamton
Vestal, NY 13901

Dr. Douglas R. Baumgardt
ENSCO, Inc
5400 Port Royal Road
Springfield, VA 22151-2388

Dr. Susan Beck
Department of Geosciences
Building #77
University of Arizona
Tuscon, AZ 85721

Dr. T.J. Bennett
S-CUBED
A Division of Maxwell Laboratories
11800 Sunrise Valley Drive, Suite 1212
Reston, VA 22091

Dr. Robert Blandford
 AFTAC/TT, Center for Seismic Studies
1300 North 17th Street
Suite 1450
Arlington, VA 22209-2308

Dr. Stephen Bratt
ARPA/NMRO
3701 North Fairfax Drive
Arlington, VA 22203-1714

Dale Breding
U.S. Department of Energy
Recipient, IS-20, GA-033
Office of Arms Control
Washington, DC 20585

Dr. Lawrence Burdick
C/O Barbara Wold
Dept of Biology
CA Inst. of Technology
Pasadena, CA 91125

Dr. Robert Burridge
Schlumberger-Doll Research Center
Old Quarry Road
Ridgefield, CT 06877

Dr. Jerry Carter
Center for Seismic Studies
1300 North 17th Street
Suite 1450
Arlington, VA 22209-2308

Dr. Martin Chapman
Department of Geological Sciences
Virginia Polytechnical Institute
21044 Derring Hall
Blacksburg, VA 24061

Mr Robert Cockerham
Arms Control & Disarmament Agency
320 21st Street North West
Room 5741
Washington, DC 20451,

Prof. Vernon F. Cormier
Department of Geology & Geophysics
U-45, Room 207
University of Connecticut
Storrs, CT 06268

Prof. Steven Day
Department of Geological Sciences
San Diego State University
San Diego, CA 92182

Dr. Zoltan Der
ENSCO, Inc.
5400 Port Royal Road
Springfield, VA 22151-2388

Dr. Stanley K. Dickinson
AFOSR/NM
110 Duncan Avenue
Suite B115
Bolling AFB, DC 20332-6448

Prof. Adam Dziewonski
Hoffman Laboratory, Harvard University
Dept. of Earth Atmos. & Planetary Sciences
20 Oxford Street
Cambridge, MA 02138

Prof. John Ebel
Department of Geology & Geophysics
Boston College
Chestnut Hill, MA 02167

Dr. Petr Firbas
Institute of Physics of the Earth
Masaryk University Brno
Jecna 29a
612 46 Brno, Czech Republic

Dr. Mark D. Fisk
Mission Research Corporation
735 State Street
P.O. Drawer 719
Santa Barbara, CA 93102

Prof. Donald Forsyth
Department of Geological Sciences
Brown University
Providence, RI 02912

Dr. Cliff Frolich
Institute of Geophysics
8701 North Mopac
Austin, TX 78759

Dr. Holly Given
IGPP, A-025
Scripps Institute of Oceanography
University of California, San Diego
La Jolla, CA 92093

Dr. Jeffrey W. Given
SAIC
10260 Campus Point Drive
San Diego, CA 92121

Dr. Indra N. Gupta
Multimax, Inc.
1441 McCormick Drive
Landover, MD 20785

Dan N. Hagedon
Pacific Northwest Laboratories
Battelle Boulevard
Richland, WA 99352

Dr. James Hannon
Lawrence Livermore National Laboratory
P.O. Box 808, L-205
Livermore, CA 94550

Prof. Danny Harvey
University of Colorado, JSPC
Campus Box 583
Boulder, CO 80309

Prof. Donald V. Helmberger
Division of Geological & Planetary Sciences
California Institute of Technology
Pasadena, CA 91125

Prof. Eugene Herrin
Geophysical Laboratory
Southern Methodist University
Dallas, TX 75275

Prof. Robert B. Herrmann
Department of Earth & Atmospheric Sciences
St. Louis University
St. Louis, MO 63156

Prof. Lane R. Johnson
Seismographic Station
University of California
Berkeley, CA 94720

Prof. Thomas H. Jordan
Department of Earth, Atmospheric &
  Planetary Sciences
Massachusetts Institute of Technology
Cambridge, MA 02139

Prof. Alan Kafka
Department of Geology & Geophysics
Boston College
Chestnut Hill, MA 02167

2

U.S. Dept of Energy
Max Koontz, NN-20, GA-033
Office of Research and Develop.
1000 Independence Avenue
Washington, DC 20585

Dr. Richard LaCoss
MIT Lincoln Laboratory, M-200B
P.O. Box 73
Lexington, MA 02173-0073

Dr. Fred K. Lamb
University of Illinois at Urbana-Champaign
Department of Physics
1110 West Green Street
Urbana, IL 61801

Prof. Charles A. Langston
Geosciences Department
403 Deike Building
The Pennsylvania State University
University Park, PA 16802

Jim Lawson, Chief Geophysicist
Oklahoma Geological Survey
Oklahoma Geophysical Observatory
P.O. Box 8
Leonard, OK 74043-0008

Prof. Thorne Lay
Institute of Tectonics
Earth Science Board
University of California, Santa Cruz
Santa Cruz, CA 95064

Dr. William Leith
U.S. Geological Survey
Mail Stop 928
Reston, VA 22092

Mr. James F. Lewkowicz
Phillips Laboratory/GPE
29 Randolph Road
Hanscom AFB, MA 01731-3010(2 copies)

Prof. L. Timothy Long
School of Geophysical Sciences
Georgia Institute of Technology
Atlanta, GA 30332

Dr. Randolph Martin, III
New England Research, Inc.
76 Olcott Drive
White River Junction, VT 05001

Dr. Robert Masse
Denver Federal Building
Box 25046, Mail Stop 967
Denver, CO 80225

Dr. Gary McCartor
Department of Physics
Southern Methodist University
Dallas, TX 75275

Prof. Thomas V. McEvilly
Seismographic Station
University of California
Berkeley, CA 94720

Dr. Art McGarr
U.S. Geological Survey
Mail Stop 977
U.S. Geological Survey
Menlo Park, CA 94025

Dr. Keith L. McLaughlin
S-CUBED
A Division of Maxwell Laboratory
P.O. Box 1620
La Jolla, CA 92038-1620

Stephen Miller & Dr. Alexander Florence
SRI International
333 Ravenswood Avenue
Box AF 116
Menlo Park, CA 94025-3493

Prof. Bernard Minster
IGPP, A-025
Scripps Institute of Oceanography
University of California, San Diego
La Jolla, CA 92093

Prof. Brian J. Mitchell
Department of Earth & Atmospheric Sciences
St. Louis University
St. Louis, MO 63156

Mr. Richard J. Morrow
USACDA/IVI
320 21st St. N.W.
Washington , DC 20451

Mr. Jack Murphy
S-CUBED
A Division of Maxwell Laboratory
11800 Sunrise Valley Drive, Suite 1212
Reston, VA 22091 (2 Copies)

3

Dr. Keith K. Nakanishi
Lawrence Livermore National Laboratory
L-025
P.O. Box 808
Livermore, CA 94550

Prof. John A. Orcutt
IGPP, A-025
Scripps Institute of Oceanography
University of California, San Diego
La Jolla, CA 92093

Prof. Jeffrey Park
Kline Geology Laboratory
P.O. Box 6666
New Haven, CT 06511-8130

Dr. Howard Patton
Lawrence Livermore National Laboratory
L-025
P.O. Box 808
Livermore, CA 94550

Dr. Frank Pilotte
HQ AFTAC/TT
1030 South Highway A1A
Patrick AFB, FL 32925-3002

Dr. Jay J. Pulli
Radix Systems, Inc.
6 Taft Court
Rockville, MD 20850

Dr. Robert Reinke
ATTN: FCTVTD
Field Command
Defense Nuclear Agency
Kirtland AFB, NM 87115

Prof. Paul G. Richards
Lamont-Doherty Earth Observatory
 of Columbia University
Palisades, NY 10964

Mr. Wilmer Rivers
Teledyne Geotech
1300 17th St N #1450
Arlington, VA 22209-3803

Dr. Alan S. Ryall, Jr.
Lawrence Livermore National Laboratory
P.O. Box 808, L-205
Livermore, CA 94550

Dr.Chandan K. Saikia
Woodward Clyde- Consultants
566 El Dorado Street
Pasadena, CA 91101

Dr. Richard Sailor
TASC, Inc.
55 Walkers Brook Drive
Reading, MA 01867

Prof. Charles G. Sammis
Center for Earth Sciences
University of Southern California
University Park
Los Angeles, CA 90089-0741

Prof. Christopher H. Scholz
Lamont-Doherty Earth Observatory
 of Columbia University
Palisades, NY 10964

Dr. Susan Schwartz
Institute of Tectonics
1156 High Street
Santa Cruz, CA 95064

Mr. Dogan Seber
Cornell University
Inst. for the Study of the Continent
3130 SNEE Hall
Ithaca, NY 14853-1504

Secretary of the Air Force
(SAFRD)
Washington, DC 20330

Office of the Secretary of Defense
DDR&E
Washington, DC 20330

Thomas J. Sereno, Jr.
Science Application Int'l Corp.
10260 Campus Point Drive
San Diego, CA 92121

Dr. Michael Shore
Defense Nuclear Agency/SPSS
6801 Telegraph Road
Alexandria, VA 22310

4

Dr. Robert Shumway
University of California Davis
Division of Statistics
Davis, CA 95616

Dr. Matthew Sibol
Virginia Tech
Seismological Observatory
4044 Derring Hall
Blacksburg, VA 24061-0420

Prof. David G. Simpson
IRIS, Inc.
1616 North Fort Myer Drive
Suite 1050
Arlington, VA 22209

Donald L. Springer
Lawrence Livermore National Laboratory
L-025
P.O. Box 808
Livermore, CA 94550

Dr. Jeffrey Stevens
S-CUBED
A Division of Maxwell Laboratory
P.O. Box 1620
La Jolla, CA 92038-1620

Prof. Brian Stump
Los Alamos National Laboratory
EES-3
Mail Stop C-335
Los Alamos, NM 87545

Prof. Jeremiah Sullivan
University of Illinois at Urbana-Champaign
Department of Physics
1110 West Green Street
Urbana, IL 61801

Prof. L. Sykes
Lamont-Doherty Earth Observatory
of Columbia University
Palisades, NY 10964

Dr. Steven R. Taylor
Los Alamos National Laboratory
P.O. Box 1663
Mail Stop C335
Los Alamos, NM 87545

Prof. Tuncay Taymaz
Istanbul Technical University
Dept. of Geophysical Engineering
Mining Faculty
Maslak-80626, Istanbul Turkey

Prof. Clifford Thurber
University of Wisconsin-Madison
Department of Geology & Geophysics
1215 West Dayton Street
Madison, WS 53706

Prof. M. Nafi Toksoz
Earth Resources Lab
Massachusetts Institute of Technology
42 Carleton Street
Cambridge, MA 02142

Dr. Larry Turnbull
CIA-OSWR/NED
Washington, DC 20505

Dr. Gregory van der Vink
IRIS, Inc.
1616 North Fort Myer Drive
Suite 1050
Arlington, VA 22209

Dr. Karl Veith
EG&G
2341 Jefferson Davis Highway
Suite 801
Arlington, VA 22202-3809

Prof. Terry C. Wallace
Department of Geosciences
Building #77
University of Arizona
Tuscon, AZ 85721

Dr. Thomas Weaver
Los Alamos National Laboratory
P.O. Box 1663
Mail Stop C335
Los Alamos, NM 87545

Dr. William Wortman
Mission Research Corporation
8560 Cinderbed Road
Suite 700
Newington, VA 22122

Prof. Francis T. Wu
Department of Geological Sciences
State University of New York
at Binghamton
Vestal, NY 13901

Prof Ru-Shan Wu
University of California, Santa Cruz
Earth Sciences Department
Santa Cruz, CA 95064

ARPA, OASB/Library
3701 North Fairfax Drive
Arlington, VA 22203-1714

HQ DNA
ATTN: Technical Library
Washington, DC 20305

Defense Technical Information Center
Cameron Station
Alexandria, VA 22314 (2 Copies)

TACTEC
Battelle Memorial Institute
505 King Avenue
Columbus, OH 43201 (Final Report)

Phillips Laboratory
ATTN: XPG
29 Randolph Road
Hanscom AFB, MA 01731-3010

Phillips Laboratory
ATTN: GPE
29 Randolph Road
Hanscom AFB, MA 01731-3010

Phillips Laboratory
ATTN: TSML
5 Wright Street
Hanscom AFB, MA 01731-3004

Phillips Laboratory
ATTN: PL/SUL
3550 Aberdeen Ave SE
Kirtland, NM 87117-5776 (2 copies)

Dr. Michel Bouchon
I.R.I.G.M.-B.P. 68
38402 St. Martin D'Heres
Cedex, FRANCE

Dr. Michel Campillo
Observatoire de Grenoble
I.R.I.G.M.-B.P. 53
38041 Grenoble, FRANCE

Prof. Hans-Peter Harjes
Institute for Geophysic
Ruhr University/Bochum
P.O. Box 102148
4630 Bochum 1, GERMANY

Prof. Eystein Husebye
IFJF
Jordskjelvstasjonen
Allegaten, 5007 BERGEN NORWAY

David Jepsen
Acting Head, Nuclear Monitoring Section
Bureau of Mineral Resources
Geology and Geophysics
G.P.O. Box 378, Canberra, AUSTRALIA

Ms. Eva Johannisson
Senior Research Officer
FOA
S-172 90 Sundbyberg, SWEDEN

Dr. Peter Marshall
Procurement Executive
Ministry of Defense
Blacknest, Brimpton
Reading FG7-FRS, UNITED KINGDOM

Dr. Bernard Massinon, Dr. Pierre Mechler
Societe Radiomana
27 rue Claude Bernard
75005 Paris, FRANCE (2 Copies)

Dr. Svein Mykkeltveit
NTNT/NORSAR
P.O. Box 51
N-2007 Kjeller, NORWAY (3 Copies)

Prof. Keith Priestley
University of Cambridge
Bullard Labs, Dept. of Earth Sciences
Madingley Rise, Madingley Road
Cambridge CB3 OEZ, ENGLAND

Dr. Jorg Schlittenhardt
Federal Institute for Geosciences & Nat'l Res.
Postfach 510153
D-30631 Hannover , GERMANY

Dr. Johannes Schweitzer
Institute of Geophysics
Ruhr University/Bochum
P.O. Box 1102148
4360 Bochum 1, GERMANY

6

Trust & Verify
VERTIC
Carrara House
20 Embankment Place
London WC2N 6NN, ENGLAND

Prof. Dr. M. Namik YALCIN
Dept. of Earth Sciences
P.O. Box 21,
41470
GEBZE-KOCAELI, TURKEY